АКУСТИЧЕСКИЙ ЖУРНАЛ

АКАДЕМИЯ НАУК СССР

SOVIET PHYSICS

Acoustics

VOLUME 2 NUMBER 1

A Translation

of the

Journal of Acoustics

of the

Academy of Sciences of the USSR

Published by the

AMERICAN INSTITUTE OF PHYSICS

INCORPORATED

SOVIET PHYSICS

Acoustics

A translation of the "Journal of Acoustics" of the USSR.

A publication of the

AMERICAN INSTITUTE OF PHYSICS

Governing Board

Allen V. Astin
Robert F. Bacher
W. S. Baird
H. A. Bethe
R. T. Birge
Frank D. Dexter
J. C. Gardner
S. A. Goudsmit
Charles Kittel
Hugh S. Knowles
R. B. Lindsay
William F. Meggers
Harry F. Olson
R. R. Palmer
R. F. Paton
Eric Rodgers
Ralph A. Sawyer
Frederick Seitz
H. D. Smyth
Mark W. Zemansky

Officers and Staff

Frederick Seitz
Chairman, Governing Board
Henry A. Barton
Director
Wallace Waterfall
Executive Secretary
Mark W. Zemansky
Treasurer
Theodore Vorburger
Advertising Manager
Ruth F. Bryans
Publication Manager
Kathryn Setze
Assistant Treasurer
Alice Mastropietro
Circulation Manager
Eugene H. Kone
Director of Public Relations

American Institute of Physics Advisory Board on Russian Translations

Elmer Hutchisson, *Chairman*
Dwight Gray, Morton Hamermesh, Vladimir Rojansky, Victor Weisskopf

"Soviet Physics—Acoustics" is published by the American Institute of Physics for the purpose of making available in English reports of current Soviet research in acoustics as contained in the "Journal of Acoustics" of the Academy of Sciences of the USSR, and will regularly consist of four issues per year.

Transliteration of the names of Russian authors follows the system employed by the Library of Congress.

This translating and publishing project was undertaken by the Institute in the conviction that dissemination of the results of research everywhere in the world is invaluable to the advancement of science. The National Science Foundation of the United States encouraged the project initially and is supporting it in large part by a grant. Translation and printing are being handled by Consultants Bureau, Inc.

The American Institute of Physics and its translators propose to translate faithfully all the scientific material in the "Journal of Acoustics" of the Academy of Sciences of the USSR appearing after January 1, 1955, the first year of its publication. The views expressed in the translated material, therefore, are intended to be those expressed by the original authors, and not those of the translators nor of the American Institute of Physics.

One volume is published annually. Volume 1 will contain all of the scientific material published in the original Russian journal during the calendar year 1955, and Volume 2 will contain all of the scientific material published in the original Russian journal during the calendar year 1956.

Subscription Prices:

Per year, beginning with Volume 2 (4 issues)	
United States and Canada	$20.00
Elsewhere	22.00
*Back Numbers (beginning with Volume 2)	
Single copies	$ 6.00

*Volume 1, consisting of two issues, is available only as a set at the yearly rates quoted above.

Subscriptions should be addressed to the American Institute of Physics, 57 East 55th Street, New York 22, New York.

Copyright by American Institute of Physics 1956

SOVIET PHYSICS

Acoustics

SOVIET PHYSICS — ACOUSTICS **VOLUME 2, NUMBER 1**

ANNOUNCEMENT

A year ago the American Institute of Physics established "Soviet Physics — JETP" as its first step in bringing before American physicists information about the scientific activities of Soviet physicists. The demand for translations of other Russian physics journals has encouraged the Institute to broaden its program. "Soviet Physics — Acoustics" and the other translation journals listed on the back cover of this issue constitute the expanded program of the Institute.

SOVIET PHYSICS — ACOUSTICS VOL. 2, NO. 1 Jan.-Feb.-March, 1956

(Published by the American Institute of Physics September, 1956)

CONTENTS

Page Russian Page

Integration of a System of Auto-Simulating Equations for the Problem of a Short-Duration Shock in a Cold Gas. V. B. Adamskii 1 3

Acoustic Nondirectional Ceramic Receiving Transducers. A. A. Anan'eva 8 10

Motion of a Gas Due to a Pressure of Short Duration (Shock). Ia. B. Zel'dovich 25 28

Sound Velocities in Individual Liquids and in Liquid Mixtures. B. B. Kudriavtsev 36 39

Calculation of Audibility of Nonlinear Distortion Arising in an Electroacoustical Channel. A. V. Rimskii-Korsakov 48 51

Dielectric and Piezoelectric Properties of Solid Solutions of (Ba, Sr) TiO_3, (Ba, Pb) TiO_3, Ba (Ti, Sn) O_3 and Ba (Ti, Zr) O_3. N. A. Roi 60 62

Acoustical Properties of a Thinly Laminated Medium. S. M. Rytov 67 71

A High-Power Ultrasonic Installation for Irradiating Microorganisms. I. V. Skards 81 84

Sound Radiation By a Rotating Dipole. L. N. Sretenskii 89 93

CHRONICLE

V. S. Grigor'ev (On His Fiftieth Birthday) 95 99

In the Acoustical Commission of the Acad. Sci. USSR. Conference Devoted to Methods of Investigating Speech 96 100

Development of Acoustics in Poland and Romania 97 101

LETTERS TO THE EDITOR

The Investigation of the Field Produced by Ultrasonic Dispersion Lenses in a Liquid. L. M. Liamshev 100 103

From the Press of the Academy of Sciences of the USSR. (Advertisement) . . . . . . 102 ....

INTEGRATION OF A SYSTEM OF AUTOSIMULATING EQUATIONS FOR THE PROBLEM OF A SHORT DURATION SHOCK IN A COLD GAS

V. B. Adamskii

A system of autosimulating equations is derived for the problem of a short duration shock in a cold gas [1]. An investigation is made of this system in general form for any adiabatic index γ. The exponent $\underline{n}$, upon which the autosimulating solution depends, may be found by numerical integration from a specially defined point to the point defined by the initial conditions. Values are given for the exponent $\underline{n}$, and graphs are given for the physical quantities in Euler and Lagrange coordinates which are obtained by numerical integration for a diatomic gas ($\gamma = 7/5$).

In the paper by Ia. B. Zel'dovich titled "The Motion of a Gas Due To A Pressure of Short Duration (Shock)" [1], it is shown that the problem of a short duration shock reduces to a system of autosimulating equations. These autosimulating equations may be obtained directly in the Lagrangian form. We introduce the independent variable

$$\eta = \frac{m}{M},$$

where $m = \int_{-\infty}^{x} \rho\, dx = \rho_0 y$ and $M = \rho_0 X$ (X is the Euler coordinate of the shock wave front, $\underline{x}$ is the Euler flow coordinate, $\underline{y}$ is the Lagrange coordinate).

Let us suppose that $p = A\rho_0 M^{-n} f(\eta)$ is the pressure, $u = \sqrt{A}\, M^{-\frac{n}{2}} w(\eta)$ is the velocity, and $\rho = \rho_0 q(\eta)$ is the density.

Let us assume that $\underline{f} = 1$ for $\eta = 1$. Then from the condition for the shock front of a strong shock wave, $p = \frac{\gamma + 1}{2} \rho_0 u^2$, we have

$$w(1) = \sqrt{\frac{2}{\gamma + 1}}.$$

We note that

$$\frac{dM}{dt} = \frac{\gamma + 1}{2} \rho_0 u^2 = \frac{\gamma + 1}{2} \rho_0 \sqrt{A}\, M^{-\frac{n}{2}}.$$

We write out the equations for the gas dynamics in Lagrangian form:

$$\frac{\partial \rho}{\partial t} = -\frac{\rho^2}{\rho_0} \frac{\partial u}{\partial y} \quad \text{or} \quad \frac{\partial \rho}{\partial t} = -\rho^2 \frac{\partial u}{\partial m} \quad \text{is the continuity equation;}$$

$$\frac{\partial u}{\partial t} = -\frac{1}{\rho_0} \frac{\partial p}{\partial y} \quad \text{or} \quad \frac{\partial u}{\partial t} = -\frac{\partial p}{\partial m} \quad \text{is the equation of motion.}$$

Beyond the shock front the flow is isentropic, and therefore we may apply the equation

$$\frac{ds}{dt} = 0 \quad \text{or} \quad \frac{d}{dt}\left(\frac{p}{\rho^{\gamma}}\right) = 0,$$

since $\frac{p}{\rho^{\gamma}}$ is a function of entropy only.

Thus, the quantity $\frac{p}{\rho^{\gamma}}$ is a function of the entropy of a particle and is independent of time for each particle.

From the equation of motion, we obtain

$$\frac{n}{2} w + \eta \frac{dw}{d\eta} = \sqrt{\frac{2}{\gamma+1}} \frac{df}{d\eta}.$$

Further, we utilize the entropy equation. For any gas particle the relationship

$$\frac{p}{\rho^{\gamma}}(m, M_1) = \frac{p}{\rho^{\gamma}}(m, M_2)$$

holds, or

$$\rho(m, M_1) = \rho(m, M_2) \left[\frac{p(m, M_1)}{p(m, M_2)}\right]^{\frac{1}{\gamma}},$$

where M_1 and M_2 are the Lagrange coordinates of the shock front at various instants in time. If we take $M_2 = m$, then we obtain

$$\rho(m, M) = \frac{\gamma+1}{\gamma-1} \rho_0 \left[\left(\frac{m}{M}\right)^n f(\eta)\right]^{\frac{1}{\gamma}},$$

whence

$$q = \frac{\gamma+1}{\gamma-1} [\eta^n f(\eta)]^{\frac{1}{\gamma}}.$$

Thus an algebraic relationship exists between the quantities $\underline{q}$ and $\underline{f}$.

Let us finally make use of the continuity equation. In autosimulating variables it will acquire the form

$$\sqrt{\frac{\gamma+1}{2}} \eta \frac{dq}{d\eta} = q^2 \frac{dw}{d\eta}.$$

Eliminating $\underline{q}$, we obtain

$$\frac{\gamma+1}{\gamma-1} \sqrt{\frac{\gamma+1}{2}} \eta \frac{d}{d\eta} [\eta^n f]^{\frac{1}{\gamma}} = \left(\frac{\gamma+1}{\gamma-1}\right)^2 [\eta^n f]^{2/\gamma} \frac{dw}{d\eta},$$

or

$$\frac{dw}{d\eta} = -\sqrt{\frac{\gamma+1}{2}} \frac{\gamma-1}{\gamma+1} \eta \frac{d}{d\eta} [\eta^n f]^{-1/\gamma}.$$

Thus we obtain a system of two ordinary differential equations, which we shall proceed to investigate:

$$\frac{n}{2} w + \eta \frac{dw}{d\eta} = \sqrt{\frac{2}{\gamma+1}} \frac{df}{d\eta},$$

$$\frac{dw}{d\eta} = -\sqrt{\frac{\gamma+1}{2}} \frac{\gamma-1}{\gamma+1} \eta \frac{d}{d\eta} [\eta^n f]^{-1/\gamma}.$$

We shall show that $1 < n < 2$.

Let us integrate the first equation from η_0 to 1; η_0 is the point where the velocity $\underline{w}$ changes sign. Then we have

$$\int_{\eta_0}^{1}\left(\frac{n}{2}w+\eta\frac{dw}{d\eta}\right)d\eta=\int_{\eta_0}^{1}\sqrt{\frac{2}{\gamma+1}}\,\frac{df}{d\eta}d\eta,$$

$$\left(1-\frac{n}{2}\right)\int_{\eta_0}^{1}w\,d\eta=\left(w\eta-\sqrt{\frac{2}{\gamma+1}}\,f\right)\Bigg|_{\eta_0}^{1};$$

Substituting the limits, we obtain

$$\left(1-\frac{n}{2}\right)\int_{\eta_0}^{1}w\,d\eta=\sqrt{\frac{2}{\gamma+1}}\,f(\eta_0).$$

At the right there is a positive quantity; in order that there be a positive quantity to the left as well, the condition n < 2 must apply.

Let us now integrate the first equation over the same limits, multiplying it by w:

$$\int_{\eta_0}^{1}\left(\frac{n}{2}w^2+\eta w\frac{dw}{d\eta}\right)d\eta=\sqrt{\frac{2}{\gamma+1}}\int_{\eta_0}^{1}w\frac{df}{d\eta}\,d\eta,$$

$$(n-1)\int_{\eta_0}^{1}\frac{w^2}{2}d\eta+\sqrt{\frac{2}{\gamma+1}}\int_{\eta_0}^{1}f\frac{dw}{d\eta}\,d\eta=-\eta\frac{w^2}{2}\Bigg|_{\eta_0}^{1}+\sqrt{\frac{2}{\gamma+1}}\,wf\Bigg|_{\eta_0}^{1}.$$

Let us now utilize the second equation

$$\sqrt{\frac{2}{\gamma+1}}\int_{\eta_0}^{1}f\frac{dw}{d\eta}\,d\eta=-\frac{\gamma-1}{\gamma+1}\int_{\eta_0}^{1}f\eta\,\frac{d}{d\eta}\,[\eta^n f]^{-\frac{1}{\gamma}}\,d\eta=$$

$$=\frac{\gamma-1}{\gamma+1}\,\frac{1}{\gamma}\int_{\eta_0}^{1}[\eta^n f]^{-\frac{1}{\gamma}}\,\frac{d}{d\eta}\,[\eta^n f]\,\frac{d\eta}{\eta^{n-1}}=\frac{1}{\gamma+1}\int_{\eta_0}^{1}\frac{d}{d\eta}\,[\eta^n f]^{\frac{\gamma-1}{\gamma}}\,\frac{d\eta}{\eta^{n-1}}=$$

$$=\frac{1}{\gamma+1}\,[\eta^n f]^{\frac{\gamma-1}{\gamma}}\,\frac{1}{\eta^{n-1}}\Bigg|_{\eta_0}^{1}+\frac{n-1}{\gamma+1}\int_{\eta_0}^{1}[\eta^n f]^{\frac{\gamma-1}{\gamma}}\,\frac{d\eta}{\eta^{n}}.$$

Whence we obtain

$$(n-1)\int_{\eta_0}^{1}\left(\frac{w^2}{2}+\frac{1}{\gamma+1}\,\eta^{-\frac{n}{\gamma}}f^{\frac{\gamma-1}{\gamma}}\right)d\eta=-\eta\frac{w^2}{2}\Bigg|_{\eta_0}^{1}+\sqrt{\frac{2}{\gamma+1}}\,wf\Bigg|_{\eta_0}^{1}-$$

$$-\frac{1}{\gamma+1}\,[\eta^n f]^{\frac{\gamma-1}{\gamma}}\,\frac{1}{\eta^{n-1}}\Bigg|_{\eta_0}^{1};$$

after substituting the limits

$$(n-1)\int_{\eta_0}^{1}\left(\frac{w^2}{2}+\frac{1}{\gamma+1}\,\eta^{-\frac{n}{\gamma}}f^{\frac{\gamma-1}{\gamma}}\right)d\eta=\frac{1}{\gamma+1}\left\{[\eta_0^n f(\eta_0)]\frac{\gamma-1}{\gamma}\,\frac{1}{\eta_0^{n-1}}+1\right\}.$$

From this it follows that the condition n > 1 must apply.

The substitution of $\varphi\,\eta^{\frac{2\gamma-n}{\gamma+1}}=\underline{f}$ and $\omega\,\eta^{\frac{\gamma-n+1}{\gamma+1}}=\underline{w}$ makes it possible to reduce the system to one equation.

In terms of the new variables, the equations transform into the form

$$\frac{n}{2}\omega+\frac{d\omega}{d\xi}+\frac{\gamma-n-1}{\gamma+1}\omega=\sqrt{\frac{2}{\gamma+1}}\left\{\frac{d\varphi}{d\xi}+\frac{2\gamma-n}{\gamma+1}\varphi\right\},$$

$$\frac{d\omega}{d\xi}+\frac{\gamma-n-1}{\gamma+1}\omega=\frac{1}{\gamma}\sqrt{\frac{\gamma+1}{2}}\,\frac{\gamma-1}{\gamma+1}\left\{\varphi^{-\left(\frac{1}{\gamma}+1\right)}\frac{d\varphi}{d\xi}+\frac{(2+n)\gamma}{\gamma+1}\varphi^{-1/\gamma}\right\},$$

where $\xi = \ln \eta$.

The system, resolved with respect to the derivatives, is of the form

$$\frac{d\varphi}{d\xi}=\frac{\sqrt{\frac{\gamma+1}{2}}\frac{n}{2}\omega-\frac{2\gamma-n}{\gamma+1}\varphi+\frac{\gamma-1}{2(\gamma+1)}(n+2)\varphi^{-1/\gamma}}{1-\frac{\gamma-1}{2\gamma}\varphi^{-\left(\frac{1}{\gamma}+1\right)}},$$

$$\frac{d\omega}{d\xi}=\frac{\frac{\gamma-1}{\gamma\sqrt{2(\gamma+1)}}n\varphi^{-1/\gamma}+\frac{(\gamma-1)^2}{4\gamma(\gamma+1)}(n+2)\omega\varphi^{-\left(\frac{1}{\gamma}+1\right)}-\frac{\gamma-1-n}{\gamma+1}\omega}{1-\frac{\gamma-1}{2\gamma}\varphi^{-\left(\frac{1}{\gamma}+1\right)}}.$$

Thus we arrive at a single equation

$$\frac{d\omega}{d\varphi}=\frac{\frac{\gamma-1}{\gamma\sqrt{2(\gamma+1)}}n\varphi^{-1/\gamma}+\frac{(\gamma-1)^2}{4\gamma(\gamma+1)}(n+2)\omega\varphi^{-\left(\frac{1}{\gamma}+1\right)}-\frac{\gamma-1-n}{\gamma+1}\omega}{\sqrt{\frac{\gamma+1}{2}}\frac{n}{2}\omega-\frac{2\gamma-n}{\gamma+1}\varphi+\frac{\gamma-1}{2(\gamma+1)}(n+2)\varphi^{-1/\gamma}}.$$

To eliminate the fractional powers and reduce the equation to a form in which all the adiabatic indices will be of uniform character, we change variables:

$$\frac{\omega}{\varphi}=u \quad \text{and} \quad \varphi^{\left(\frac{1}{\gamma}+1\right)}=z.$$

Then we obtain

$$u+\left(\frac{1}{\gamma}+1\right)\frac{du}{dz}z=\frac{\frac{\gamma-1}{\gamma\sqrt{2\gamma+1}}n\frac{1}{z}+\frac{(\gamma-1)^2}{4\gamma(\gamma+1)}(n+2)\frac{u}{z}-\frac{\gamma-1-n}{\gamma+1}u}{\sqrt{\frac{\gamma+1}{2}}\frac{n}{2}u-\frac{2\gamma-n}{\gamma+1}+\frac{\gamma-1}{2(\gamma+1)}(n+2)\frac{1}{z}}$$

After simple transformations, the equation acquires the form:

$$\frac{du}{dz}=\frac{1}{z}\frac{\frac{\gamma-1}{\sqrt{2(\gamma+1)}}n-\frac{\gamma-1}{4}(n+2)u+\gamma uz-\frac{n\gamma}{2}\sqrt{\frac{\gamma+1}{2}}u^2z}{\frac{n}{2}(\gamma+1)\quad\sqrt{\frac{\gamma+1}{2}}uz-(2\gamma-n)z+\frac{\gamma-1}{2}(n+2)}.$$

We shall now make a qualitative analysis of this equation.

The equation for the isocline of infinities is

$$z=\frac{\frac{\gamma-1}{2}(n+2)}{2\gamma-n-\frac{n}{2}(\gamma+1)u} \quad \text{and } z=0.$$

The equation for the isocline of zeros is

$$z = \frac{\frac{\gamma-1}{\sqrt{2(\gamma+1)}}n - \frac{\gamma-1}{4}(n+2)u}{\frac{n\gamma}{2}\sqrt{\frac{\gamma+1}{2}u^2 - \gamma u}}.$$

Let us now plot the general shapes of the integral curves. During this process we shall not be interested in the region of the integral curves where $z < 0$, i.e., at negative pressure, nor for $u > \sqrt{\frac{2}{\gamma+1}}$, i.e., for velocities which are greater than the velocity of mass in the shock front.

From the asymptotic shape (when $u \longrightarrow \infty$) of the isocline of infinities

$$z = -\frac{\gamma-1}{\gamma+1}\,\frac{n+2}{n}\sqrt{\frac{2}{\gamma+1}}\,\frac{1}{u}$$

and the isocline of zeros

$$z = -\frac{\gamma-1}{\gamma}\,\frac{n+2}{2n}\sqrt{\frac{2}{\gamma+1}}\,\frac{1}{u}$$

it follows that they must intersect in the region of negative u. Their intersection forms a nodal point in a kind of saddle, which can readily be seen from the picture of the shape of the integral curves, which is given in Figure 1.

The integral curve satisfying the boundary conditions must pass through this nodal point.

In fact, a curve which does not pass through the nodal point either never reaches the value of $z = 0$ (i.e., $p = 0$ and such a result is clearly meaningless) or goes to infinity, but more weakly than the isocline of zeros

$$|u| < \frac{\gamma-1}{2\gamma}\,\frac{n+2}{n}\sqrt{\frac{2}{\gamma+1}}\,\frac{1}{z}.$$

It is easy to convince ourselves that in this case

$$u = -\frac{C}{z},$$

where C is an arbitrary positive constant.

Returning to the previous variables, we have

$$\omega = -\frac{C}{\varphi^{\frac{1}{2}\left(\frac{1}{\gamma}-1\right)}}.$$

If we now substitute this relationship into the equation relating φ and η near $\eta \longrightarrow 0$, we obtain

$$\eta\frac{d\varphi}{d\eta} \approx -\frac{\gamma(n+2)}{\gamma+1}\varphi,$$

which after integration yields

$$\varphi \approx \frac{1}{\eta^{\frac{\gamma(n+2)}{\gamma+1}}}.$$

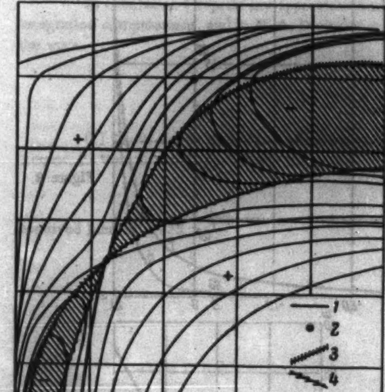

Figure 1. Approximate shape of the integral curves. 1) The integral curve satisfying the initial conditions; 2) point of the initial conditions; 3) isocline of infinities; 4) isocline of zeros; 5) region of positive values for the derivative, 6) region of negative values for the derivative.

Now, turning to the function $f = \varphi\eta^{\frac{2\gamma - n}{\gamma + 1}} \approx \eta^{-n}$, we do not obtain zero pressure at the point $\eta = 0$.

We now find the coordinates of the nodal point in terms of the variables u and z. Setting the numerator and denominator equal to zero, and eliminating z, we obtain the equation

$$\frac{\frac{\gamma-1}{2}(n+2)}{(2\gamma - n) - \frac{n}{2}(\gamma+1)\sqrt{\frac{\gamma+1}{2}}\,u} = \frac{\frac{\gamma-1}{4}(n+2)\,u - \frac{\gamma-1}{\sqrt{2(\gamma+1)}}\,n}{\gamma u - \frac{n\gamma}{2}\sqrt{\frac{\gamma+1}{2}}\,u^2}$$

or, converting it to a standard quadratic equation, we have

$$(2+n)\frac{\gamma-1}{2}\sqrt{\frac{\gamma+1}{2}}\,u^2 - (2 - n\gamma)\,u - \frac{4(2\gamma - n)}{\sqrt{2(\gamma+1)}} = 0.$$

From this,

$$u = \frac{2 - n\gamma \pm \sqrt{[n(\gamma-2)]^2 + 2n(\gamma-2)\,2(2\gamma-1) + [2(2\gamma-1)]^2}}{(\gamma-1)(2+n)\sqrt{\frac{\gamma+1}{2}}}$$

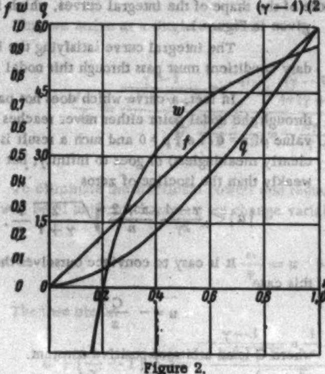

Figure 2.

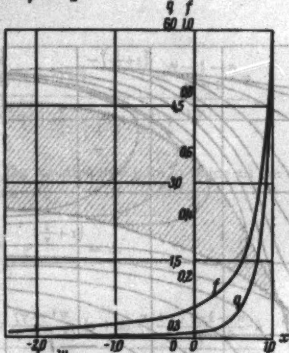

Figure 3.

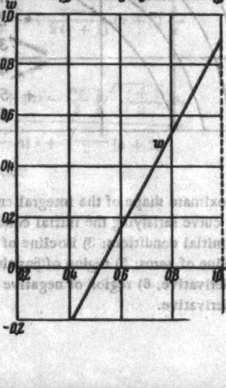

Figure 4.

Figures 2, 3, 4. Diatomic gas:
η is the Lagrange coordinate, x is the Euler coordinate,
f is the pressure variable, q is the density variable,
w is the velocity variable.

We take the negative root $u = -2\sqrt{\frac{2}{\gamma+1}}$, and then

$$z = \frac{\gamma-1}{2\gamma}.$$

In order to determine n, it is necessary to conduct numerical integration from the nodal point by the method of trial and error. Only for one value of n will the curve for numerical integration lead to the point of initial conditions. For our initial path to numerically follow the separatrix when we start from the nodal point, it is necessary to know the resolution near the nodal point,

$$u - u_0 = k(z - z_0),$$

where

$$u_0 = -2\sqrt{\frac{2}{\gamma+1}}, \quad z_0 = \frac{\gamma-1}{2\gamma}, \quad k = \frac{5n+4+\sqrt{(5n+4)^2 - 16n(1+n)\frac{\gamma+1}{\gamma}}}{n\frac{\gamma^2-1}{\gamma^2}\sqrt{\frac{\gamma+1}{2}}}.$$

The plus sign in front of the root is taken because, as can be seen from Figure 1, the integral curve which is the solution coincides with that saddle separatrix which has the greater slope.

The value of the index n is obtained for a diatomic gas. It is n = 1.333 for $\gamma = \frac{7}{5}$.

We have also plotted the quantities f, g, w in Euler and Lagrange coordinates (Figures 2, 3, and 4).

In conclusion I express my appreciation to I. A. Adamskaya and M. S. Zhdanova for the numerical-integration computations, and to N. A. Dmitriev and Ia. B. Zel'dovich for their participation in discussing the work.

LITERATURE CITED

[1] Ia. B. Zel'dovich, "The Motion of a Gas Due to a Pressure of Short Duration (Shock)," Acoust. J. Vol. 2, No. 1, pp. 22-38 (1956).

Received June 11, 1955

Institute of Chemical Physics
Academy of Sciences of the USSR
Moscow

ACOUSTIC NONDIRECTIONAL CERAMIC RECEIVING TRANSDUCERS

A. A. Anan'eva

The paper examines piezoelectric acoustic receiving transducers with spherical and cylindrical directivity, which represent thin shells of barium titanate ceramic. The concept of the transformation coefficient of mechanical stresses is introduced, and it is shown that when the character of the transformation is properly selected and the corresponding arrangement of electrodes properly executed, we may obtain a high sensitivity for the receiving transducers when the directional characteristics are good.

It is known that barium titanate ceramic, used as a material for acoustic receiving transducers, has a low sensitivity in comparison to other piezoelectric substances. For a medium-quality barium titanate ceramic, the piezoelectric modulus in the direction of polarization is $d_{33} = 3.6 \cdot 10^{-6}$ CGSE, the modulus in a direction perpendicular to polarization is $d_{31} = -1.5 \cdot 10^{-6}$ CGSE and the dielectric constant is $\epsilon = 1{,}000$ to 1,200. The ratio of the piezoelectric moduli to the dielectric constant (this ratio determines the sensitivity of the acoustic receiving transducers in the no-load regime [1]) is small and in the usual transducer assemblies with plain or package transducing elements the utilization of barium titanate proves impractical. In these cases, preference may be given to barium titanate solely because of its greater strength.

However, there is one field of acoustic instrumentation where the utilization of polarized barium titanate ceramic considerably simplifies the solution of the problem posed – that is in the field of designing nondirectional acoustic receivers, for example, nondirectional radio-broadcasting microphones, nondirectional acoustical and hydroacoustical measuring receivers, etc.

Spherical nondirectional measuring hydrophones of barium titanate ceramic, and later cylindrical receiving transducers as well, had been produced in the acoustics laboratory of the Phys. Inst. Acad. Sci. as early as 1950.

For receivers with a spherical directional characteristic, hollow spheres of barium titanate glued together out of two halves (Figure 1a) were used in the capacity of a detecting element, and they were polarized radially; for receivers with a circular directional characteristic, radially polarized hollow cylinders were used (Figure 1b).

We should note that it is difficult to obtain an ideal spherical directional characteristic, since the unavoidable structural elements serving as output leads and as cable connectors disrupt the spherical symmetry. As an example, the directional characteristics of a spherical receiver made of barium titanate are shown in an equatorial plane (Figure 2) and in a plane containing an output lead (Figure 3).** In the given case the output lead from the inner electrode was passed through a metal tube which was soldered to the outer metal surface of the sphere. As we can see, the directional characteristics in the equatorial plane were satisfactory, where they are substantially distorted in the plane containing the output lead.

---

* Presented at the Second All-Union Conference on Piezoelectricity, May 26, 1955

** The polar characteristics given in this paper were obtained under conditions of an unbounded medium by means of an automatic pulse arrangement for obtaining the directional characteristics for the hydroacoustic emitters and receivers.

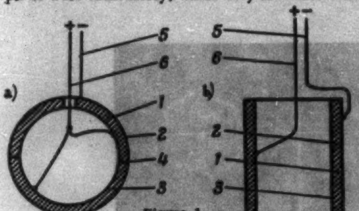

Figure 1.

1) Ceramic; 2 and 3) metallization layer; 4) splice of two hemispheres along equatorial plane; 5 and 6) outlets.

In a cylindrical receiver the problem of constructing the output lead is not as sharply posed, since the cylindrical output lead, naturally, does not disrupt cylindrical symmetry. However the presence of the output lead still affects the directional characteristics in the axial planes, which is easy to see from Figure 6. Let us note that the directional characteristics of cylindrical receivers in the plane perpendicular to the axis (Figures 4 and 5) are, generally speaking, better than the characteristics of spherical receivers in an equatorial plane. The presence of the glued joint in the great-circle of the spherical receivers does not produce a noticeable effect upon the directional characteristics; this was verified with an experimental receiver in which the joint was located in the axial plane of the output lead.

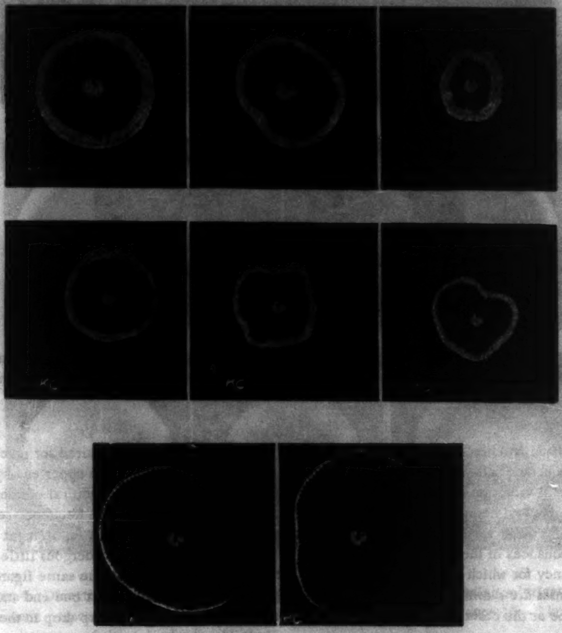

Figure 2. Directional characteristics for a radially polarized spherical receiver in the equatorial plane. The outer diameter of the sphere, D = 16 mm

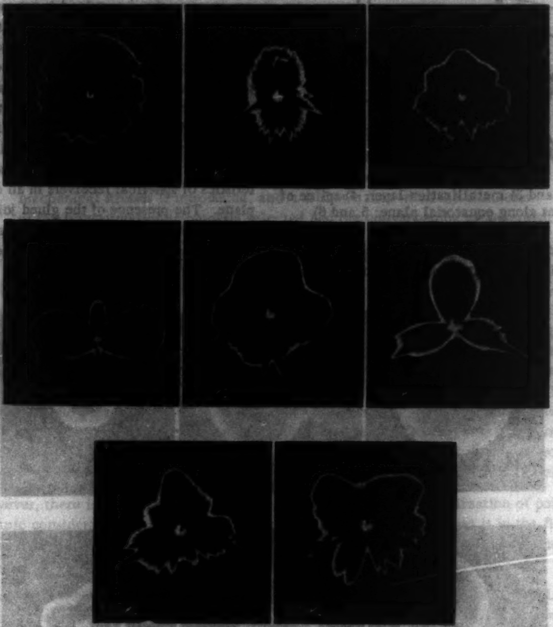

Figure 3. Directional characteristics of a spherical receiver with radial polarization in the plane containing the output lead. The external diameter of the sphere D = 16 mm.

Wide-band nondirectional acoustic receivers are the ones most often required for practical purposes. The working frequency-band, in which the sensitivity is constant, is limited at the upper end by the frequencies of natural vibration of the ceramic or the resonant frequencies of the structural elements serving to lead in the cable and hermetically seal it. As an example, Figure 7a shows the frequency response for the sensitivity of a cylindrical receiving transducer with rubber end caps and a soft cable input lead; in this case the resonances of the cable attachments are absent and the sensitivity undergoes little change right up to the frequency for which longitudinal resonance occurs in the cylinder. In the same figure (b), the frequency responses are shown for a cylinder of the same type having a brass cap at one end and a cap with a brass input tube at the other end. The presence of these elements leads to a sharp drop in the frequency near 15 kc.

We should note that the piezoelement in the form of the cylindrical tube has three fundamental types of internal resonances: 1) that determined by longitudinal vibrations of the cylinder (first resonance for $\lambda = 2h$, where λ is the wave length in the ceramic, h is the height of the cylinder); 2) that related to the diameter of the cylinder (first resonance for $\lambda \approx \pi D$, where D is the diameter of the cylinder); and 3) that related to the wall thickness (first resonance for $\lambda \approx 2a$, where a is the wall thickness). Figure 8 gives

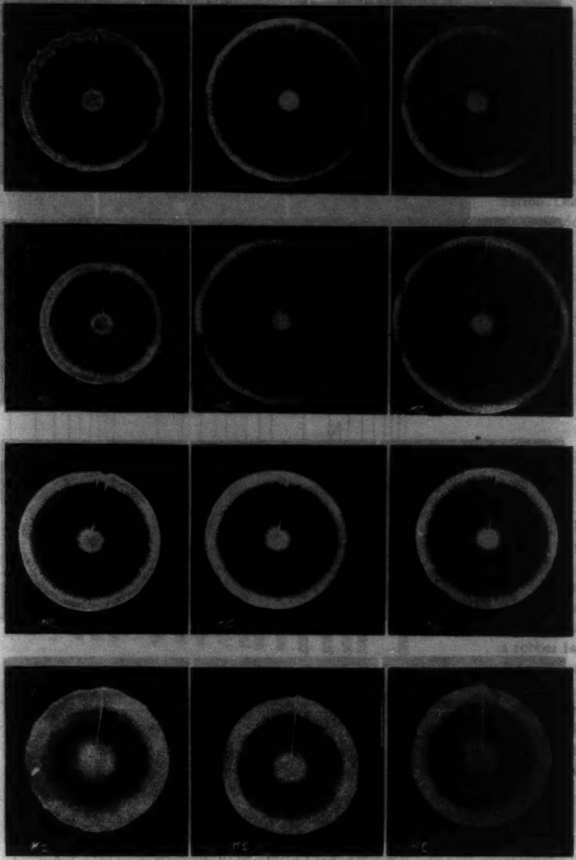

Figure 4. Directional characteristics for a cylindrical receiver with radial polarization in a plane perpendicular to the axis of the cylinder in the frequency range 15-45 kc. Outer diameter of the cylinder D = 32 mm.

the frequency characteristic of the electrical impedance of the cylindrical detecting element, and the enumerated resonances are clearly seen in it. For a piezoelement in the form of a hollow sphere, the resonant frequencies may be calculated; however, when a joint is present, generally speaking, which does

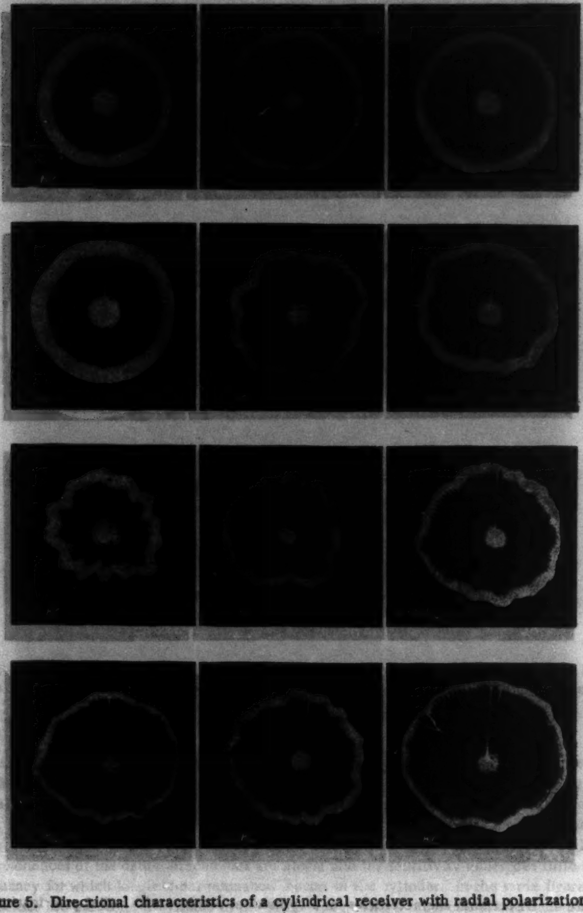

Figure 5. Directional characteristics of a cylindrical receiver with radial polarization in a plane perpendicular to the axis of the cylinder in the frequency range 50-300 kc. Outer diameter of the cylinder D = 32 mm.

not possess a sufficiently high rigidity, the hemispheres vibrate "freely" to a considerable degree and the experimental resonant frequencies do not coincide with the ones calculated for a hollow sphere without a joint. It has been experimentally discovered that the following two types of resonances take place: 1) those which depend on the diameter $\left(\lambda \approx \frac{\pi D}{2}\right)$ and 2) those which depend upon the wall-thickness ($\lambda \approx 2a$).

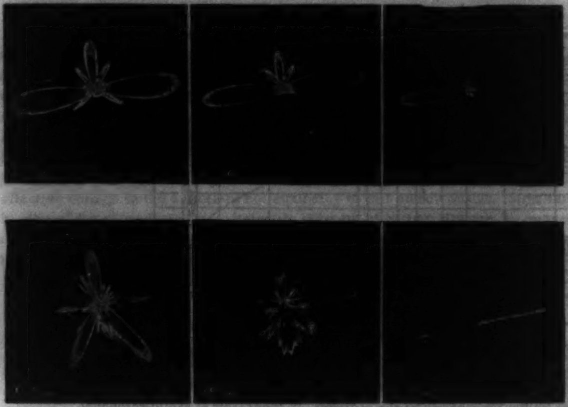

Figure 6. Directional characteristics in an axial plane of a cylindrical receiver with radial polarization. Outer diameter of the cylinder D=32 mm.

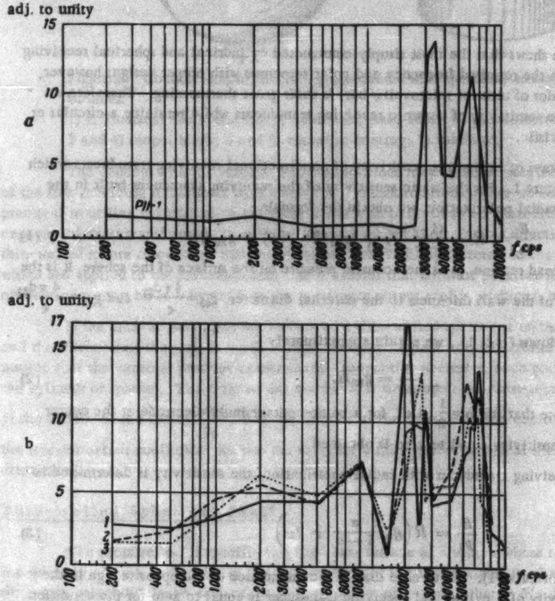

Figure 7. Examples of the frequency responses for the sensitivity of cylindrical receiving transducers with radial polarization.

a) Cylinder ends capped by a rubber layer; b) the cylinders possess metal membrane end-caps (1, 2, 3 are the characteristics of three receiving transducers with identical geometric dimensions).

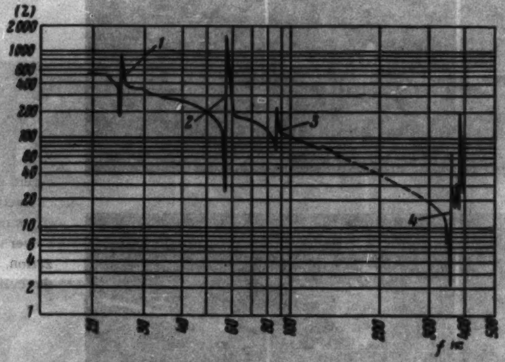

Figure 8. Spectrum of the internal vibrations in the cylindrical receiving transducer. 1) Fundamental longitudinal resonance of the cylinder; 2) fundamental radial resonance of the cylinder; 3) first harmonic radial oscillations; 4) resonance of thickness vibrations in the cylinder.

The above discussion shows that the most simply constructed cylindrical and spherical receiving transducers enable us to obtain the required frequency and polar responses with proper design; however, their low sensitivity (of the order of units of microvolts/ bar) is their great shortcoming. Therefore, we pose the problem of raising the sensitivity of ceramic receiving transducers while retaining a circular or spherical directional characteristic.

Let us examine the ways of raising the sensitivity of nondirectional receiving transducers which are constructed as shown in Figure 1. For the static sensitivity of the receiving transducer built in the form of a hollow sphere with radial polarization, we obtain the formula

$$\frac{E}{p_0} = R\frac{(1-2\sigma)^2}{(3-6\sigma+4\sigma^2)}\left[g_{31}(3-5\sigma)+g_{33}\sigma\right], \qquad (1)$$

where E is the emf in the no-load regime; p_0 is the acoustic pressure on the surface of the sphere, R is the external radius, σ is the ratio of the wall thickness to the external diameter, $g_{33} = \frac{4\pi d_{33}}{\epsilon}$ and $g_{31} = \frac{4\pi d_{31}}{\epsilon}$.

For a small wall thickness ($\sigma \ll 1$) , we obtain approximately

$$\frac{E}{p_0} = g_{31}R. \qquad (2)$$

It is interesting to note that for $\sigma = \frac{1}{2}$, i.e., for a point-contact inner electrode at the center of a solid ceramic sphere, a sensitivity equal to zero is obtained.

For a cylindrical receiving transducer with radial polarization, the sensitivity is determined in the following manner [2]:

$$\frac{E}{p_0} = R\left(g_{33}\frac{\sigma}{1-\sigma} + g_{31}\right) \qquad (3)$$

with the same notation as in formula (1). Let us note that as a consequence of the opposite sign in the moduli d_{33} and d_{31}, the sensitivity of a cylindrical receiving transducer is equal to zero for the condition

$$\sigma = \frac{d_{31}}{d_{31}-d_{33}}.$$

As in the case of the sphere, the sensitivity is approximately equal to Rg_{31}, when the wall is thin.

On the basis of the above it is plain that only two fundamental methods exist for increasing the sensitivity of such receiving transducers: direct increase of the piezo modulus d_{33}, and increase of the external diameter of the sphere or cylinder. The first method as yet shows little promise. The second method may be used, but only until diffractional limitations begin to apply. Therefore, we selected a different method for increasing the sensitivity of ceramic receiving transducers with spherical or cylindrical symmetry. Actually, the problem is one of utilizing a piezoelectric material which has an excessively large dielectric constant in the most practical manner. For that purpose, evidently, it is necessary to utilize the maximum piezomodulus inherent in the given material on the one hand, and on the other hand, to increase the effective voltage in the directions corresponding to this piezomodulus. Simultaneously, it is permissible, in view of the excessively large dielectric constant of barium titanate, to increase the effective size of the detecting element in the direction of greatest piezomodulus. We shall define as mechanical stress transformers those mechanical arrangements which simultaneously resolve all of these three problems.

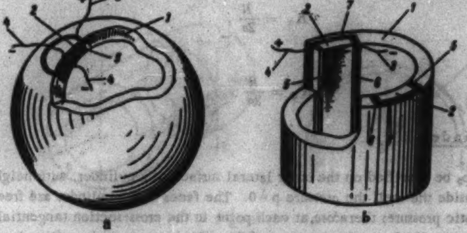

Figure 9. Construction of receiving transducers with spherical and cylindrical receiving surfaces.
1) Cylindrical shell (metallic), spherical (glass) shell; 2) piezoelectric ceramic element; 3 and 4) output leads; 5 and 6) metallic coating; 7) insulator.

The concept of a mechanical stress transformer may be illustrated very clearly by the example of the first receiving transducers with mechanical transformations which we built. We first thought it practical to utilize cylindrical or spherical shells with built-in small piezoelements (Figure 9) in the capacity of stress transformers, in order to retain a spherical or circular directional characteristic. A thin-walled sphere or cylinder will transform external radially directed forces into tangential forces which are applied to the piezoelements It is natural that both the polarization and the arrangement of electrodes must be so selected that the maximum output emf is produced, as is shown in Figure 9.

If the pressure acts upon the surface of a thin-walled sphere (or on the lateral surface of a cylinder) and the thickness of the wall is small enough, we may neglect normal stresses in the material (i.e., we may assume that the external pressure causes chiefly tangential stresses at each point in the cross-section of the cylinder or sphere). The ratio of the mechanical stress upon the cross-section to the acoustic pressure at the surface of the sphere $\frac{\sigma_T}{p_0}$ shall be defined as the transformation coefficient K. We shall calculate the transformation coefficient for two cases: 1) for a thin-walled spherical shell, 2) for a thin-walled cylindrical shell.

Thin-Walled Spherical Shell

The pressure, p_0, is specified on the outer surface of a sphere whose radius is equal to R. Inside the sphere p = 0. At each point in the cross-section of the sphere equal mechanical stresses will act in two directions perpendicular to each other $\sigma_T = \sigma_\phi$; let us compute them. We shall mentally take a cross-section of the sphere through a great-circle. The sum of the normal forces acting upon the circular cross-section (Figure 10a) with an area $S = 2\pi R^2$, is equal to $F = \int_0^{\pi/2} p\,ds$.

where

$$p = p_0 \sin \vartheta, \quad dS = 2\pi\rho R d\vartheta = 2\pi R^2 \cos \vartheta d\vartheta.$$

Therefore,

$$F = 2\pi R^2 p_0 \int_0^{\pi/2} \sin 2\vartheta d\vartheta = p_0 \pi R^2,$$

the stress in the direction τ is

$$\sigma_\tau = \frac{F}{S} p_0 \frac{R}{2a}.$$

From this,

$$K_\tau = \frac{R}{2a},$$

and since $\sigma_\tau = \sigma_\phi$,

$$K_\phi = \frac{R}{2a}.$$

Thin-Walled Cylinder

Let a pressure p_0 be specified on the outer lateral surface of a cylinder, with height $\underline{h}$, radius R and wall thickness $\underline{a}$. Inside the shell the pressure p = 0. The faces of the cylinder are free, i.e., shielded from the action of acoustic pressure; therefore, at each point in the cross-section tangential stresses σ_τ will act in a direction perpendicular to the generant of the cylinder; stresses in a direction parallel to the generant of the cylinder are equal to zero.

Let us mentally take a cross-section of the cylinder through a generant (Figure 10b) and set aside one-half of the cylinder; we shall replace its effect upon the other half of the cylinder by equivalent forces which are normal to the plane of the cross-section. The sum of the projections of all forces acting on two rectangular cross-sections with an overall area S = 2ha, is equal to

$$F = h \int_0^{\pi} p dS,$$

where

$$p = p_0 \sin \vartheta,$$

$$dS = R d\vartheta.$$

Therefore,

$$F = h \int_0^{\pi} p_0 R \sin \vartheta d\vartheta = 2hRp_0;$$

$$\sigma_\tau = \frac{F}{S} = p_0 \frac{R}{a}.$$

From this, the transformation coefficient is

$$K_\tau = \frac{R}{a}.$$

When the dimensions of the sphere or cylinder are sufficiently great, and the wall is sufficiently thin, large values of the transformation coefficient may be obtained.

It is evident that the mechanical transformation may be utilized independently of how the polarization of the detecting element is oriented, and even independently of what type of element is selected.

In this particular case, however, we may fully utilize the advantages of barium titanate only by tangential polarization of the detector element. When this is done we make use of the largest piezomodulus d_{33}, and it is possible to select a sufficiently large effective length for the detector element (along the arc of

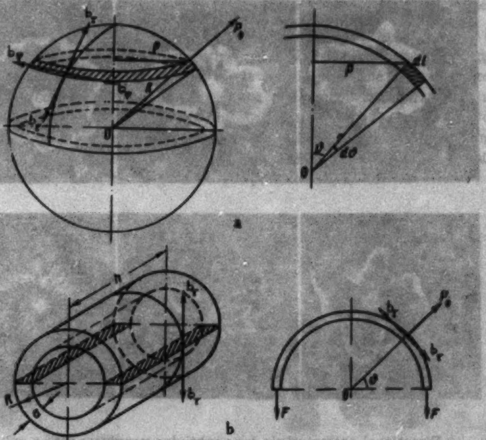

Figure 10

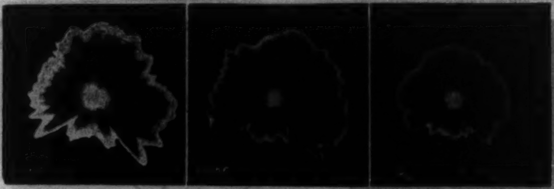

Figure 11. Directional characteristics of a receiving transducer with a spherical receiving surface (diameter of the sphere 29 mm)

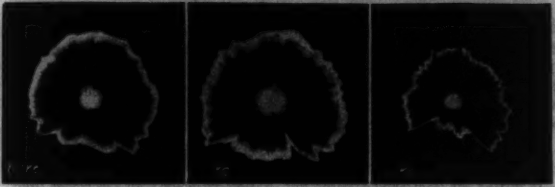

a great-circle for a sphere and along the circumference for a cylinder). Under these conditions the large dielectric constant of ceramic barium titanate is not a disadvantage, but on the contrary is an advantage.

We prepared cylindrical and spherical receivers according to the diagrams in Figure 9. However, the directional characteristics of such receivers proved to be unsatisfactory (Figures 11 and 12), and therefore we decided to utilize the very same piezoelectric material in the capacity of a material for the mechanical transformer. Thus, we arrived at a construction in which the piezoelement is a thin-walled shell with a special electrode arrangement.

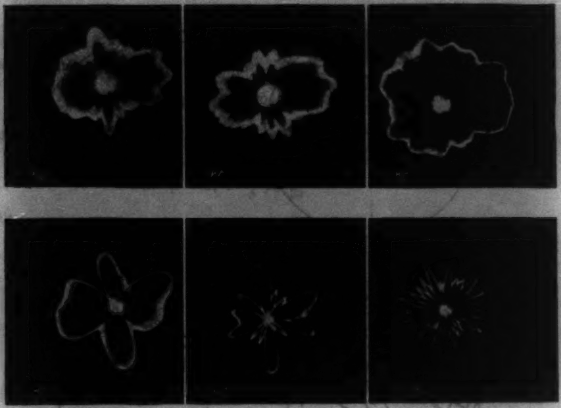

Figure 12. Directional characteristic for a receiving transducer with a cylindrical receiving surface (diameter of the cylinder 38 mm).

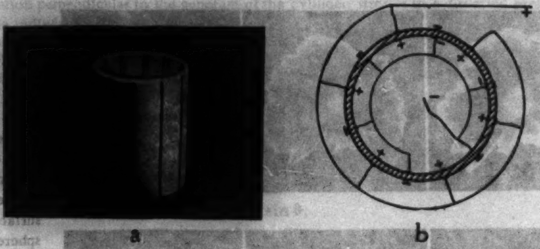

Figure 13. a) External view of a ceramic detecting element in the form of a continuous cylinder with electrodes fired onto its lateral surfaces; b) circuit for combining the electrodes when polarizing the ceramic and when the acoustic receivier is in operation.

When the construction is cylindrical, the large magnitude of the dielectric permeability of the ceramic made it possible to utilize non-sectioned ceramic thin-walled cylinders with electrodes fired onto the lateral surfaces of the cylinder. With an electrode distribution over the cylindrical surfaces which is shown in Figures 13, a and b, tangential polarization of the ceramic is effected. In utilizing the method of surface application of the electrodes, it is also possible to effect the tangential polarization of a thin-walled ceramic sphere, as is shown in Figure 14.

In a case when a cylindrical or spherical acoustical receiver possessing surface applied electrodes is utilized in the capacity of an air microphone, there is no necessity for using any shielding devices whatsoever, except, perhaps, a shielding grid. For hydrophones it is necessary to utilize an external shielding layer of a dielectric with a dielectric constant which is substantially lower than that of barium titanate.

Various plastics may be utilized as material for such a layer; in particular, we utilized a layer made of rubber.

The external view of the latest models of our highly-sensitive cylindrical hydrophones is shown in Figure 15. An example of the directional characteristics of cylindrical hydrophones with tangential polarization is shown in Figures 16 and 17. The band of frequencies in which the polar characteristics remain circular is narrowed in comparison to that for a receiver with a homogeneous radial polarization, since we changed the character of the piezoelement's symmetry. The internal resistance of hydrophones of the specified type is considerably higher than that of hydrophones having the same dimensions but possessing radially-polarized elements; however, the internal resistance remains within permissible limits for engineering application, due to the large dielectric permeability of the ceramic.

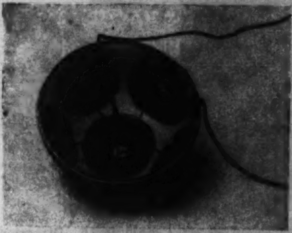

Figure 14. Element of a spherical acoustical receiver-hemisphere with surface electrodes, allowing tangential polarization of the ceramic to be effected.

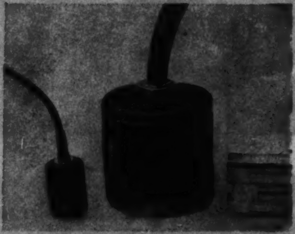

Figure 15. Overall view of hydrophones with detecting elements in the form of a radially-polarized ceramic cylinder.

TABLE 1

Polarization	Shapes of receiving surface	
	Sphere	Cylinder (with free faces)
Radial	$Rg_{32} = 4.7 \cdot R$	$Rg_{32} = 4.7R$
Longitudinal	—	$Rg_{32}\frac{1}{a} = 4.7R\frac{1}{a}$
Tangential	$\frac{2\pi R^2}{an} g_{33} = 71.0 \frac{R^2}{an}$	$\frac{2\pi R^2}{an} g_{33} = 71.0 \frac{R^2}{an}$

Notation in the table: a is the wall-thickness of the ceramic shell in cm; 1 is the distance between electrodes, in cm; R is the radius of the cylinder or sphere in cm; n is the number of cells (on a great-circle of the sphere or on a diameter of the cylinder).

Let us compute the static sensitivity of thin-walled spherical and cylindrical receivers of barium titanate ceramic, utilizing the definition for the coefficient of mechanical transformation which was introduced earlier. The sensitivity of the piezoelectric receiver of the simplest type, in a no-load regime, is determined by the formula

$$\frac{E}{P_0} = gl$$

where E is the emf developed across the coatings of the piezoelement for a specified acoustic pressure upon its surface, g is the corresponding piezoconstant, "1" is the effective length of the piezoelement (the distance between electrodes).

In utilizing systems with mechanical transformation, we gain an additional advantage in receiver sensitivity:

$$\frac{E}{p_0} = Kgl,$$

where K is the transformation coefficient of mechanical stress. For the cases of a thin-walled sphere and a thin-walled cylinder with free ends, the expressions for K were given above.

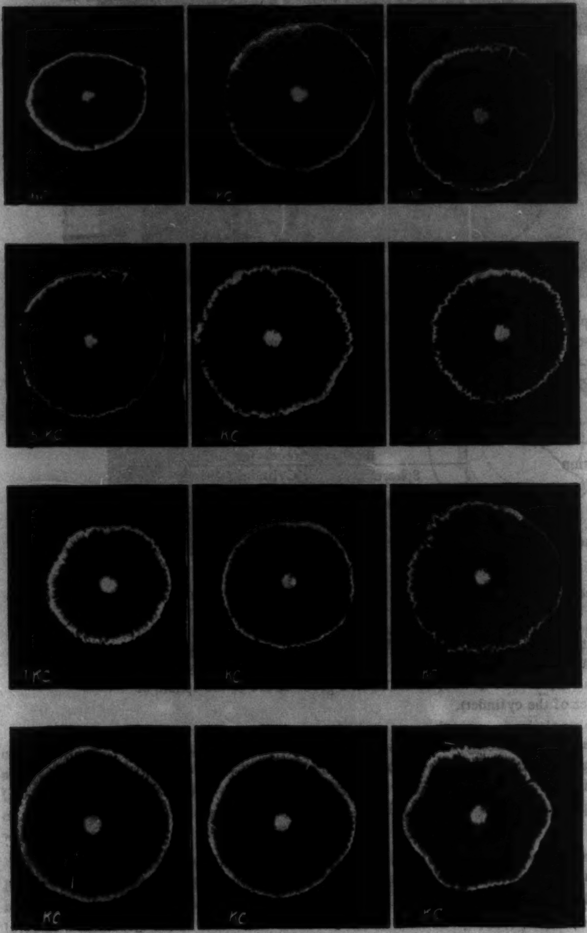

Figure 16. Directional characteristics of a ceramic acoustic receiver with tangential polarization in the frequency range 10-55 kc. Diameter of the cylinder D = 32 mm; height h = = 40 mm.

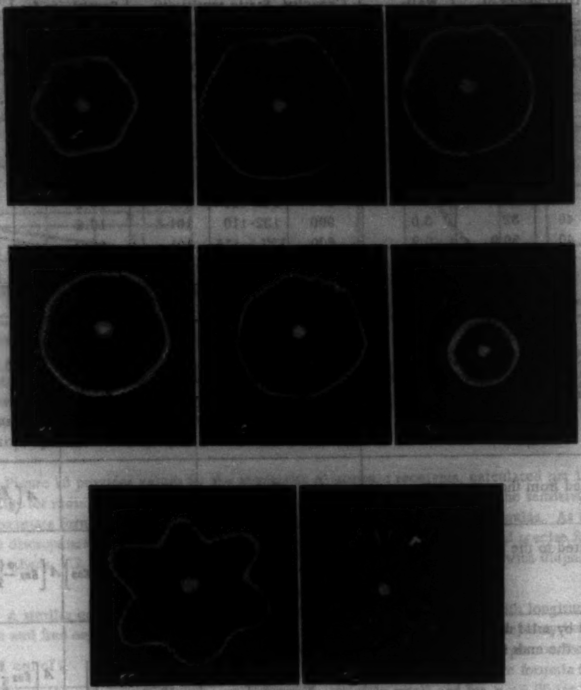

Figure 17. Directional characteristics of a ceramic acoustic receiver with tangential polarization in the frequency range of 60-239 kc. The diameter of the cylinder D = 32 mm; height h = 40 mm.

In Table 1, formulas are given for calculating the sensitivity in the no-load regime in µv/bar, for ordinary barium titanate ceramic with a dielectric permeability $\epsilon = 1200$ and a piezoelectric modulus $d_{33} = 3.6 \times 10^{-6}$ CGSE.

In Table 2, data is given for cylindrical piezoelements for hydrophones with tangential polarization. For comparison, the maximum sensitivity which may be obtained for radial polarization of cylinders with the same dimensions are given (cylinders with rigid diaphragms capping the ends, which increase the longitudinal amplification in the shell for a specified sound pressure). The table indicates two values for the calculated sensitivity: the lesser value is calculated for the case when the portion of the surface occupied by the electrodes is taken into account, and the larger value for the case when the electrodes are infinitely narrow.

The design of cylindrical tubes with a finite wall thickness when various methods are used for capping the ends [2] results in the formulas provided in Table 3.

TABLE 2

Specified piezoelement No.	Dimensions of cylinders		Wall-, thickness, (mm)	Capacity (μμf)	Static sensitivity, (μv/bar)		Sensitivity for radial polarization* (μv /bar)	Working frequency band
	Height (mm)	Diameter (mm)			Calculated values	Average measured values		
1	40	52	1.5	500	264-238	234	17	up to 20 kc
2	40	52	1.5	500	264-238	250	17	up to 20 kc
3	40	52	1.5	500	264-238	240	17	up to 20 kc
4	40	52	3.0	900	132-110	135	16.2	up to 20 kc
5	40	52	3.0	900	132-110	106.5	16.2	up to 20 kc
6	40	52	3.0	900	132-110	101.5	16.2	up to 20 kc
7	40	30.9	0.9	690	127.5-115	101	10.9	up to 50 kc
8	40	32.0	1.5	—	73	64.4	10.7	up to 50 kc
9	23.6	14.6	1.0	—	19	—	4.75	up to 100 kc

TABLE 3

	Method of securing ends	Method of polarization		
		I, radial polarization	II, longitudinal polarization	III, tangential polarization
1	Ends shielded from the pressure	$R\left(g_{33}\frac{\sigma}{1-\sigma}+g_{31}\right)$	$h\frac{g_{31}}{2(\sigma-\sigma^2)}$	$A\left(\frac{g_{31}\sigma}{1-\sigma}+g_{33}\right)$
2	Ends subjected to the pressure	$R\left[g_{33}\frac{\sigma}{1-\sigma}+ +g_{31}(1-2\sigma)\right]$	$h\left[\frac{g_{31}}{2(\sigma-\sigma^2)}+g_{33}\right]$	$A\left[g_{31}\frac{\sigma(3-2\sigma)}{1-\sigma}+g_{33}\right]$
3.	Ends closed by solid diaphragm (pressure on the ends is amplified).	$R\left(g_{33}\frac{\sigma}{1-\sigma}+g_{31}\times \times\frac{3-2\sigma}{2-2\sigma}\right)$	$h\left[\frac{2g_{31}+g_{33}}{4(\sigma-\sigma^2)}\right]$	$A\left[g_{31}\frac{1+2\sigma}{2(1-\sigma)}+g_{33}\right]$

In Table 3, the parameter A has the form

$$A=\frac{1}{h}\frac{2\pi R}{\ln\frac{2}{1-2\sigma}},$$

σ is the ratio of wall thickness to the external diameter of the cylinder, h is the height of the cylinder; the remaining definitions are the same as before.

When we place $\sigma = 0$, it is easy to prove that the approximate expressions for the static sensitivities of thin-walled spherical and cylindrical shells given in Table 1 are the limiting cases of the generalized calculation of the sensitivities of a cylinder and sphere with finite wall-thicknesses.'

It is of interest to clarify to what degree the approximate formula is usable for practical computation in a case which differs from the limiting case, i.e., for finite values of σ. It is evident that it is impractical to select large values of σ, even if we do not approach the region near σ = 0 where the sensitivity decreases rapidly, since for a thick wall the sensitivity falls sharply. Therefore, we selected values of σ which were no greater than 0.05 – 0.06.

---

* For a cylinder with rigid diaphragms as end caps. For a cylinder with free ends, when it is radially polarized, the sensitivity would be 1.5 times smaller.

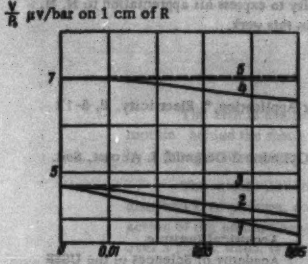

Figure 18. Calculation of static sensitivity of ceramic cylindrical and spherical acoustic receivers with radial polarization
1 and 3 (Sphere); 2 and 3 (cylinder) (ends are shielded from pressure); 4 and 5 (cylinder) (ends are closed by rigid membranes which amplify the pressure upon them).

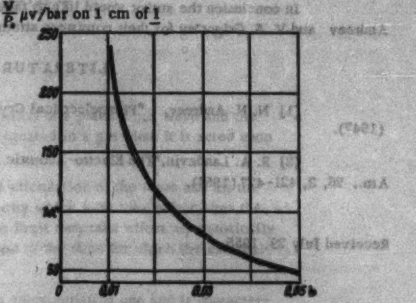

Figure 19. Calculation of the static sensitivity of a cylinder with longitudinal polarization (ends of the cylinder are shielded from pressure).

Figure 18 provides values for the sensitivity of acoustic receivers, calculated per 1 cm external radius for radial polarization. The dotted horizontal straight lines depict the sensitivity calculated by the approximate formulas, the solid curves depict calculation by the precise formulas. As we can see, for σ = 0.05 the discrepancies between the results of calculation by the approximate and precise formulas are 2.1 db for a sphere, 1.2 db for a cylinder with free ends, and 0.73 db for a cylinder with diaphragms capping its ends.

A similar comparison is given in Figure 19 for the case of a cylinder with longitudinal polarization and free ends. Here the advantage of small σ is clearly seen; the discrepancy between the results of computation by the precise formula (solid curve) and by the approximate formula (dotted curve) is extremely small and for σ = 0.05 is only 0.46 db. Finally, Figure 20 shows a comparison with the case of a cylinder with tangential polarization. Here the error in calculation by the approximate formula for σ = 0.05 is 1.16 db. Thus, it is always possible in practice to calculate the static sensitivity of an acoustic receiver by the approximate formulas.

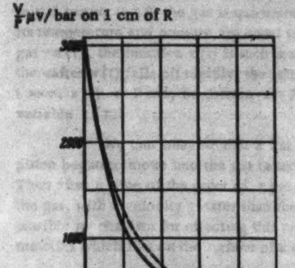

Figure 20. Calculation of the static sensitivity of a cylinder with tangential polarization (the ends are shielded from pressure).

Let us note that for cylindrical receivers with tangential polarization the limit of the sensitivity when σ is decreased is determined in practice by the conditions imposed by the piezoelement strength and by the necessity of obtaining an electrical impedance which is not too high.

Summarizing, it may be said that piezoelectric acoustic receivers in the form of thin shells of barium titanate ceramic with surface-attached electrodes permit us to obtain good directional characteristics with high sensitivity and an internal electrical impedance which is not too great. It should be said that the above statement applies not only to piezoelements in the form of closed shells, but also to dome-shaped and even flat shells; the latter may be utilized in case a high axial concentration coefficient is required.

In conclusion the author would like to take this opportunity to express his appreciation to N. N. Andreev and V. S. Grigor'ev for their consistent attention and help in this work.

LITERATURE CITED

[1] N. N. Andreev, "Piezoelectrical Crystals and Their Application," Electricity, 2, 5-13 (1947).

[2] R. A. Landevin, "The Electro-Acoustic Sensitivity of Cylindrical Ceramic," J. Acoust. Soc. Am., 26, 3, 421-427 (1954).

Received July 29, 1955

Acoustical Institute
Academy of Sciences of the USSR
Moscow

MOTION OF A GAS DUE TO A PRESSURE OF SHORT DURATION (SHOCK)

Ia. B. Zel'dovich

The article examines the propagation of a plane shock wave and the motion behind the shock front which is created in a gas when it is acted upon by a strong brief external pressure.

The article finds the laws for the attenuation of the wave and for the distribution of pressure, density and velocity which must take effect after the action of the pressure has ceased — in the limit they take effect asymptotically over a period which is large in comparison to the time for which the external pressure acts.

The solution which is found is an autosimulating one and is characterized by a power-function relationship of the wave amplitude to time and to the path traversed by the wave; however, in contrast to the analogous problem of an explosion, the exponent is not found by dimensional concepts, but by integrating ordinary differential equations.

A unique case is examined from the point of view of an asymptotic solution by means of the equations of conservation of impulse and energy; the problem concerning the conditions required for the practical achievement of such motion is also discussed.

---

1. Posing The Problem; The General Nature Of The Motion

Let us examine a half-space (the region $x > 0$), occupied by an ideal monatomic gas. At the initial instant ($t = 0$) the gas is quiescent, its density is everywhere identical ($\rho = \rho_0$ for $x > 0$; $\rho = 0$, $x < 0$), its temperature and pressure are equal to zero. A brief pressure impulse acts on the external surface of this gas — $\pi(t)$; the function $\pi(t)$ is such that $\pi(t) = 0$ for $t < 0$, then $\pi(t)$ attains a maximum value P and thereafter $\pi(t)$ falls off rapidly; the fall-off time is defined by the quantity τ in such a way that for $t \gg \tau$, $\pi(t) \ll P$ may be written $\pi = Pf(t/\tau)$, where $\underline{f}$ is a dimensionless function of the dimensionless variable t/τ.

We can imagine that a flat piston was located at the origin, and that at the initial moment the piston began to move into the gas in such a way that $\pi(t)$ was the gas pressure on the surface of the piston. Then after a time of the order of τ the piston was taken away, or began to move to the left, away from the gas, with a velocity greater than the expansion velocity of the gas which it had compressed. Another possible mechanism for effecting this type of motion is the explosion of a thin plane layer of explosive material which lies on the surface of a cold gas.

The characteristic feature of the definition of the problem is the free space in the left half-space for $x < 0$ at the initial moment. The gas particles which are located on the surface at the initial moment (for $x = 0$), fly out into the free space after the external pressure of the piston has ceased.

The problem is to find the motion of the gas, the distribution of density, pressure and other quantities with respect to an elapsed time which is large in comparison to the effective period τ for which the pressure acts.

Thus, an asymptotic solution is sought for the unidimensional equations of the gas dynamics for a specified pressure curve $\pi(t)$ which is characterized by a sufficiently rapid fall-off of pressure. The same problem may be formulated somewhat differently thus: while retaining the form of the dimensionless function $f(t/\tau)$, we shall force the pressure duration τ toward zero and the maximum pressure toward infinity, and then we shall seek the limiting form of the solution which is obtained for these conditions — the distribution of velocity, pressure and other quantities — after a finite time $\underline{t}$ at a finite distance $\underline{x}$.

It is evident that the solution of the problem must also provide the answer to the problem of specifically how and according to what law P must rise when τ decreases, in order to guarantee the specified finite pressure in the gas and the end of a finite time $\underline{t}$. If, for example, the combination $p^k \tau^1$ is included in the answer, then $\underline{p}$ must rise as $\tau^{-\frac{1}{k}}$ as τ decreases.

The general nature of the unknown motion is shown in Figure 1. A shock wave is propagated in an undisturbed cold gas; a limiting compression which depends upon the adiabatic index of the gas is attained at the shock front of this wave; the speed of propagation of the shock wave and the velocity of the mass in the shock front are related in an elementary way to the pressure of the shock wave. Behind the front, the pressure, density and velocity decrease.[*]

The amplitude of the shock wave decreases with the passage of time. The solution of the problem must provide the answer to the peculiar problem of finding the maximum possible rate at which the amplitude decreases for a plane shock wave with a constant initial density, propagated in an ideal gas: the solution being sought is related to the problem of an instantaneous pressure impulse (τ goes to zero); it is evident that any extended application of pressure and any delay in the fall of the pressure upon the piston can only diminish the rate at which the pressure of the shock wave falls off.

The nature of the solution does not depend upon the specific form of the law for the fall-off of the pressure upon the piston $\pi(t)$, which is defined by the nondimensional function $f(t/\tau)$, if $\underline{f}$ falls off sufficiently rapidly[**] for large values of t/τ.

In particular, it is immaterial whether $\underline{f}$ rises discontinuously or smoothly for $t < \tau$; even when the growth of pressure in the gas is smooth, a shock wave is formed with a pressure amplitude of the order of the maximum pressure exerted by the piston P. The velocity of the shock wave under these conditions is of the order of $D \approx \sqrt{P/\rho_0}$, so that some small mass of gas of the order of $D\rho_0\tau \approx \tau\sqrt{P\rho_0}$ was subjected to a shock compression with an amplitude P. Expanding out into free space after the pressure upon the piston has become zero, this gas develops an expansion velocity of the order of $u \approx \sqrt{P/\rho_0}$, and at the instant $\underline{t}$ is located at the point $x = u_0 t \approx t\sqrt{P/\rho_0}$. Thus, for example, if $f(t/\tau) = 1$ for $0 < t/\tau < 1$ and $f = 0$ for $t/\tau > 1$, we can easily find that u_0 for a diatomic gas is the difference between the velocity of expansion, which is equal to 5c ($\underline{c}$ is the sonic velocity of the compressed gas) and the velocity of the mass in the wave, $\underline{u}$. In the limit, when P increases without limit, the absolute value of u_0 undergoes an unlimited increase, and thus in the solution being sought the distribution of ρ, $\underline{p}$, $\underline{u}$ shown in Figure 1 should be imagined as extending limitlessly to the left to $x = -\infty$.

2. Autosimulating Solution and Laws Of the Conservation of Energy and Impulse

The postulate concerning the independence of the unknown solution from the specific form of $\pi(t)$ leads us to the idea that the solution (for example, the instantaneous pressure distribution $p(x, t)$ when

---

[*] In order to compare waves of various amplitudes in gases with different densities, it is convenient to define the speed with which the pressure falls off by a nondimensional quantity (by, the logarithmic derivative $\frac{d \ln p}{d \ln t} = \frac{t}{p}\frac{dp}{dt}$, or by its equivalent — the value of the exponent in the formula $p \approx t^{-g}$.)..

[**] We can specifically indicate what is meant by "sufficiently rapidly" only after the solution has been found.

$t >> \tau$) should be sought in autosimulating form

$$p(x, t) = AP^{k}\tau^{l}\rho_0^{h}t^{-g}\tilde{p}(x/X),$$

where $X = X(t)$ is the coordinate of the shock wave (Figure 1).

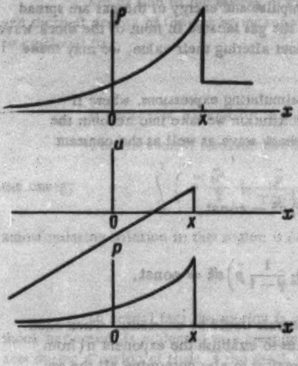

Figure 1.

For the sake of being precise, let us agree that $\tilde{p}(1) = 1$ so that the pressure at the shock front is $p(X, t) = P^{k}\tau^{l}\rho_0^{h}t^{-g}$.

The form of the function $X(t)$ can be found in an elementary manner:

$$\frac{dX}{dt} = D \approx \sqrt{p(x, t)/\rho_0}$$

so that $X \approx t^{1-g/2}$; from the law describing the decreasing amplitude of the wave as a function of time, $p \approx t^{-g}$, it is easy to derive the law describing the amplitude decrease as a function of the path traversed by the wave:

$$p(x, t) \approx X^{-\frac{2g}{2-g}};$$

$$p(x, X) \approx BP^{k'}\tau^{l'}\rho_0^{h'}X^{-n}; \quad n = \frac{2g}{2-g}.$$

The basic result accomplished by this paper consists of the evaluation of the exponents $\underline{k}$, $\underline{l}$, $\underline{h}$, $\underline{g}$ or $\underline{k'}$, $\underline{l'}$, $\underline{h'}$, $\underline{n}$, as well as the definition of the dimensionless function $\underline{\tilde{p}}$ and of the analogous functions $\underline{\tilde{u}}$, $\underline{\tilde{\rho}}$ which define the distribution of speed, density and other quantities.

It is easy to verify that dimensional concepts establish only three relationships between the four exponents (since all quantities are expressed in a system of measurement using three basic units: mass, length and time).

The missing relationship can be obtained by examining those ordinary differential equations which can be obtained (from the partial differential equations of gas-dynamics) for the dimensionless functions $\tilde{p}$, $\tilde{\rho}$, $\tilde{u}$ of one variable $\xi = x/X$.

In a series of problems, for example in the well-known problem of a point explosion solved by L. I. Sedov [1], the exponents can be found in an elementary way from the laws of conservation of mechanics (from the conservation of energy in Sedov's example).

How is the problem being examined different, and may we not, in the case of a shock, find the exponents from elementary concepts ?

After the pressure upon the piston has gone to zero no external forces act upon the gas, because the pressure is equal to zero both for $x \longrightarrow -\infty$ (in the limit at the boundary of the expansion), and for $x \longrightarrow \infty$ (it is sufficient if $x > X$) in a cold gas. Therefore, the motion conserves the full amount of gas momentum $\int_{-\infty}^{\infty} \rho u \, dx$ which is equal to the impulse of the piston pressure $T = \int_0^{\infty} \pi \, dt = P\tau \int_0^{\infty} f(t/\tau)\, dt/\tau = aP\tau$ (all quantities are referred to a unit cross-sectional area of the YZ plane, i.e., to a unit area of the piston). It is evident that the full energy of the entire gas, which is equal to $\int_{-\infty}^{\infty} \left(\rho \frac{u^2}{2} + \frac{1}{\gamma-1} p\right) dx$, is also conserved ($\gamma$ is the adiabatic index); the energy must be equal to the work done by the piston during the period that the pressure acts.

The velocity of the piston is fully defined by specifying the pressure upon the piston, however finding u(t) according to the specified function $\pi(t)$ requires the solution of the equations of gas-dynamics. In any case, it is easy to establish from dimensional concepts that $E = bP^{3/2}\tau\rho_0^{-1/2}$, where b is the dimensionless number which depends in some way upon the dimensionless function $f(t/\tau)$.

From a strictly theoretical viewpoint, the integrals of impulse and energy of the gas are spread over the entire space occupied by the gas. In actual fact, however, the gas located in front of the shock wave is immobile and cold, and produces no yield in these integrals; without altering their value, we may make X the upper limit of integration.

Let us substitute $p(x,t) = \Pi\tilde{p}(x/X)$ into the integral autosimulating expressions, where $\Pi = BP^{k'}\tau^{l'}\rho_0^{m'}X^{-n}$, $u = \sqrt{\Pi/\rho_0}\ \tilde{u}(x/X)$, $\rho = \rho_0(x/X)$; in making this substitution we take into account the relation between the pressure and velocity in the shock front of the shock wave as well as the constant value of density in the shock front. We obtain

$$I = \int \rho u\, dx = \sqrt{\Pi\rho_0}\, X \int_{-\infty}^{1} \tilde{\rho}(\xi)\tilde{u}(\xi)\, d\xi = \text{const},$$

$$E = \int \left(\rho\frac{u^2}{2} + \frac{1}{\gamma-1}p\right)dx = \Pi X \int_{-\infty}^{1}\left(\tilde{\rho}\frac{\tilde{u}^2}{2} + \frac{1}{\gamma-1}\tilde{p}\right)d\xi = \text{const}.$$

It would be natural to assume that the dimensionless integrals would be constants. Then each of the two conditions written above, taken separately, would permit us to establish the exponent n (from the impulse equation n = 2, from the energy equation n = 1), and thereafter to also determine all the remaining exponents in an elementary way.

However, taken together, these two equations contradict one another! The impression is created that no autosimulating solution may simultaneously satisfy both conditions which necessarily follow from the equations of mechanics, and therefore, the problem has no autosimulating solution at all.

Below we shall specifically find an autosimulating solution of the power-function type. It will be shown that the true exponent is always confined within the limits $1 < n < 2$; for a diatomic gas $n = 1.333 \approx \frac{4}{3}$.

It is already practical here, even before we obtain the specific solution, to be clear concerning the manner in which this solution agrees with the laws of conservation. It is difficult to imagine a reader who would agree to follow algebraic derivations and the integration of differential equations while expecting to obtain a solution which satisfied neither the law of conservation of momentum nor the law of conservation of energy!

The full expression for the pressure:

$$p = \left(\frac{\tau\sqrt{P/\rho_0}}{X}\right)^n BP\tilde{p} = BX^{-4/3}\rho_0^{-2/3}\tau^{4/3}P^{5/3}\tilde{p}(x/X)$$

corresponds to the exponent $n \sim \frac{4}{3}$ found by V. B. Adamskii in [3], so that for obtaining a finite (not zero and not ∞) pressure at a finite distance when $\tau \longrightarrow 0$ and $P \longrightarrow \infty$, it is necessary that P grow as $\tau^{-4/5}$.

When P increases according to such a law the impulse of external force caused by the motion (the shock impulse), I, goes toward zero in the limit: $I \approx P\tau \approx \tau^{1/5}$. Therefore, the impulse equation for autosimulating motion is written thus:

$$B'X^{1/3}\int_{\infty}^{1}\tilde{p}(\xi)\tilde{u}(\xi)\, d\xi = 0.$$

This leads to a condition which the dimensionless functions $\tilde{p}$, $\tilde{u}$ must satisfy: $\int_{-\infty} \tilde{p}\ \tilde{u} d\xi = 0$.

Let us turn to the energy equation. According to what has been said the work done by the piston (by the shock) on the gas being examined is (for the relationship between the pressure P and the period of the shock τ which has already been found) proportional to

$$E \approx P^{\text{[illegible]}}\tau \approx (\tau^{-\text{[illegible]}})^{\text{[illegible]}}\tau \approx \tau^{-\text{[illegible]}}.$$

In the limit the work done by the shock is $E \longrightarrow \infty$ for $\tau \longrightarrow 0$.

Let us turn to the energy of the gas which is calculated as the volume-integral of the kinetic and thermal energy of the gas by means of the autosimulating solution. The dimensional multiplier is proportional to

$$\Pi X = P^{\text{[illegible]}}\tau^{\text{[illegible]}}X^{-\text{[illegible]}}.$$

It decreases without limit as the wave is propagated; this is impermissible at first glance.

The paradox is resolved due to the fact that the dimensionless integral in the expression for the energy $\int_{-\infty}^{1}\left(\tilde{\rho}\,\frac{\tilde{u}^2}{2}+\frac{\tilde{p}}{\gamma-1}\right)d\xi$ is divergent in the region of large negative ξ. The autosimulating solution in this region is of asymptotic form:

$$\tilde{u} = k\xi; \qquad \rho = r(-\xi)^{-\text{[illegible]}}.$$

In actual fact the motion is such that a definite mass of gas, located at the surface upon which the shock has acted, is subjected to a pressure different from the autosimulating pressure. For a pressure P which acts during a period of time τ the shock wave traverses a distance $\tau\sqrt{P/\rho_0}$ and compresses a mass of gas m_0 $\tau\sqrt{P\rho_0}$ (on a unit surface).

Only for $t > \tau$ do we have a right to expect that the amplitude of the shock wave will approach the autosimulating solution which we have found. Because of the adiabatic nature of the motion, the entropy of a mass m_0 always remains constant and differs from the value which is obtained by extrapolating the autosimulated entropy distribution to that mass.

The approach of the true solution (for finite P and τ) to the autosimulating solution occurs non-uniformly with respect to time (as the wave is propagated, i.e., as X increases). As X grows, the pressure and all the other quantities in almost the entire mass of gas embraced by motion approach values which correspond to the autosimulating solution. At the same time, the approximation does not occur in a small mass m_0; however, with the passage of time, this mass comprises an ever-diminishing portion of the entire mass embraced by the motion.* In the limit we may neglect this small mass both in the differential equations and in the convergent impulse integral; however in the energy integral, due to the fact that this integral diverges, it is essential to stop the integration in the region to which the autosimulating solution is inapplicable.

The boundary of this region x_2, $\xi_2 = x_2/X \cdot (x_2 < 0;\ \xi_2 < 0)$, can be found from the condition

$$m_0 \approx \tau\sqrt{P\rho_0} \approx \int_{-\infty}^{x_2}\rho\,dx = \rho_0 X\int_{-\infty}^{\xi_2}\tilde{\rho}\,d\xi \approx \rho_0 X(-\xi_2)^{-\text{[illegible]}}.$$

The meaning of the condition is that we have taken the autosimulating solution and found in it the boundary of the region in which the mass m_0 is located (Figure 2).

Such a method must yield a proper order of magnitude and a correct dependency of x_2 and ξ_2 upon the parameters.

---

* With the passage of time the approximation of the true solution to the autosimulating solution proceeds analogously to the manner in which the increase in the number of terms in a Fourier series causes the sum of these terms to approximate a discontinuous function: the known Gibbs phenomenon leads to the fact that near the discontinuity the difference between the series and the function does not go to zero for any number of terms; however, the width of the region in which the series appreciably differs from the function goes to zero with an increase in the number of terms.

We obtain

$$\xi_2 \approx -\left[\frac{X}{\tau\sqrt{P/\rho_0}}\right]^{2/3}, \quad x_2 \approx X^{5/3}(\tau\sqrt{P/\rho_0})^{-2/3}.$$

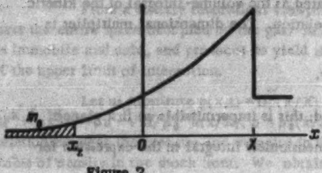

Figure 2.

As X grows, the region in which the autosimulating solution is inapplicable (lined area in the figure) is ever more squeezed over to the left, even further from the main region of the motion. However, due to the fact that the main portion of the kinetic energy is also concentrated at the left in the zone of low density and rapid motion, the presence of the lined area always (even when the growth in X and the decrease in m_0/X is unlimited) remains essential to the evaluation of the energy integral.

We shall take this integral not from $-\infty$, but from x_2 or ξ_2:

$$E = \Pi X \int_{\xi_2}^{1} \left(\tilde{\rho}\frac{\tilde{u}^2}{2} + \frac{1}{\gamma-1}\tilde{p}\right) d\xi.$$

Substituting $\rho \approx (-\xi)^{-5/2}$, $\tilde{u} \approx \xi$, we find that the value of the integral is determined by the lower limit, when $|\xi_2| >> 1$, $\xi_2 < 0$.

$$\int_{\xi_2}^{1} \left(\tilde{\rho}\frac{\tilde{u}^2}{2} + \frac{1}{\gamma-1}\tilde{p}\right) d\xi \to |\xi_2|^{1/2}.$$

Let us express Π and ξ_2 in terms of X; $\Pi \sim X^{4/3}$, $\xi_2 = X^{2/3}$. Let us substitute them into the expression for the energy. We obtain

$$E \sim \Pi X |\xi_2|^{1/2} \sim X^{-4/3} X (X^{2/3})^{1/2} = X^0 = \text{const},$$

which should follow from the law of conservation of energy.

It is also easy to verify that in utilizing the above dependencies of Π and ξ_2 upon P and τ, we obtain $E \sim P^{3/2}\tau$. The impulse integral converges and it is not necessary to examine ξ_2 in it.

Thus, the postulate that the full impulse is equal to zero and that a small region exists which does not obey the autosimulating solution, resolves the paradoxes which arise when the solution is compared with the conservation equations.

3. General Properties of the Solution

The value of the exponent given above, n=1.333, which defines the dependency of the shock wave amplitude Π upon the path X traversed by the wave, $\Pi \sim X^{-4/3}$, results in a maximum rate of attenuation with respect to distance for a plane shock-wave in a diatomic gas.

As is evident from the formula, the amplitude of the wave is 2.5 times smaller when the traversed distance is twice as great.

It is also not difficult to find the dependency of the shock front location and its amplitude upon time; we obtain $X \sim t^{3/5}$ and $\Pi \sim t^{-4/5}$. When the time is doubled, the amplitude of the wave is 1.74 times smaller.

The autosimulating nature of the motion means that the distribution of all the quantities at various instants in time are similar. In particular, such a quantity as the ratio of the mass located between the origin and the shock wave to the entire mass involved in motion is a constant; this quantity in the case of a diatomic gas equals 0.90.

Thus, one tenth of the gas was expelled to the left of the initial location of the gas boundary (to the left of the origin) as a result of the compression and subsequent expansion. We may also find the fraction of the gas which moves to the right, in the direction of the shock. For this purpose, we find ξ_1 such that $U(\xi_1) = 0$. The unknown portion of the gas is given by the formula

$$\beta = \int_{\xi_1}^{1} \tilde{\rho}\, d\xi = 0.78.$$

It is not difficult to compose formulas for the impulse and energy of this fraction of the gas:

$$I_1 = \rho_0 X \sqrt{\Pi} \int_{\xi_1}^{1} \tilde{\rho}\tilde{u}\, d\xi, \quad E_1 = \Pi X \int_{\xi_1}^{1} \left(\tilde{\rho}\frac{\tilde{u}^2}{2} + \frac{\tilde{p}}{\gamma - 1}\right) d\xi.$$

Both expressions under the integral are positive and (in the interval $\xi_1 < \xi < 1$ $\tilde{u} > 0$) are bounded in such a way that both integrals are finite and positive numbers.

Substituting $\Pi \sim X^{-n}$, we find that $I_1 \sim X^{1-n/2}$, and $E_1 \sim X^{1-n}$.

It is not difficult to verify without calculation that with the passage of time Υ_1 must rise and E_1 must fall; thus we have been able to show in advance, before integrating the equations, that for any adiabatic index,

$$1 - \frac{n}{2} > 0, \quad 1 - n < 0, \quad 1 < n < 2.$$

Let us note that for this case the point $\xi = \xi_1$, i.e., the quiescent point at which the particle velocity of the gas is equal to zero, moves from left to right; $x_1 = \xi_1 X$ grows.

Since the gas at this point is quiescent, we may say that this point also moves from left to right relative to the gas.

Let us examine the volume of gas for which we have written out the expressions for impulse and energy — the volume enclosed between the quiescent point and the shock wave: $x_1 < x < X$.

A cold undisturbed gas enters this volume from the right through the surface of the shock wave at a pressure equal to zero. It is evident that this gas will introduce neither impulse nor energy into the volume which we are examining. The gas leaves this volume through the surface $x = x_1$; the gas has a finite pressure and temperature and a velocity equal to zero.

Because the quiescent point was selected to be the second boundary of the volume being examined, the momentum (impulse) of the gas leaving the volume is equal to zero.

The momentum of the gas located in the volume grows, since a pressure different from zero acts on the surface x_1:

$$\frac{dI_1}{dt} = p_1 > 0,$$

whence $1 - \frac{n}{2} > 0$.

The variation of the energy contained in the volume under examination is governed by the fact that the work done by the pressure-forces, pu dt upon this surface is equal to zero ($u = 0$); when the point x_1 moves to the right relative to the gas, the gas emerges from the volume with a thermal energy different from zero (its kinetic energy equals zero since $u = 0$). Finally

$$\frac{dE_1}{dt} = -\frac{1}{\gamma - 1}\frac{p_1}{\rho_1}\rho_1\frac{dx_1}{dt} = -\frac{1}{\gamma - 1}p_1\xi_1\frac{dX}{dt} =$$

$$= \frac{d\,(aX^{1-n})}{dt} = (1 - n)\frac{E_1}{X}\frac{dX}{dt};$$

Whence it follows that $n > 1$

The overall picture of the motion is such that the energy contained in a specified fraction of th mass (for example in the region $x_1 < x < X$ or $0 < x < X$) decreases continuously; an irreversible flow of energy into the zone of expanding, low-density gas takes place.

The shorter the shock duration, the greater the decrease in the energy E_1 in comparison to the initial work done by the shock piston. It is not surprising that in the limit an infinite piston energy is required for a shock duration of $\tau \longrightarrow 0$.

The impulse of the entire gas equals zero or, more precisely, is equal to the small initial impulse of the shock in the true solution and not in the autosimulating solution. The impulse of a definite portion of the gas, for example of that portion I_1 which moves to the right, increases without limit according to the extent of the motion. The impulse of that portion of the gas is very large in comparison to the initial impulse of the shock and is balanced by the impulse ("reaction") of the gas expanding to the left. Let us notice that as far as the order of magnitude is concerned, the following formula holds: $I_1 = \sqrt{M_1 E_1}$ ("the Staniukovich formula"). However, as a consequence of the substantially nonuniform distribution of velocities in the expanding gas, such a formula cannot be applied in the zone of expansion which encloses the energy $E_{exp} = E_{piston} - E_1$, and whose mass equals $M_{exp} = M - M_1 = \rho_0 X - M$ in this zone

$$I_{exp} / \sqrt{M_{exp} E_{exp}} \longrightarrow 0.$$

In order to complete the solution of the problem of the motion of a gas due to a short-duration shock it is not only necessary to determine the exponents and the dimensionless functions (which is accomplished by integrating ordinary differential equations). It is necessary, in addition, to evaluate the numerical multipliers A and B in the formulas.

The dimensionless numbers A, B depend upon the adiabatic index and upon the specific form of the shock pressure-curve, $f(t/\tau)$. It was not possible for us to obtain closed expressions for them however.

At the present time we see only one path toward the complete solution of the problem: for $t \approx \tau$, (for example, up to $t = 5\tau$ or 10τ) the partial differential equations are explicitly solvable when a specific law is given for the pressure on the piston; continuing the solution for $t \gg \tau$ in the asymptotic (autosimulating) form, we find the constants A and B from the condition of coincidence for the two solutions at the boundary point to which the calculation is carried.

The law of pressure fall-off, $f(t/\tau)$, is limited by the evident condition that the pressure upon the piston must fall off more rapidly than the amplitude of the pressure in the autosimulating solution itself, i.e., more rapidly (with a negative exponent which has a greater modulus) than $t^{-4/5}$.

4. Explosion At The Separation Boundary Of Gases Possessing Different Densities

The shock delivered to a gas by a piston under the condition of subsequent expansion into a vacuum is the limiting idealization of this problem. A more realistic statement of the problem is the examination of a thin plane layer of explosive material (EM), separating a gas with an initial density ρ_0 (in which motion is examined as well) located to the right of the origin ($x > 0$), and a gas with an initial density R ($R \ll \rho_0$). We shall define the mass of the EM distributed over a unit surface by $\underline{m}$, and the calorie-content of the EM (the specific energy in ergs/g) by Q. Following M. A. Laurent'ev's method, we subdivide the initial process into stages.

At the instant of the explosion chemical energy is transformed into thermal energy and energy of elasticity; then the thermal and elastic energy is transformed into kinetic energy by the expansion of the explosion products (EP). Only in the subsequent stage are the EP braked, releasing some of their energy to the gas.

The velocity of the EP is of the order of $w \sim \sqrt{Q}$. Their total energy is mQ, their impulse is $m\sqrt{Q}$. In a gas with a density ρ_0 the EP create a shock wave with a pressure of the order of $P = \rho_0 w^2 = \rho_0 Q$. From the condition that during the time that the pressure P is acting the EP must release their energy and impulse to the gas, we find the duration of pressure action

$$\tau = \frac{m\sqrt{Q}}{\rho_0 Q} = \frac{m}{\rho_0 \sqrt{Q}};$$

During that time the shock wave will traverse a path of the order of m/ρ_0 in the gas and the mass of the gas brought into motion will be of the order of m. As we should have expected, the postulated autosimulating solution is applicable to the problem concerning the action of the EM only after the mass of gas brought into motion, $M = \rho_0 X$, exceeds the mass of the EM.

Omitting the numerical multipliers, we substitute the values which we have found for the magnitude and duration of the pressure into the autosimulating expression for the amplitude of the shock wave. We obtain

$$\Pi = \rho_0^{-1/3} Q X^{-4/3} m^{4/3} = Q\rho_0 \left(\frac{m}{X\rho_0}\right)^{4/3} = Q\rho_0 \left(\frac{m}{M}\right)^{4/3}$$

for $M \gg m$.

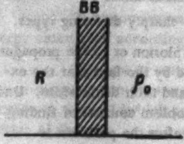

Figure 3.

When gas is present at the left, even though it is lower in density ($R \ll \rho_0$), instead of a vacuum, the applicability of the solution is also limited by the late stages of the process.

For the late stages, when the mass of the EM is small in comparison to the mass of the gases brought into motion from both sides, all the prerequisites exist for utilizing the theory of a powerful explosion (developed by L. I. Sedov) for solving the problem. It is not difficult to generalize the theory of a unidimensional plane explosion to include the case of an explosion at the boundary of two gases with different densities.

In each half-space we take the Sedov solution which satisfies the condition that the velocity must equal zero at the origin and make the two solutions obey the condition that the pressure must be equal. Since the law for pressure fall-off with time in a powerful explosion does not depend upon gas density (in the plane case this law is $p \sim t^{-2/3}$), then such an interlacing of the two solutions is possible. When the pressures are equal, the paths traversed by the two shock waves, Y to the left, and X to the right, are in a ratio which is the inverse of the ratio of the square roots of the gas densities:

$$\frac{Y}{X} \sim \sqrt{\rho_0/R}.$$

By normalizing to the entire energy of the explosion, we find the order of magnitude of the pressure amplitude Π_S in the shock wave (the index "S" next to the letter Π indicates: "the pressure calculated according to the Sedov theory") at the instant when the wave has traversed the path X in the gas being examined:

$$mQ = (Y + X)\,\Pi_s; \quad \Pi_s = \frac{mQ}{X\left(1 + \sqrt{\rho_0/R}\right)} = \frac{mQ}{X}\sqrt{\frac{R}{\rho_0}} =$$

$$= Q\rho_0\left(\frac{m}{\rho_0 X}\right)\sqrt{\frac{R}{\rho_0}} = Q\rho_0\left(\frac{m}{M}\right)\sqrt{\frac{R}{\rho_0}}.$$

Thus in the limit, which occurs for large values of time and large values of X and M, the presence of a gas at the left (with a small density, $R \ll \rho_0$) causes the pressure to fall off more slowly (Π_S falls as M^{-1} or X^{-1}), than in the case of expansion into a vacuum which we examined earlier, where Π falls as $M^{-4/3}$ or $X^{-4/3}$.

We should expect that, beginning with these values of M and X for which $\Pi = \Pi_S$, a greater value of Π_S will be attained during further motion. Such a criterion will provide the upper limit of applicability for the proposed autosimulating solution, if we use the condition

$$\rho_0 Q\left(\frac{m}{M}\right)^{4/3} = \rho_0 Q\left(\frac{m}{M}\right)\sqrt{\frac{R}{\rho_0}}; \quad M = m\left(\frac{\rho_0}{R}\right)^{3/2}.$$

Thus the region in which the solution is applicable is finally given by the inequality

$$m < M < m\left(\frac{\rho_0}{R}\right)^{3/2}.$$

For a large value of the ratio ρ_0/R, this region may be sufficiently broad.

If we compare the pressures in our proposed solution and in the theory of a powerful explosion at identical instants in time (and not for equal X's, as was done above), we will obtain the same result.

The dimensionless numerical multipliers in the expression for the pressure and for the boundaries of applicability cannot be obtained without extremely difficult calculations which require the integration of partial differential equations, and without specific postulates concerning the equations for the state of the EP and the explosion process.

5. Remarks Concerning the Two Types of Autosimulating Solutions

It is well known that autosimulating solutions are separated into two sharply differing types.

The first type, to which, for example, the problems of a powerful explosion or of the propagation of heat in a medium with nonlinear heat-conductivity [4] belong, is distinguished by the fact that the exponents are evaluated from physical conceptions, from the laws of conservation and their dimensions. Under these conditions the exponents prove to be rational numbers. The calculation problem consists of finding the dimensionless functions by integrating ordinary differential equations. Thereafter the problem is completely solved, since the numerical constants are determined by normalizing the solution with respect to the conserved quantity (the total released energy in the examples given).

The second type of problem is typified, for example, by the problem examined by Huderle (cited from [2]) concerning the convergence of a cylindrical shock wave into a line or the convergence of a spherical wave into a point. In this case the very finding of the exponent requires the integration of ordinary differential equations. The exponent is found from the condition that the integral curve may pass through a specially defined point; without this it is not possible to satisfy the boundary conditions.

It would seem that it would be possible to easily determine whether problems belong to one or the other type. Thus in the examples given, the problem concerning a powerful explosion is "closed"; the mass of gas involved in motion is finite and is easily expressed by the radius of the wave. In the problem of the convergence of a shock wave only the vicinity of the origin and a small portion of the gas which is involved in motion are examined; in this case we cannot pose the problem of the motion of the entire gas. It is natural therefore that in the first case we may make use of the equation of conservation of energy, but cannot do so in solving the second problem; in the case where the wave converges, the energy of the autosimulating region continuously diminishes and the exponent is found from other concepts.

The problem examined in this paper is of methodological interest, because from the manner in which it is posed it would seem to belong to the first type, since at every moment a quantity of material governed by the position of the wave is involved in motion (in the very same way as it is in the problem of a powerful explosion). Therefore,the impossibility of determining the exponent by means of the law of the conservation of energy proved to be a non-trivial factor. As we have explained in detail above, the energy integral diverges in our case, and the finite value of energy is determined by a small region which bears the imprint of the initial conditions (the autosimulating solution is inapplicable to this small region).

In the example analyzed we can see the necessity of great care and thoroughness during the derivation of the autosimulating solution.

In conclusion I take this opportunity to express my appreciation to V. B. Adamskii who performed the calculations and to N. A. Dmitriev for his participation in discussing the paper.

CONCLUSIONS

The problem of the motion of a gas bounded by a vacuum is examined when the motion is produced by a short duration pressure impulse.

An autosimulating solution is found for which the pressure Π at the shock front of the shock wave propagated in the gas decreases as a power function of the distance traversed, X: $\Pi \sim X^{-n}$, where $1 < n < 2$. In a general way, for any adiabatic index of the gas, it was proven that $1 < n < 2$; the numerical value for $\gamma = \frac{7}{5}$ was $n = 1.333$. The law which we found results in the maximum possible attenuation rate for a plane shock wave under any and all conditions.

The dependency of shock front pressure at a specified distance upon the duration τ and the magnitude P of the shock pressure was found; the pressure at the shock front depends upon the product $P\tau^{-k}$ where $1 < k < \frac{3}{2}$ where k is expressed in terms of n.

In the limit, for small τ, the pressure impulse of the shock goes to zero and the work done by the shock is infinite.

The momentum of the gas involved in autosimulating motion is identically equal to zero. The energy calculated according to the autosimulating solution is expressed by a diverging integral.

The law of conservation of energy cannot be utilized for evaluating the exponent of autosimulation; conservation of energy is guaranteed due to the deviation of the true solution from the autosimulating solution in a small (which goes to zero in a manner determined by the degree to which the process develops) portion of the gas.

The paper has examined the problem of specifying the region of applicability for the solution describing the propagation of a shock wave from an explosion produced upon a plane surface separating two gases of different density.

LITERATURE CITED

[1] L. I. Sedov, Methods of the Theory of Similarity and Dimensional Analysis, GTTI (State Tech. Theor. Press) Moscow, 1954.

[2] R. Courant and Friedrichs, Supersonic Flow and Shock Waves, Foreign Lit. Press., Moscow, 1950.

[3] B. V. Adamskii, "Integration of a System of Autosimulating Equations for the Problem of a Short Duration Shock in a Cold Gas," Acoust. J. 2, No. 1, 3-9 (1956).*

[4] Ia. B. Zel'dovich, A. S. Kompaneets, Selected Works Devoted to the Seventieth Birthday of Academician A. F. Ioffe, Acad. Sci. USSR Press, Moscow-Leningrad, 1950.

Received June 11, 1955

Institute of Chemical Physics
Academy of Sciences, USSR
Moscow

---

*Soviet Physics - Acoustics, p. 1.

SOUND VELOCITIES IN INDIVIDUAL LIQUIDS AND IN LIQUID MIXTURES

B: B: Kudriavtsev

The paper develops a thermodynamic calculation of the velocity of sound in pure liquids and in binary liquid mixtures. The theoretical calculations are compared with experimental data. The calculated values for the velocity of sound agree satisfactorily with those observed experimentally both in individual liquids and in binary mixtures. The theory which is developed permits the calculation of the velocity of sound in anomalous mixtures (aqueous solutions), and the values agree satisfactorily with experimental results. Equations are obtained for calculating the velocity of sound in triple mixtures as well as in more complex mixtures.

Notwithstanding the many papers devoted to the calculation of the velocity of sound in liquids [1 – 8], this problem cannot be considered solved.

We may separate the attempts to calculate the velocity of sound into two groups. The first group includes papers in which the velocity of sound is calculated on the basis of a specific model of the liquid, allowing for the size of the molecules and their interaction [3,4]. In papers which belong to the second group the velocity of sound is calculated on the basis of the thermodynamic relationships which exist between various physical characteristics of the liquid [2, 6, 9].* Since only a few liquids possess a known structure and since that structure is undoubtedly dependent upon temperature in a complex way, the practical application of the results of analyses which belong to the first group is extremely limited [10]. The thermodynamic theory in this case offers great possibilities, although here also it is not possible to avoid reliance upon several postulates which have not yet been fully justified theoretically. In this paper an attempt is made to analyze the reasoning made during the calculation of the velocity of sound on the basis of thermodynamic relationships, to discuss the validity of the assumptions which are inescapable in the process of obtaining a final expression for the velocity of sound, and to compare the theoretically calculated quantities with the results of the experimental measurement of the velocity of sound.

Thermodynamically, we can produce full theoretical proof that

$$\left[\frac{\partial U}{\partial v}\right]_T = -P + T\left[\frac{\partial P}{\partial T}\right]_v. \qquad (1)$$

Here U is the internal energy, v is the volume, P is the pressure and T is the temperature.

Differentiating Equation (1) with respect to v for T = const., and utilizing the expression:

$$c^2 = -v^2\gamma\left[\frac{\partial P}{\partial v}\right]_T, \qquad (2)$$

for evaluating the velocity of sound, c, in which $\gamma = c_p/c_v$ is the ratio of the entropy of the substance at a constant pressure, c_p, to the entropy at a constant volume, c_v, we obtain

---

* Sometimes the relationship between the velocity of sound c, the density ρ and the pressure p is used for this purpose: $c^2 = dp/d\rho$. It is not always possible to make the indicated separation strictly, since the theoretical analysis may use a combination of the indicated methods (see [24]).

$$v^2\gamma\left[\frac{\partial^2 U}{\partial v^2}\right]_T = c^2 - T\left[\frac{\partial c^2}{\partial T}\right]_v. \tag{3}$$

In order to solve this equation it is first necessary to know the dependency of the internal energy of the liquid, U, upon the volume v. The internal energy of the liquid, as can that of any substance, can be represented by the sum of two terms:

$$U = \Phi + E;$$

of which Φ is the potential energy and E is the kinetic energy.

We must further assume that the kinetic energy E of the liquid depends only upon temperature and that therefore $\left[\frac{\partial E}{\partial v}\right]_T = 0$. In this case Equation (3) will become:

$$\gamma v^2\left[\frac{\partial^2 \Phi}{\partial v^2}\right]_T = c^2 - T\left[\frac{\partial c^2}{\partial T}\right]_v. \tag{4}$$

In order to integrate this equation, we must know the relationship between the potential energy of the liquid Φ and its volume v. As a rule we attempt to find this relationship by basing ourselves upon the law of paired interaction between the molecules of the liquid. According to modern concepts the potential energy of the interaction between two molecules may be defined by the expression

$$\varphi = R(r)\,e^{-r/\rho} - Br^{-\mu}, \tag{5}$$

in which r is the distance between the molecules under examination, B, μ and ρ are quantities which are constant for the specified molecules, and R(r) is a polynomial containing positive and negative powers of the intermolecular distance r. The utilization of Equation (5) is so difficult that in practice it is always replaced by one of the approximate expressions given below:

$$\varphi = \frac{A}{r^{\nu}} - \frac{B}{r^{\mu}}, \tag{6}$$

where A, B, ν, μ are constants;

$$\varphi = \varphi_0 + b(r - r_0)^2 + d(r - r_0)^3 + \cdots \tag{7}$$

where b, d, ··· are constants, r_0 is the equilibrium distance between molecules, and $\varphi_0 = \varphi$ for $r = r_0$;

$$\varphi = C + D\{e^{-2a(r-r_0)} - 2e^{-a(r-r_0)}\}, \tag{8}$$

where C, D, a are constants, r_0 is the equilibrium distance between molecules.

We should turn our attention to two facts,first, the expressions written above for φ are valid only at absolute zero, and second, the transition from the potential energy of interaction between two isolated molecules to the potential energy of the liquid as a whole is not feasible without postulating a fully-defined structure for the liquid. In practice the expressions written above are directly applied (with more or less of a basis for doing so) to the calculation of the potential energy of the liquid [1, 11]. We believe that the success of such attempts is explained simply by the fact that all of the expressions written above for the computation of φ yield the minimum value of φ for some specified value of $r = r_0$, and by the fact that these expressions go to zero for $r = \infty$. It is completely evident that the internal energy of the liquid taken as a whole must also possess the same kind of properties.

As a matter of fact, the thermodynamic equilibrium condition

$$\left[\frac{\partial \Phi}{\partial v}\right] = 0 \text{ for } v = v_0,$$

where v_0 is the equilibrium volume, defines the presence of a minimum in the curve which depicts the dependency of the potential energy upon the volume; the equality of the potential energy to zero when the volume is increased to infinity follows from the very definition of potential energy. Since every liquid may be in equilibrium with a saturated vapor at all temperatures, from the temperature of fusion right up to the critical temperature, then the equation for the dependency of potential energy upon volume may be used for various temperatures, taking into consideration, of course, the fact that the constants contained in the equation may have different values at different temperatures. In such a case, the indicated expressions become interpolating formulas and the preference for one of them over the others is decided only by how well the test material can be depicted by it and how convenient it is for calculation. As practice shows, satisfactory results may be obtained with a simple two-term equation

$$\Phi = \frac{A_1}{v^n} - \frac{B_1}{v^m}, \tag{9}$$

which is derived from Equation (6). In Equation (9), the first term is governed by the repelling forces, and the second term is governed by the attracting forces. According to modern concepts, the exponent m in the term governed by attraction must be equal to two. The situation involving the exponent n in the term governed by the mutual repulsion of the molecules is in a much worse state.

In Equation (6) fully satisfactory results are obtained for a ν which is equal to 8, 10, 12, 14 (12), and therefore for n = $\frac{8}{3}, \frac{10}{3}, \frac{12}{3}, \frac{14}{3}$. Such arbitrariness makes the utilization of Equation (9) somewhat difficult. The quantities A_1 and B_1 in Equation (9) are functions of temperature, but at constant temperature they are constants which are characteristic for the specified liquid. Utilizing Equation (9), we may write

$$\gamma v^2 \left[\frac{\partial^2\Phi}{\partial v^2}\right]_T = nm\gamma\Phi_0, \tag{10}$$

where Φ_0 is the potential energy of the liquid occupying an equilibrium volume at the specified temperature.

Thus, for determining the velocity of sound, we obtain

$$nm\gamma\Phi_0 = c^2 - T\left[\frac{\partial c^2}{\partial T}\right]_v. \tag{11}$$

The integration of this equation presents no difficulties* and leads to the expression

$$c^2 = nm\gamma\Phi_0 + fT + g(v), \tag{12}$$

where g(v) is an arbitrary function of volume, f is a constant.

Assuming that the velocity of sound at critical temperature or above critical temperature is the same as the velocity of sound in the gas, and assuming that the latter velocity does not depend upon pressure (volume), we find that

$$g(v) = 0 \text{ и } f = \gamma\frac{R}{M},$$

where R is the universal gas constant and M is the molecular weight.

The final calculating equation is of the form:

$$c^2 = nm\gamma\Phi_0 + \frac{\gamma RT}{M}, \tag{13}$$

therefore, in order to calculate the velocity of sound it is necessary to know the values of n, m, γ and Φ_0. We discussed the magnitudes of n and m above, γ is known for many liquids; we must still discuss the problem of what we shall set the potential energy of the liquid, Φ_0, equal to. At first glance it is natural to set the potential energy Φ_0 of the liquid equal to the latent heat-of-vaporization λ. In this case, however, the relative agreement (deviations are less than 20%) between the calculated and experimentally observed values for the velocity of sound may only be achieved by assuming, as it is assumed in the theory of Van der Vaals, that m = 1, i.e., $\mu = 3$ (see Table 1). Such a postulate, however, does not agree with modern concepts of the nature of molecular interaction.

In addition, even when the above postulates are made, the discrepancy between theory and experiment is still 16-20% on the average. The reason for this can easily be discovered. Let us actually assume, for example, that the liquid consists of dimeric molecules which dissociate during evaporation. In such a case the experimentally determined heat-of-vaporization will include the heat of dimerization. At the same time the presence of dimers will have practically no effect upon the velocity of sound in the liquid. During the calculation of the velocity of sound it is more correct to utilize the relationship which exists between the potential energy of the liquid and its surface tension*. As must follow from elementary theory [13]:

---

* During integration, it is assumed that n, m and γ are constant.

$$\Phi_0 = 2\sigma v_m^{2/3} N^{1/3}, \tag{14}$$

where σ is the coefficient of surface tension, v_m is the molecular volume, and N is Avogadro's number.

Having substituted this value of Φ_0 into Equation (13), we find that

$$c^2 = (2mn\gamma N^{1/3}) \frac{\sigma}{M^{1/3} \rho^{2/3}} + \gamma \frac{RT}{M}. \tag{15}$$

In order to provide the possibility of conducting an oriented check of Equation (15), which it is desirable to perform on the greatest possible amount of numerical data, we assumed that for all liquids, $\gamma = 1.4$, $n = 4$ ($\nu = 12$), $m = 2$ ($\mu = 6$), and on the basis of data for the surface tension and densities of the liquids (this data can be obtained from tables in [14]) the velocity of sound in 50 different liquids was calculated. The results obtained are graphically depicted in Figure 1 in which the experimental values for the velocity of sound ($c_{observed}$) are plotted along the axis of abscissas and the values calculated by means of Equation (15) are plotted along the axis of ordinates; the individual points define values of velocity calculated according to Equation (15). Examining this diagram, we may be sure that the vast majority of the calculated values is distributed in a comparatively narrow band which encompasses a ± 10% deviation from a central line. At the same time, the slope of this line is not the same as that required by the construction (45 degrees). Since at room temperature (the calculation was performed at 20 degrees) there is no basis for using a value of γ greater than 1.4, the value of n should evidently be increased. Therefore in all subsequent calculations it was assumed that $n = \frac{14}{3}$ ($\nu = 14$). More accurate results are obtained if we utilize values found in the tables. Figures 2 and 3 compare the experimentally obtained values for the velocity of sound with the calculated results obtained from Equation (15) in the case when data from the tables in [14] is used for the values of density, surface tension and entropy ratio γ. In these calculations the maximum deviation is only 5%. It is necessary to note that the theory does not always agree so well with the experiment. For chlorobenzene (Figure 4) for example, the discrepancy between the calculated and observed values for the velocity of sound attains 12-15%.

Sometimes, in comparing theoretical calculations with experimental results, not only the absolute values of the sound velocities are compared, but also the temperature coefficients of the sound velocities [4]. The results of such a comparison, applied to Equation (15), are given in Table 2.

TABLE 1

Substance	t°	$c_{calc.}$ (m/sec)	c_{expt} (m/sec)	$\frac{c_{expt} - c_{calc}}{c_{expt}}$ (%)
Benzene	10	1140	1370	+20
Carbon tetrachloride	0	800	1010	+20
Heptane	0	1050	1230	+18
Chloroform	0	920	1070	+14
Octane	125	836	750	−10

---

* It would be more correct to speak of the surface energy; however, this would introduce only insignificant variations into the numerical results.

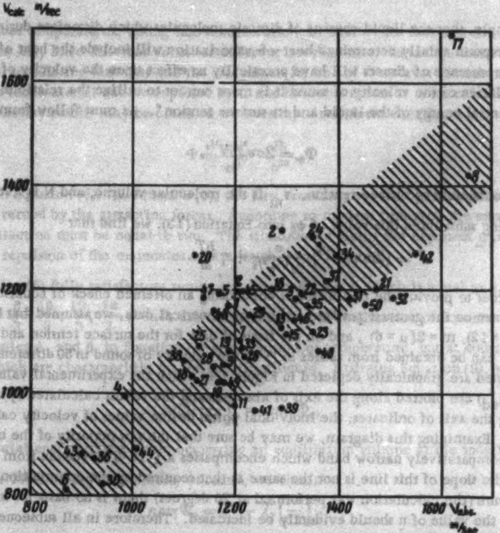

Figure 1. Calculation of sound velocity in liquids from data on their density and surface tension. 1) Acetone; 2) acetonitrile; 3) ethyl acetate; 4) ethyl ether; 5) ethyl alcohol; 6) ethyl iodide; 7) amyl acetate; 8) aniline; 9) benzene; 10) bromobenzene; 11) bromotoluene; 12) isobutyl alcohol; 13) chlorobenzene; 14) chloroform; 15) o-chlorotoluene; 16) cyclohexane; 17) formamide; 18) hexane; 19) methyl acetate; 20) methyl alcohol; 21) nitrobenzene; 22) nitromethane; 23) m-xylene; 24) formic acid; 25) octane; 26) n-propyl alcohol; 27) isopropyl alcohol; 28) carbon bisulfide; 29) toluene; 30) carbon tetrachloride; 31) cyclohexanon; 32) ethyl analine; 33) ethylene-chloride; 34) pyridine; 35) pipiridine; 36) bromoform; 37) dioxane; 38) tertiary butyl alcohol; 39) palmitic acid; 40) octyl alcohol; 41) stearic acid; 42) quinoline; 43) ethyl bromide; 44) ethylene bromide; 45) amyl alcohol; 46) n-butyl alcohol; 47) butyl chloride; 48) acetic acid; 49) methylene chloride; 50) cyclohexanol.

TABLE 2

Substance	$\left(\frac{1}{c}\frac{\Delta c}{\Delta t}\right)_{calc}$	$\left(\frac{1}{c}\frac{\Delta c}{\Delta t}\right)_{expt}$	Temp. interval in deg C
Benzene	$-3.1\cdot10^{-3}$	$-3.6\cdot10^{-3}$	10-50
Ethyl alcohol	$-1.9\cdot10^{-3}$	$-2.9\cdot10^{-3}$	0-50
Methyl alcohol	$-1.6\cdot10^{-3}$	$-2.8\cdot10^{-3}$	0-50
Chlorobenzene	$-2.9\cdot10^{-3}$	$-2.9\cdot10^{-3}$	20-50
Ethyl ether	$-3.0\cdot10^{-3}$	$-4.7\cdot10^{-3}$	0-30
Carbon tetrachloride	$-2.1\cdot10^{-3}$	$-3.5\cdot10^{-3}$	0-50

TABLE 3

Substance	$\left(\frac{1}{c}\frac{\Delta c}{\Delta t}\right)_{expt}$	$\left(\frac{1}{c}\frac{\Delta c}{\Delta t}\right)_{calc}$	$\left(\frac{1}{c}\frac{\Delta c}{\Delta t}\right)_{II}$
Bromoform	$-3.4\cdot10^{-3}$	$-0.45\cdot10^{-3}$	$-2.63\cdot10^{-3}$
Benzene	$-3.6\cdot10^{-3}$	$+0.01\cdot10^{-3}$	$-1.83\cdot10^{-3}$
Nitrobenzene	$-2.5\cdot10^{-3}$	$+0.2\cdot10^{-3}$	$-1.65\cdot10^{-3}$
Aniline	$-2.8\cdot10^{-3}$	$+0.22\cdot10^{-3}$	$-1.86\cdot10^{-3}$

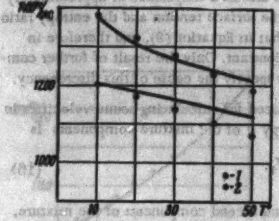

Figure 2. Comparison of calculated and observed values for the velocity of sound.
1) In benzene and ethyl alcohol; 2) at various temperatures.

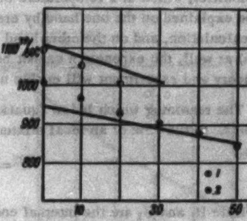

Figure 3. Comparison of calculated and observed values for the velocity of sound.
1) In ethyl ether and carbon tetrachloride; 2) at various temperatures.

In order to appraise the results obtained, we provide a table taken from a paper by L. G. Mikhailov and Iu. P. Syrnikov [4], in which the observed temperature coefficients of sound velocity are compared with the calculated ones on the basis of the "hole" theory of liquids. In the last column of the table values are given for the temperature coefficient of velocity $\left(\frac{1}{c}\frac{\Delta c}{\Delta t}\right)_{II}$, which are obtained if the theoretical volume of the substance at absolute zero is arbitrarily replaced by the volume of the substance at fusion. As can easily be verified, the "hole" theory does not even lead to a qualitative agreement with the experiment; such qualitative agreement may be achieved only as a result of unproven postulates (the replacement of the volume at absolute zero by the volume at fusion).

Allowing for the discrepancy between the calculated and observed temperature coefficients of sound velocity, it was desirable to calculate the sound velocities according to Equation (15) over a wide range of temperatures. The possibility of making such calculations is limited by the data on the temperature dependency of the surface tension σ and the ratio of the entropys γ. Nevertheless, utilizing the data in the tables of [14] and the results of the investigations by Lependin [6], Nozdrev [16] and Akhmetzianov [15] we were able to calculate the sound velocities in ethyl alcohol in the temperature range from 0° to 240°, i.e., practically up to the critical temperature, which for ethyl alcohol equals 243 degrees. Figure 5, which depicts the results of the calculation proves to us that the above-mentioned agreement between the theory and the experiment is not accidental. The discrepancy between the calculated and observed values

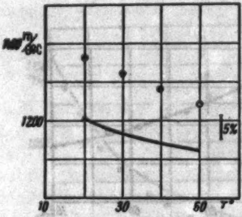

Figure 4. Comparison of calculated and observed values for the velocity of sound in chlorobenzene for various temperatures.

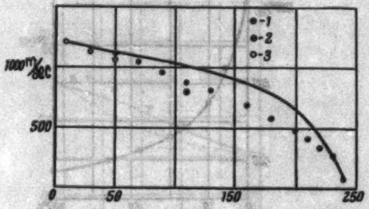

Figure 5. Comparison of calculated and observed values of the sound velocity in ethyl alcohol in the temperature range from 0° to the critical temp.
1) According to Akhmetzianov [15]; 2) according to Nozdrev [16]; according to Hubbard [14].

for sound velocities, which at a temperature of about 180 degrees attains a magnitude of approximately 20 %, may be explained on the one hand by errors in the data on the surface tension and the entropy ratio, used in the calculation, and on the other hand by the possibility that in Equation (9), and therefore in Equation (15) as well, the exponent n cannot be assumed strictly constant. Only the result of further comparison of theory and experiment will enable us more precisely to specify the cause of this discrepancy.

The reasoning which led to Equation (15) may be utilized for calculating sound velocities in liquid mixtures. In the case of an ideal mixture the internal energy U of the mixture components is additive, i.e.,

$$U = \mu U_1 + (1 - \mu) U_2. \tag{16}$$

Here U_1 and U_2 are the internal energies of the first and second components of the mixture, taken separately, and μ is the molar fraction of the first component. The same relationship will be valid with respect to the volume, i.e.,

$$v = \mu v_1 + (1 - \mu) v_2. \tag{17}$$

Differentiating Equation (16) twice with respect to the volume v at a constant entropy S, and noting the fact that

$$\left[\frac{\partial^2 U}{\partial v^2}\right]_S = \frac{c^2 M}{v^2},$$

where c is the velocity of sound and M is the molecular weight, it is not difficult to obtain an expression for the sound velocities in the mixture

$$c^2 = \mu \frac{M_1}{\bar{M}} c_1^2 + (1 - \mu) \frac{M_2}{\bar{M}} c_2^2, \tag{18}$$

where c is the sound velocity in the mixture, c_1 and c_2 are respectively the sound velocities in the first and second components, $\bar{M}$ is the average molecular weight of the mixture, M_1 and M_2 are the molecular weights of the components and μ is the molecular fraction of the first component.

In order to check Equation (18) it is natural to select binary mixtures for which conditions (16) and (17) are fulfilled as rigidly as is possible, and such mixtures are gas mixtures. In Figures 6 and 7 the solid curves depict the results of the calculation of sound velocity in the mixtures of hydrogen-nitrogen and carbon monoxide-carbon dioxide gas by means of Equation (18); the solid circles depict the values of the velocities which were found experimentally [17]. The agreement of theory with experiment is fully satisfactory.

Of the liquid mixtures, those that are close to ideal are: carbon tetrachloride-benzene and chlorobenzene-bromobenzene. In Figures 8 and 9

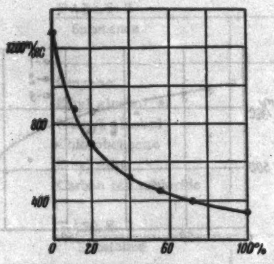

Figure 6. Comparison of calculated and observed sound velocities in hydrogen-nitrogen mixtures of varying composition at 0°.
Abscissa: percent nitrogen.

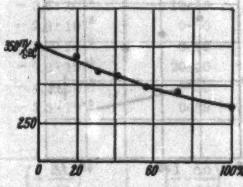

Figure 7. Comparison of the calculated and observed sound velocities in carbon monoxide-carbon dioxide gas mixtures of varying composition at 20°.
Abscissa: percent carbon dioxide.

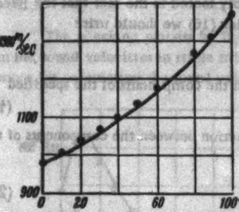

Figure 8. Comparison of the calculated and observed values of the sound velocity in carbon tetrachloride-benzene mixtures of varying composition at 10°. Abscissa: percent benzene.

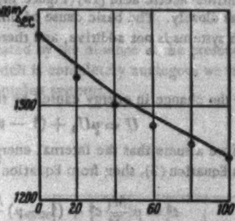

Figure 9. Comparison of calculated and observed values of sound velocity in chlorobenzene-bromobenzene mixtures of varying composition at 0°. Abscissa: percent bromobenzene..

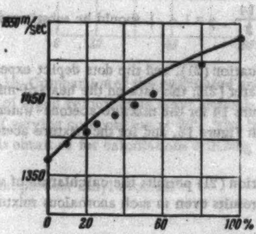

Figure 10. Comparison of calculated and observed values of sound velocity in benzene-nitrobenzene mixtures of varying composition at 10°. Abscissa: percent nitrobenzene.

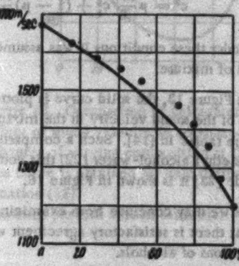

Figure 11. Comparison of calculated and observed values of sound velocity in aniline-acetic acid mixtures of varying composition at 15°. Abscissa: percent acetic acid.

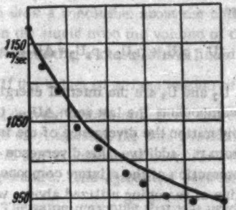

Figure 12. Comparison of calculated and observed values of sound velocity in carbon tetrachloride-ethyl alcohol mixtures of varying composition at 20°. Abscissa: percent carbon tetrachloride.

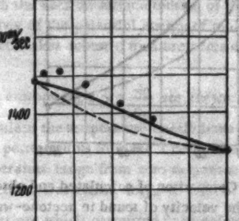

Figure 13. Comparison of calculated and observed values of sound velocity in formic acid-water mixtures of varying composition at 20°. The broken-line curve is obtained for calculations which use Equation (18). Abscissa: percent formic acid.

the solid curves are drawn on the basis of calculations which use Equation (18); the dots depict values of sound velocity which were found experimentally [18]. The agreement of theory with experiment in this case is fully satisfactory. The calculated and observed values of velocity in the mixtures benzene-nitrobenzene [18] (Figure 10), aniline-acetic acid [19] (Figure 11) and carbon tetrachloride-ethyl alcohol [20] (Figure 12). do not coincide as closely. The basic cause of this discrepancy is probably rooted in the fact that the internal energy of such systems is not additive, and therefore instead of Equation (16) we should write

where ΔU_{12} is the change in energy caused by the interaction between the components of the specified mixture.

$$U = \mu U_1 + (1-\mu) U_2 + \Delta U_{12}, \tag{19}$$

If we assume that the internal energy of molecular interaction between the components of the mixture obeys Equation (9), then from Equation (19) we can find

$$c^2 = \mu \frac{M_1}{M} c_1^2 + (1-\mu) \frac{M_2}{M} c_2 + mn\gamma\Delta U^0 \tag{20}$$

During the calculation we may use the approximation which consists of substituting ΔU^0 for the specific heat of a mixture of given composition L; then we shall obtain, for calculating the velocities of sound in mixtures, the expression

$$c^2 = \mu \frac{M_1}{M} c_1^2 + (1-\mu) \frac{M_2}{M} c_2^2 + 5.5 \cdot 10^8 L. \tag{21}$$

Under these conditions it was assumed that m = 2, n = $\frac{14}{3}$, γ = 1.4. L should be substituted in calories/gram of mixture.

In Figure 13, the solid curve is plotted by means of Equation (21), and the dots depict experimental values of the sound velocity in the mixture: formic acid-water [21]; the data on the heat-of-mixture is taken from the tables in [14]. Such a comparison is shown in Figure 14 for the mixture acetone-water [19]; for the mixture ethyl alcohol-water [22] this comparison is shown in Figure 15, and for the mixture acetone-carbon bisulfide [23] it is shown in Figure 16.

As we may conclude from examining the graphs, Equation (21) permits the calculation of sound velocity so that there is satisfactory agreement with experimental results even in such anomalous mixtures as aqueous solutions of alcohols.

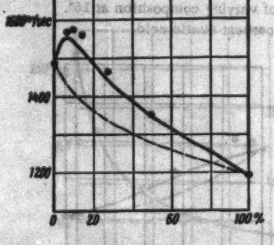

Figure 14. Comparison of calculated and observ values for the velocity of sound in acetone-water mixtures of varying composition at 20.5°. The broken-line curve is obtained for calculations utilizing Equation (18).
Abscissa: percent acetone.

It is not difficult to obtain an expression which is analogous to Equation (21) for calculating the velocities of sound in a triple-system or even in a more complex system than that. In fact, defining the molar fractions of the components in a triple mixture respectively by p_1, p_2 and p_3, we may write

$$U = p_1 U_1 + p_2 U_2 + p_3 U_3 + \Delta U_{123}. \tag{22}$$

Here U_1, U_2 and U_3 are the internal energies of the mixture components the last term, ΔU_{123}, takes into consideration the divergence of the internal energy from the additive (this divergence is caused by the interaction of the mixture components). Applying the line of reasoning utilized above, we obtain

$$c^2 = p_1 \frac{M_1}{M} c_1^2 + p_2 \frac{M_2}{M} c_2^2 + p_3 \frac{M_3}{M} c_3^2 + 5.5 \cdot 10^8 L. \tag{23}$$

In the simplest case, when we may assume that the internal energy is additive, expression (23) becomes:

$$c^2 = p_1 \frac{M_1}{M} c_1^2 + p_2 \frac{M_2}{M} c_2^2 + p_3 \frac{M_3}{M} c_3^2. \qquad (24)$$

The checking process for Equation (24) is complicated by the absence at the present time of data on the sound velocities in triple mixtures. In a manner which is completely analogous we may obtain expressions for calculating the sound velocity in even more complex systems.

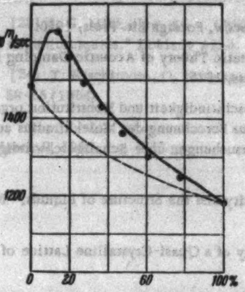

Figure 15. Comparison of the calculated and observed values of sound velocities in ethyl alcohol-water mixtures of varying composition at 20°. The broken-line curve is obtained for calculations utilizing Equation (18).
Abscissa: percent ethyl alcohol.

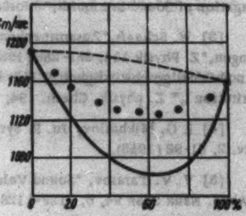

Figure 16. Comparison of calculated and observed values of sound velocity in acetone-carbon bisulfide mixtures of varying composition at 20°. The broken-line curve is obtained for calculations utilizing Equation (18).
Abscissa: percent carbon bisulfide.

SUMMARY

Utilizing the thermodynamic relationships between various physical parameters which characterize the liquid, we are able to establish the relationship between the sound velocity in the liquid and the surface tension of the liquid. Under these conditions, the calculated values of sound velocity agree satisfactorily with the experimental values.

Comparing the results of acoustic measurements with the data on surface tension of the liquids permits us to draw a conclusion about the nature of the dependency of the potential energy of molecular interaction in the liquid upon the volume of the liquid. This fact makes acoustic measurements extremely valuable in formulating a theory of the liquid state.

If the values of surface tension of the liquid and the entropy ratio $\gamma = \frac{c_p}{c_v}$ are known at various temperatures, then the equations derived make it possible to calculate the temperature coefficients of sound velocity. For ethyl alcohol, the data available in the literature permitted us to make a comparison between the theoretical and experimental values of velocity in the temperature range from zero degrees to the critical temperature. The agreement between theory and experiment was satisfactory.

The same reasoning that was used to obtain the equations which permitted us to calculate the sound velocity in individual liquids may be applied to the calculation of sound velocities in ideal binary mixtures. The values of sound velocity which were calculated for a series of mixtures using an equation so obtained, were in satisfactory agreement with values found experimentally.

In those cases when a significant discrepancy is observed between the sound velocity values which are calculated and those which are found experimentally, this discrepancy is caused first of all by the divergence of the internal energy of the system from the additive. Taking into consideration the presence of mutual interaction between the components of the mixture, we are able to calculate sound velocities even in such anomalous mixtures as aqueous solutions of alcohols in such a way that they agree with experimental values. The equations obtained for sound velocity in binary mixtures are extended to apply to triple and to even more complex mixtures.

LITERATURE CITED

[1] S. Glesston, Theoretical Chemistry, Ch.IX. Moscow, Foreign Lit. Press, 1950.

[2] B. B. Kudriavtsev, Dissertation, "Molecular-Kinetic Theory of Acoustic Damping in Gases and Propagation of Sound in Liquids," Moscow Chem. Tech. Press, 1945.

[3] W. Schaafs,"Zusammenhang zwischen Schallgeschwindigkeit und Konstitution organischer. Verbindungen,"Z. Physik 114, 251-256 (1939); "Bemerkungen zur Berechnung des Molekülradius aus Mol volumen und Schallgeschwindigkeit," 115, 69-76 (1940); "Untersuchungen über Schallgeschwindigkeit und Konstitution I," Z. physik. Chem. 194, 28-38 (1944).

[4] I. G. Mikhailov, Iu. P. Syrnikov, "Sound Velocity and the Structure of Liquids," Bull. Leningrad Univ. 2, 81-98 (1953).

[5] V. V. Tarasov, "Sound Velocity and Null Energy of a Quasi-Crystalline Lattice of Liquids," Doklady Akad. Nauk SSSR 94, 6, 1125-1128 (1954).

[6] A. F. Lependin, Dissertation, "The Problems of Sound Propagation in Liquids and Gases Enclosing a Critical Region," MOPI, 1953.

[7] T. H. Barron, C. Domb,"The Velocity of Elastic Waves in the Solidified Inert Gases"," Phil. Mag. 45, 654-655 (1954).

[8] B. B. Kudriavtsev, Application of Ultrasonic Methods in Practical Physical and Chemical Research, State Tech. and Theor. Press, Moscow-Leningrad, 1952.

[9] B. B. Kudriavtsev, "Sound Velocity in Liquids and Physico-Chemical Properties of Liquids," J. Phys. Chem. (USSR) 28, 5, 930-935 (1954).

[10] A. A. Adkhamov, Dissertation, "Concerning a Molecular-Kinetic Theory of the Propagation of Ultrasonic Waves in Liquids," Moscow State Univ., 1954.

[11] Ia. I. Frenkel, Kinetic Theory of Liquids, Acad, Sci. USSR Press, 1954.

[12] H. S. Green, Molecular Theory of Fluids, 1952, p. 201.

[13] A. Aiken, A Course in Chemical Physics, Edition No. I, United Sci. Tech. Press, Moscow, 1935.

[14] Landolt-Bornstein,Physikalische Chemische Tabellen, 1923-1936.

[15] K. T. Akhmetzianov, "Propagation Velocity of Ultrasonic Waves in Methyl and Ethyl Alcohol in a Critical Region," Bull. Moscow State Univ. 9, 31-41 (1949).

[16] V. F. Nozdrev, Dissertation, "Investigation of the Propagation of Ultrasonic Waves in Organic Liquids and Their Saturated and Reheated Vapors," MOPI, 1950.

[17] B. B. Kudriavtsev, "Molecular-Kinetic Theory of the Sound Propagation Process In Gases," Moscow Chem. Tech. Press, 1940, Vol. 5, pp. 19-34.

[18] B. N. Suslov, B. B. Kudriavtsev, "Investigation of Liquid Binary Systems with Molecular Interaction of Different Kinds," in the Symposium "Application of Ultrasonics to the Investigation of Substances," No. 2, Moscow, MOPI Press, 1955, pp. 5-23.

[19] I. G. Mikhailov, "Velocity of Ultrasonic Waves in Aqueous Mixtures of Several Organic Liquids," Doklady Akad. Nauk SSSR 31, 4, 324-326 (1941).

[20] K. Sacher, "Die Abhängigkeit der Schallgeschwindigkeit von Konzentration in einem dipol-dipolloser Flüssigkeitgemisch," Physik. Z. 41, 360-362 (1940).

[21] I. G. Mikhailov, "Velocity of Ultrasonic Waves in a Mixture of Formic Acid and Water," Doklady Akad. Nauk SSSR 31, 551-552 (1941).

[22] N. I. Larionov, "Investigation of Propagation Velocity of Ultrasonic Waves in Mixtures Containing Associated Components," J. Phys. Chem. (USSR) 27, 7, 1002-1012 (1953).

[23] I. G. Mikhailov, A. A. Chistorazum, "Velocity of Ultrasonic Waves in Several Binary Mixtures of Organic Liquids," Doklady Akad. Nauk SSSR 81, 779-782 (1951).

[24] T. Kischimoto, O. Nomoto, "On Molecular Sound Velocity of Liquids I," J. phys. Soc. of Japan 9, 1, 59-65 (1954).

Received March 2, 1955 Moscow Regional Pedagogical Institute

CALCULATION OF AUDIBILITY OF NONLINEAR DISTORTION ARISING IN AN ELECTROACOUSTICAL CHANNEL

A. V. Rimskii-Korsakov

The article sets out to calculate the audibility of nonlinear distortion by calculating the probability that the products of nonlinear distortion will exceed both the masked threshold created by the basic signal which is transmitted by an electro-acoustical channel, and the threshold of audibility under the conditions of the specified auditorium.

An approximate theoretical calculation of this probability is given and the result of this calculation is given for the simplest case – a constant-amplitude frequency spectrum for the input signal and a quadratic nonlinearity characteristic. The real "threshold of perceptibility" for the distortion in this case is defined by a harmonic coefficient of 2-3%.

An approximate calculation of the audibility of nonlinear distortion in an electroacoustical channel may be performed by utilizing data specifying the spectral density $S_1(\omega)$ of the fundamental (undistorted) signal I_1 at the output of the channel and specifying the spectral density $S_{2,3}\ldots$ of the distortion products $I_{2,3}\ldots$

The spectral density of the nonlinear distortion products may in turn be obtained by known methods, methods which are utilized in examining a nonlinear transformation of a random wave process [1]. In all these calculations the simplest procedure is to examine the original signal as a random stationary process which has a normal distribution.

For such an assumption, every portion of the fundamental signal and the nonlinear products, occupying a narrow frequency band $\omega \pm \frac{\Delta\omega}{2}$, may be examined as random signals whose average intensity can be found from their spectral densities:

$$\overline{I^2_{1\omega}} = S_1(\omega)\,\Delta\omega;\quad \overline{I^2_{2\omega}} = S_2(\omega)\,\Delta\omega;\ \ldots\ \overline{I^2_{n\omega}} = S_n(\omega)\,\Delta(\omega) \qquad (1)$$

(the subscript 2 denotes "quadratic", the subscript 3 denotes "cubic" etcetera nonlinear products).

The instantaneous values of $I_{1\omega}$ and $I_{n\omega}$ will have definite probability densities $W_1(I_{1\omega})$ and $W_n(I_{n\omega})$, and the total probability density of the simultaneous appearance of the quantities $I_{1\omega}$ and $I_{n\omega}$ will, in the general case, be

$$W_{1n}(I_{1\omega}, I_{n\omega}) = W_{1/n}(I_{1\omega}/I_{n\omega})\,W_n(I_{n\omega}). \qquad (2)$$

From the direct comparison of S_n with S_1, it is difficult to draw any conclusion as to whether the products of nonlinearity will be audible against the "background" of the fundamental signal or not. However if the magnitude of W_{1n} is known, then we may calculate what the probability will be of $I_{n\omega}$ exceeding the threshold of audibility, i.e., the probability of distortion being audible in the band $\omega \pm \Delta\omega/2$. In order to determine this we must merely determine how the audibility threshold depends upon S_1, i.e., we must take into consideration the masking effect created by the fundamental signal in the band $\omega \pm \Delta\omega/2$, which tends to mask the distortion signal. A precise quantitative evaluation of masking is complex, but simplified relationships are used for a series of acoustic calculations; it is assumed that the examined signal, which has a frequency ω, is masked by masking spectrum components which lie in the so-called critical auditory band (or integration band) – a comparatively narrow band of frequencies for which the center frequency is the frequency of the masked wave. In addition, it is evident from the masking curves of pure tones [2] that for masking tone intensities that are not too great the audibility threshold of the masked tone in a band of frequencies surrounding the frequency of the masked tone is approximately 20 db below the level of the masking tone. For the sake of generality, therefore, we may write that the masked wave $I_{n\omega}$ becomes audible if

$$I_{n\omega} \geqslant I_{1\omega}/\beta, \tag{3}$$

where β should be made equal to 20 db, i.e., equal to 10, and $\Delta\omega$ should be made equal to the critical frequency band. Inequality (3) combined with (2) permits us to find the probability of $I_{n\omega}$ being perceptible to the ear:

$$P_0(I_{n\omega} \geqslant I_{1\omega}/\beta) = \iint W_{1n}\, dI_{1\omega}\, dI_{n\omega} \qquad (I_{n\omega} \geqslant I_{1\omega}/\beta). \tag{4}$$

Here the index $(I_{n\omega} \geq I_{1\omega}/\beta)$ shows that integration is conducted over all values of $I_{n\,\omega}$, which are greater than or equal to $I_{1\,\omega}/\beta$.

If the quantity P_0, calculated for a series of values of ω which embrace the pass-band of the channel, proves to be very small (let us assume it is less than 0.005), we may assume that for all practical purposes there will be no audible distortion in the channel.

Two substantial inaccuracies are contained in this elementary scheme of calculation.

1. For the auditory process not all cases where $I_{n\omega}$ exceeds the magnitude if $I_{1\omega}$ are important, and in particular those cases where $I_{n\omega} > I_{1\omega}$ occurs for a very short time are of little importance; only cases when $I_{n\omega} > I_{1\omega}$ for a sufficiently long period of time are of importance. In other words, it is of importance that the amplitudes of $I_{n\omega}$ and $I_{1\omega}$ be in a relationship determined by the inequality (3) and not their instantaneous values. Of course, the random signals $A_{1\omega}$ and $A_{n\omega}$ will also have random amplitudes, and for us it is most convenient to examine them as signals with random amplitudes $\varphi_{1\omega} = \omega t + \theta_{1\omega}$ and $\varphi_{n\omega} = \omega t + \theta_{n\omega}$. Here $\underline{t}$ is time, $\theta_{1\omega}$ and $\theta_{n\omega}$ are phase fluctuations.

Thus we should find a method of depicting the fundamental signal of intensity $S_1(\omega)\Delta\omega$ and the distortion products of intensity $S_n(\omega)\Delta\omega$ as signals, with random amplitudes $A_{1\omega}$ and $A_{n\omega}$, and then find the quantity $W_a(A_{1\omega}, A_{n\omega})$ and from it the probability which is of interest to us:

$$P_{0a}(A_{n\omega} \geqslant A_{1\omega}/\beta) = \iint W_a\, dA_{1\omega}\, dA_{n\omega} \qquad (A_{n\omega} \geqslant A_{1\omega}/\beta). \tag{5}$$

2) If in some band $\omega \pm \Delta\omega/2$, the magnitude of $S_1 = 0$, and $S_n \neq 0$, then the distortion may still be inaudible since a natural audibility threshold exists; under the ordinary conditions of listening to transmitted intelligence this threshold is raised because of noise at the place of reception.*

Defining this threshold magnitude by $A_{0\,\omega}$, we obtain a second inequality

$$A_{n\omega} \geqslant A_{0\omega}, \tag{6}$$

which must also be included in the limits of integration of expression (5).

EVALUATION OF THE PROBABILITY DENSITY OF W_a

The condition which we assumed (that I_1 is a random stationary process obeying a normal law of distribution) and the usual assumptions in this case for finding S_n according to the nonlinear characteristic of the channel and the magnitude of S_1, are insufficient for finding the magnitude of W_a which is basic to our calculation. In order to find W_a we should make several additional postulates with respect to the character of the signal I_1. Dwelling upon the case of the transmission of music, we may postulate that the input signal of the system (u) consists of the sum of a large number of components u_k with random amplitudes and phases. These components define individual musical tones and their harmonics, so that

---

* We do not examine the case of noise in the channel.

$$u = \sum_{k=1}^{k=r} u_k = \sum U_k \cos \varphi_k. \tag{7}$$

U_k are random amplitudes, $\varphi_{1k} = \omega_k t - \theta_{1k}$, where θ_{1k} is the phase fluctuation; ω_k is the frequency of the k-th tone or harmonic.

We shall assume that U_k possess a normal law of distribution, then;

$$\left.\begin{aligned} W_{u_k} &= \frac{1}{\sqrt{2\pi\overline{u_k^2}}} e^{-u_k^2/2\overline{u_k^2}} \\ W_{\varphi_k} &= \frac{1}{2\pi},\ 0 \leqslant \varphi \leqslant 2\pi \\ W_{U_k} &= \frac{U_k}{\overline{u_k^2}} e^{-U_k^2/2\overline{u_k^2}} \\ U_k &\geqslant 0. \end{aligned}\right\} \tag{8}$$

In this case $a = \Sigma u_k$ will also possess a normal distribution. This permits us to evaluate the average intensity of the distortion $S_n(\omega)\Delta\omega$ by ordinary methods from the magnitude of $S_1(\omega)$. In order to determine the nature of W_a, however, we should directly examine the nonlinear transformation of the magnitude of (7) in the channel containing the specified characteristic of nonlinearity $I = F(u)$.

Let us assume that the characteristic of nonlinearity contains the simplest even and odd distortion:

$$I = au + bu^2 + cu^3. \tag{9}$$

Substituting (7) into (9), we obtain

$$\begin{aligned} I = a \sum_{(k)} U_k \cos \varphi_k + \frac{1}{2} b \sum_{(j)} \sum_{(k)} U_j U_k [\cos(\varphi_k + \varphi_j) + \\ + \cos(\varphi_k - \varphi_j)] + \frac{1}{4} c \sum_{(j)} \sum_{(k)} \sum_{(l)} U_j U_k U_l [\cos(\varphi_k + \varphi_j + \varphi_l) + \\ + \cos(\varphi_k + \varphi_j - \varphi_l) + \cos(\varphi_k - \varphi_j + \varphi_l) + \cos(\varphi_k - \varphi_j - \varphi_l)]. \end{aligned} \tag{10}$$

The possible frequencies of these products when there is quadratic distortion will be

$$\omega_k + \omega_j \text{ and } |\omega_k - \omega_j|, \tag{11}$$

and when there is cubic distortion,

$$\omega_k + \omega_j + \omega_l, \quad |-\omega_k + \omega_j + \omega_l|, \quad |\omega_k + \omega_j - \omega_l|, \quad |\omega_k - \omega_j + \omega_l|. \tag{12}$$

We assume that all the original frequencies in (7) are positive.

Let us examine the quadratic products which fall in a frequency band $\omega \pm \Delta\omega/2$. They evidently satisfy the inequality

$$\omega - \Delta\omega/2 \leqslant \omega_k + \omega_j \leqslant \omega + \Delta\omega/2, \quad \omega - \Delta\omega/2 \leqslant |\omega_k - \omega_j| \leqslant \omega + \Delta\omega/2. \qquad (13)$$

A graphical depiction of these inequalities is given in Figure 1.

If the number of frequencies in our signal is r and these frequencies lie within the limits of from ω_L to ω_H then a number of intersections between the straight lines $\omega_k = \text{const}$ and $\omega_j = \text{const}$ (for j, k that are within the limits of 1 to r) which is equal to r^2 produces the full number of all the products with frequencies of $\omega_k + \omega_j$ or $\omega_k - \omega_j$. The number of intersections which occur in the lined areas between the straight lines:

$$\left.\begin{aligned} \omega_k + \omega_j &= \omega \pm \Delta\omega/2 \\ |\omega_k - \omega_j| &= \omega \pm \Delta\omega/2 \end{aligned}\right\} \qquad (14)$$

corresponds to the number of products which satisfy the conditions of (13).

The number of intersections occurring in the cross-hatched areas formed by the intersections of the straight lines of (14) with the straight lines $\omega_j = \omega \pm \Delta\omega/2$ and $\omega_k = \omega \pm \Delta\omega/2$, corresponds to the number of products which fall in the selected frequency band $\omega \pm \Delta\omega/2$ and which depend upon the fundamental signals possessing those same frequencies.

When a large number of frequencies is uniformly distributed in the interval $\omega_H - \omega_L$, the lined areas are proportional to the number of products which satisfy (13), and the cross-hatched areas are proportional to the number of those products which depend upon fundamental signals which lie in that same band of the spectrum. The ratio of these areas is $\Delta\omega/(\omega_H - \omega_L)$; i.e., it is small for a sufficiently narrow band $\Delta\omega$. The integration (critical) auditory bands comprise a band from 30 to 150 cps in the fundamental portion of the range of audible frequencies; the band of transmitted frequencies $\omega_H - \omega_L$ usually comprises not less than 5000 cps. We may thus assume that the quadratic nonlinearity products in the specified band of frequencies will contain only a very small number of those products which depend upon the fundamental signals in this same band; i.e., they may be assumed to be approximately independent of these latter ones.* Analogous reasoning may also be applied to cubic products by constructing a 3-dimensional diagram with axes $\omega_k\omega_j\omega_l$ and by sectioning the cubic volume $(\omega_H - \omega_L)$ in it by means of planes which isolate the products falling in the region of frequencies $\omega \pm \Delta\omega/2$, namely:

$$\left.\begin{aligned} \omega_j + \omega_k + \omega_l &= \omega \pm \Delta\omega/2 \\ |\omega_j - \omega_k + \omega_l| &= \omega \pm \Delta\omega/2 \end{aligned}\right\} \qquad (15)$$

etc.

The intersection of the system of planes (15) with the planes $\omega_{j,k,l} = \omega \pm \Delta\omega/2$ which are parallel to the coordinate planes would permit us to isolate the volumes containing the "dependent" products, and in so doing, it would again be proven that the ratio of volumes occupied by the dependent products to the overall volume occupied by the products in the specified band is the ratio $\Delta\omega/(\omega_H - \omega_L)$

---

* Such a conclusion with respect to the independence of the nonlinearity products in the specified band from the fundamental signals in the same band is of course obtained here in a manner which is insufficiently justified from a theoretical viewpoint, since only the number and not the intensity of the products is considered. However, it is impossible to perform the calculation for the intensity without knowning the spectrum of the signal in advance.

In European music the frequencies of the fundamental tones of the musical sounds grow in geometric progression so that the number of frequencies enclosed between ω_L and ω_k comprises

$$k = \frac{12}{\ln 2} \ln \frac{\omega_k}{\omega_L}. \tag{16}$$

Assuming that the number of frequencies is very large, and substituting integration for the process of summing within the boundaries shown in Figure 1, we can show that the number of possible additive quadratic products which are formed solely by the fundamental tones in the band $\omega \pm \Delta\omega/2$ is

$$\left.\begin{aligned} m_0 &\approx \frac{288\,\Delta\omega}{\omega(\ln 2)^3} \ln \frac{\omega - \omega_L}{\omega_L} \\ 2\omega_L &< \omega < \omega_B + \omega_L \\ m_c &\approx \frac{288\Delta\omega}{\omega(\ln 2)^3} \ln \frac{\omega_H}{\omega - \omega_H} \\ \omega_H + \omega_L &< \omega < 2\omega_H, \end{aligned}\right\} \tag{17}$$

and the number of difference products is

$$\begin{aligned} m_p &\approx \frac{288\Delta\omega}{\omega(\ln 2)^3} \ln \frac{(\omega + \omega_L)(\omega_H - \omega)}{\omega_H \omega_L}, \\ \omega_L + \Delta\omega &< \omega < \omega_H - \Delta\omega. \end{aligned} \tag{18}$$

The number of these products which depend upon the fundamental tones of the very same band will be

$$\Delta m \approx \frac{576}{(\ln 2)^3} \left(\frac{\Delta\omega}{\omega}\right)^2. \tag{19}$$

from which we find

$$\mu = \frac{\Delta m}{m_c + m_p} = \frac{\Delta\omega}{\omega} \frac{1}{\ln(\omega^2/\omega_L^2 - 1)(1 - \omega/\omega_H)}. \tag{20}$$

Table 1 gives the magnitudes of $m_c + m_p$ and μ for the frequency range from 50 to 4000 cps in the critical auditory bands.

TABLE 1

Average frequency of the band, cps	100	200	400	800	2000	4000	8000
Width of the critical band, cps	56	40	32	35	63	126	158
Relative band-width	0.56	0.2	0.08	0.044	0.031	0.031	0.02
$m_c + m_p$	930	610	400	280	350	170	–
μ	0.4	0.07	0.019	0.0075	0.0038	0.007	–

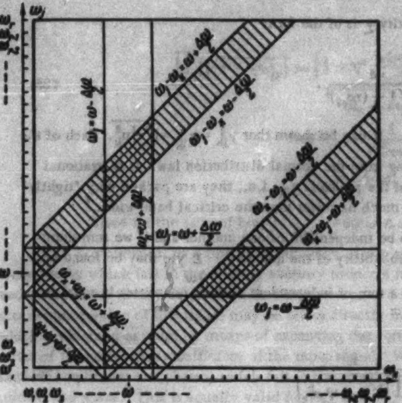
ω_j
ω_k
$\omega_j = \omega - \frac{\Delta\omega}{2}$
$\omega_j = \omega + \frac{\Delta\omega}{2}$
$\omega_j - \omega_k = \omega + \frac{\Delta\omega}{2}$
$\omega_j - \omega_k = \omega - \frac{\Delta\omega}{2}$
$\omega_k - \omega_j = \omega - \frac{\Delta\omega}{2}$
$\omega_k - \omega_j = \omega + \frac{\Delta\omega}{2}$
$\omega_k = \omega + \frac{\Delta\omega}{2}$
$\omega_k + \omega_j = \omega + \frac{\Delta\omega}{2}$
$\omega_k + \omega_j = \omega - \frac{\Delta\omega}{2}$
ω
$\omega_1 \omega_2 \omega_3$
ω_i

Figure 1.

From Table 1 it follows that only in the region of the very lowest frequencies does a significant portion of the products of quadratic distortion depend upon the fundamental tones lying in the same band. This means that the probability of hearing these distortion products will be less than if these products were independent, because large values of the distortion products would be obtained mainly for large values of the fundamental signal and would therefore be masked.

In the greater portion of the band, however, the dependency of the nonlinear products upon the fundamental signal in that same critical band is very weak, and we may assume without appreciably overestimating the audibility of the distortion that these quantities are independent. This permits us, from here on, to write

$$W_{1_n} = W_1 W_n \tag{21}$$

in place of (2) for the distortion products of second and third order, and in place of (5)

$$P_{0n} = \iint W_{A1\omega} W_{An\omega} dA_{1\omega} dA_{n\omega} . \tag{22}$$

EVALUATION OF THE PROBABILITY OF $W_{An\omega}$

The next problem is to evaluate the probability of $W_{An\omega}$ on the basis of the properties (8) of the fundamental signal. The third of the equalities (8), containing the fundamental postulate concerning the fact that individual component tones of the musical signal also obey a normal law of distribution, allows us to seek a law of distribution for the individual components of combined tones in the same manner as for products of random quantities with a normal distribution.

Let us dwell upon the case of quadratic products which consist of products of the type $\frac{1}{2} bu_k u_j$. Utilizing the known relationship for independent random quantities

$$W(y) = \int W_{x1}(x) W_{x2}\left(\frac{y}{x}\right) \frac{dx}{|x|}, \tag{23}$$

where $y = x_1 x_2$ is a random quantity which is the product of the random quantities x_1 and x_2 with probability densities W_{x1} and W_{x2} respectively, we obtain

$$W(y_{jk}) = \frac{1}{\pi \sigma_j \sigma_k} K_0\left(\frac{y_{jk}}{\sigma_j \sigma_k}\right), \tag{24}$$

where K_0 is a Bessel function, $\sigma_j^2 = b\overline{u_j^2}$, $\sigma_k^2 = b\overline{u_k^2}$, $y_{jk} = bu_j u_k$.

The characteristic function for the quantity y is of the form

$$\theta_y(\eta) = \frac{1}{\sqrt{1+(\eta\sigma_{jk})^2}}. \tag{25}$$

Here for the sake of brevity, $\sigma_{jk} = \sigma_j\sigma_k$. It can be shown that $y_{jk}^2 = \sigma_{jk}^2 = b^2\overline{u_j^2 u_k^2}$. Each of the products y_{jk} evidently has a law of distribution differing from the normal distribution law. It is irrational to attempt to find the audibility probability for each of the products y_{jk}, i.e., they are packed very "tightly" in the spectrum and each of them has a band which is much narrower than the critical band width.*

If, for simplicity, we shall assume y_{jk} to be independent of one another and if we sum them within the limits of the critical band $\Delta\omega$, then the probability of the quantity $\sum\limits_{\Delta\omega} y_{jk}$ may be found on the basis of the fact that the characteristic function of a sum of independent random quantities is equal to the product of their characteristic functions:

$$\theta_{I_{2\omega}}(\eta) = \frac{1}{\prod\limits_{(\Delta\omega)}\left[\sqrt{1+\eta^2\sigma_{jk}^2}\right]}. \tag{26}$$

Here $I_{2\omega} = \sum\limits_{\Delta\omega} y_{jk}$ is the quadratic-type nonlinearity product which is of interest to us in the critical band $\omega \pm \Delta\omega/2$. The sign of $(\Delta\omega)$ shows that the product is taken for products which fall in the specified critical band. On the basis of the properties of the characteristic function, we obtain

$$W_2(I_{2\omega}) = \frac{1}{2\pi}\int\limits_{-\infty}^{+\infty} \frac{e^{-i\eta I_{2\omega}}d\eta}{\prod\limits_{(\omega\Delta)}\left[\sqrt{1+\eta^2\sigma_{jk}^2}\right]}. \tag{27}$$

The calculation of such an integral is difficult, since in the general case σ_{jk} are different and the number of factors entering into the products may be very large; thus, for example, it can be seen from Table 1 that the number of products $(m_c + m_p)$ comprises hundreds in the critical band $\Delta\omega$. We may obtain a simplification of expression (27) by going to the limiting case $m_c + m_p \longrightarrow \infty$, and by assuming that all $\sigma_{jk} \longrightarrow 0$ so that $\sum\limits_{\Delta\omega}\sigma_{jk}^2$ remains constant. In this case we may assume that $\sum\limits_{\Delta\omega}\sigma_{jk}^2$ defines the value of the average intensity of the quadratic products in the band $\omega \pm \Delta\omega/2$; comparing this magnitude with the spectral density of the linear products, we obtain**

$$\sum_{(\Delta\omega)}\sigma_{jk}^2 \approx S_2(\omega)\,\Delta\omega,$$

where S_2 is the spectral density of the quadratic products. It is simplest to postulate that all σ_{jk} are equal to one another. This is absolutely true if all $\overline{u_k^2}$ which comprise the fundamental signal are equal to each other and if S_1 = constant within the limits of some frequency band $\omega_H - \omega_L$. Then

---

* This can be shown by taking into consideration the average duration of individual musical tones.

** The inaccuracy of this expression is due to the fact that each of the products does not occupy a finite band of the spectrum, but merely has a sharp maximum in the band of the spectrum which is of interest to us; thus some portion of the energy of a product belongs to other portions of the spectrum.

$$\prod_{(\Delta\omega)}\left[\sqrt{1+\eta^2\sigma_{jk}^2}\right]=\left[1+\eta^2\frac{S_2(\omega)\,\Delta\omega}{m_c+m_p}\right]^{(m_c+m_p)/2}\to e^{\eta^2 S_2(\omega)\Delta\omega/2},$$

$$m_c+m_p\to\infty$$

$$\lim W_2=\frac{1}{\sqrt{2\pi\sigma_{2\omega}}}e^{-I_{2\omega}/2\sigma_{2\omega}^2}, \qquad (29)$$

$$m_c+m_p\to\propto$$

Here for the sake of brevity $\sigma_{2\omega}^2 = S_2(\omega)\,\Delta\,\omega$.

Therefore, to a first approximation, if the amplitudes of individual modulation tones of the second order which fall in the critical auditory band are not dependent upon one another, and if there are enough of them, it may be assumed that they comprise a signal with a normal law of distribution;* the mean-square value of this signal may be taken directly from the calculation of the magnitude of $S_2(\omega)$ which is obtained as usual by means of expanding the correlation function of the output signal into a power series of the correlation coefficient of the input signal. We may also examine the sum of the signals with random amplitudes and phases, which fall in the small frequency band $\Delta\omega$, as a signal with a random amplitude and phase. This is equally valid for $I_{1\omega}$ and $I_{n\omega}$. Under these conditions the length of time for which the amplitudes $A_{1\omega}$ and $A_{n\omega}$ remain within the specified range of values will be of the same order, since in the final analysis they depend upon the duration of the individual tones u_k.

Assuming that (29) is an approximate value for $W_2(I_{2\omega})$, we may therefore write the amplitudes of the second-order products as

$$W_{A_{2\omega}}=\frac{A_{2\omega}}{\sigma_{2\omega}^2}e^{-A_{2\omega}^2/\sigma_{2\omega}^2}. \qquad (30)$$

AN APPROXIMATE EXPRESSION FOR P_{0a}

Making use of (22) and (30), we obtain

$$P_{0\omega}=\iint\frac{A_{2\omega}A_{1\omega}}{\sigma_{2\omega}^2\sigma_{1\omega}^2}\exp\left\{-\frac{A_{2\omega}^2}{2\sigma_{2\omega}^2}-\frac{A_{1\omega}^2}{2\sigma_{1\omega}^2}\right\}dA_{1\omega}dA_{2\omega}, \qquad (31)$$

$$A_{2\omega}\geqslant A_{1\omega}/\beta,\qquad A_{2\omega}\geqslant A_{0\omega}.$$

We introduce the variables

$$\omega=A_{2\omega}/\sigma_{2\omega}=\rho\cos\psi,\ \ z=A_{1\omega}/\sigma_{1\omega}=\rho\sin\varphi. \qquad (32)$$

---

* This result is confirmed by experimental work [3]. When a signal is subjected to a nonlinear transformation, and when that signal obeys a normal law of distribution and occupies a wide band of frequencies, the experimentally obtained distribution curve for the instantaneous values of the quadratic distortion products does not, as a whole, have a normal distribution law, but for each small portion of these products which are in a narrow band of frequencies this curve, to a good approximation, is the same as that for a normal law. B. A. Fersman was successful in experimentally showing the validity of this postulate for cubic distortion products as well, so that the derivations of this paper can evidently be developed to include the case of cubic distortion.

Then the boundaries of the region in which we integrate (31) will be determined thus:

$$w \geqslant (\sigma_{1\omega}/\sigma_{2\omega}\beta)z \quad \text{or} \quad \psi \leqslant \psi_0 = \operatorname{arc\,tan}\frac{\sigma_{1\omega}}{\sigma_{2\omega}\beta}, \tag{33}$$

$$w = \rho\cos\psi \geqslant A_0/\sigma_{2\omega}. \tag{34}$$

These conditions are depicted in Figure 2. The region of integration lies between the axis w, the inclined straight line $w = (\sigma_{1\omega}/\sigma_{2\omega\beta})z$ and the straight line (parallel to the z axis) $w = A_{0\omega}/\sigma_{2\omega}$.

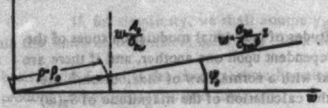
z
$w=\frac{A_0}{\sigma_{2\omega}}$
$w=\frac{\sigma_{1\omega}}{\sigma_{2\omega}\beta}z$
$\rho=\rho_0$
ψ_0
w

Figure 2.

For the case when the average power of the nonlinearity products is small in comparison to the undistorted signal (and that case is of greatest interest for evaluating the allowable nonlinear distortion) we may replace the condition (34) by the condition $\rho = \rho_0 = A_{0\omega}/\sigma_{2\omega}$. The error which results from this substitution leads to a slight re-evaluation of the magnitude of P_{0a}. Thus, instead of (31), we may write

$$P_{0a} \approx \int_{\rho_0}^{\infty}\int_{0}^{\psi_0} \frac{\rho^2\sin 2\psi}{2}\exp\left\{-\frac{\rho^2}{2}\right\}d\rho\, d\psi = \left(1+\frac{A_{0\omega}^2}{2\sigma_{2\omega}^2}\right)\exp\left\{-\frac{A_{0\omega}^2}{2\sigma_{2\omega}^2}\right\}\frac{\sigma_{2\omega}^2\beta^2}{\sigma_{2\omega}^2\beta^2+\sigma_{1\omega}^2}. \tag{35}$$

Let the average signal level at the ear of the listener be L_{av} db and let it be defined by the quantity $\overline{I_1^2}$, i.e., by the average intensity of the output signal; let the threshold value of $A_{0\omega}$ be the threshold of audibility under the auditory conditions in the auditorium ($L_{0\omega}$). Then we may write

$$\sigma_1^2 = \overline{I_1^2} = \int_{\omega_1}^{\omega_\mu} S_1(\omega)\,d\omega = a^2\overline{u_1^2} \to I_0\cdot 10^{L_{av}/10}, \tag{36}$$

$$A_{0\omega}^2 \to I_0\cdot 10^{L_{0\omega}/10},$$

$$\frac{\sigma_{2\omega}^2}{A_{0\omega}^2} = \frac{\sigma_{2\omega}^2}{\sigma_1^2}10^{(L_{av}-L_{0\omega})/10}. \tag{37}$$

Here I_0 is the standard null level of the intensity; $L_{0\omega}$ is the relative level of the audibility threshold at a frequency ω, expressed in db above I_0.

Let us be reminded that when the nonlinearity characteristic is of the form (9), the correlation function for the signal fluctuations at the output is of the form:

$$\begin{aligned}\overline{II_\tau} - (\overline{I})^2 = a^2\overline{u_1^2}R(\tau) + 2b^2(\overline{u_1^2})^2R^2(\tau) + \\ + 3c^2(\overline{u_1^2})^3[2R^3(\tau) + 3R(\tau)].\end{aligned} \tag{38}$$

This permits us to evaluate the spectral density of the fluctuations of quadratic products at the output:

$$S_2 = 2b^2(\overline{u_1^2})^2\int_0^\infty R^2(\tau)\cos\omega\tau\, d\tau,$$

whence

$$\sigma_{2\omega}^2 = 2b^2(\overline{u_1^2})^2\Delta\omega\int_0^\infty R^2(\tau)\cos\omega\tau\, d\tau, \tag{39}$$

and likewise

$$\sigma_{1\omega}^2 = a^2\overline{u_1^2}\Delta\omega\int_0^\infty R(\tau)\cos\omega\tau\, d\tau. \tag{-40}$$

By means of (36), (37), (39) and (40) all the quantities included in the expression for P_{t_a} are evaluated in terms of the characteristics of the input signal, its average intensity and correlation coefficient $R(\tau)$, the transfer coefficients of the channel a, b (which characterize the nonlinearity of the channel) and the listening conditions (the average level L_{av} and the level of the audibility threshold $L_{a\omega}$).

COMPUTATION OF THE AUDIBILITY OF SECOND-ORDER NONLINEAR PRODUCTS FOR AN INPUT SIGNAL WITH A SPECTRUM OF UNIFORM AMPLITUDE

Let the input signal of the system have a spectrum of uniform amplitude within the frequency limits of 100 to 5100 cps. The character of the spectrum of the fundamental signal and of the quadratic products at the output is shown in Figure 3. Let the average power of the output device be N_{av} and the average intensity level of the fundamental signal at the ear of the listener be 80 db. Let a level of 100 db be created at the ear of the listener for a nominal output power of N_{nom} from the output device. Let us perform calculations for five cases corresponding to a harmonic coefficient of $k_f = 1, 2, 3, 5, 10$ % for a nominal power output from the device. It follows from (9) that the harmonic coefficient for c = 0 (pure quadratic distortion) is

$$k_f = \frac{b}{2a} u_m, \tag{41}$$

where u_m is the amplitude of the input signal at nominal output. This amplitude is related to the quantity $\overline{u_1^2}$ by the obvious relationship

$$u_m^2/\overline{2u_1^2} = N_{nom}/N_{av}. \tag{42}$$

On the basis of (38), assuming R = 1 and utilizing (41) and (42), we obtain the intensity for the quadratic nonlinearity products:

$$2b^2 (\overline{u_1^2})^2 = 2k_f^2 (N_{av}/N_{nom}) a^2 \overline{u_1^2}. \tag{43}$$

Further utilizing the law for the intensity distribution of these products over the spectrum [1] shown in Figure 3, and the relationship (39), we obtain

$$\frac{\sigma^2_{2\omega}}{\sigma^2_1} = 2k_f^2 \frac{N_{av.}}{N_{nom.}} \frac{\Delta\omega}{\omega_H - \omega_L} \begin{cases} \dfrac{\omega_H - \omega_L - \omega}{\omega_H - \omega_L} & \text{for } 0 \le \omega \le \omega_H - \omega_L \\[2ex] \dfrac{\omega - 2\omega_L}{2(\omega_H - \omega_L)} & \text{for } 2\omega_L \le \omega \le \omega_L + \omega_H \\[2ex] \dfrac{2\omega_H - \omega}{2(\omega_H - \omega_L)} & \text{for } \omega_L + \omega_H \le \omega \le 2\omega_H. \end{cases} \tag{44}$$

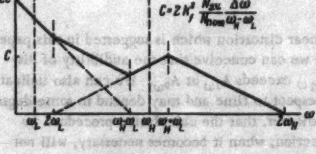

Figure 3.

The values for the audibility threshold under the conditions of the auditorium which were assumed in our calculation are given in Table 2. The magnitude of β^2 is assumed equal to 100 (the threshold intensity of the masked signal is 20 db lower than the masking signal in the critical band). The magnitude of the average intensity of the fundamental signal in the band $\Delta\omega$ is $\sigma^2_{1\omega} = \sigma_1^2 \Delta\omega/(\omega_H - \omega_L)$, since the spectrum of the input signal is of uniform amplitude. On this basis we may write

$$\frac{\sigma^2_{2\omega}}{\sigma^2_{1\omega}}\beta^2 = 2k_f^2\beta^2\,\frac{N_{\text{av.}}}{N_{\text{nom.}}}\begin{cases}\dfrac{\omega_H-\omega_L-\omega}{\omega_H-\omega_L} & \text{for } 0 \le \omega \le \omega_H-\omega_L\\[2ex] \dfrac{\omega-2\omega_L}{2(\omega_H-\omega_L)} & \text{for } 2\omega_L \le \omega \le \omega_H+\omega_L\\[2ex] \dfrac{2\omega_H-\omega}{2(\omega_H-\omega_L)} & \text{for } \omega_H+\omega_L \le \omega \le 2\omega_H.\end{cases} \qquad (45)$$

The Equalities (44) and (45) permit us to calculate P_{0a} by means of (35), according to the procedure suggested above. The results of the calculations are given in Table 2. The calculations were performed for eight values of average frequency for corresponding critical bands (the specified widths of the critical bands are given in Table 1).

TABLE 2

Average frequency in the critical band, db	50	100	200	400	800	2000	4000	8000
Audibility threshold, db	70	45	35	25	18	15	18	25
			The probability P_{0a} for five values of k_f:					
$k_f = 1\%$		A negligibly small probability				$4.6 \cdot 10^{-10}$	$4.6 \cdot 10^{-10}$	
$k_f = 2\%$					$0.48 \cdot 10^{-5}$	0.004	$8.3 \cdot 10^{-5}$	
$k_f = 3\%$				$1.5 \cdot 10^{-9}$	0.005	0.035	0.013	$0.63 \cdot 10^{-12}$
$k_f = 5\%$				0.005	0.14	0.19	0.08	$0.4 \cdot 10^{-4}$
$k_f = 10\%$			$1.8 \cdot 10^{-8}$	0.05	0.66	0.55	0.31	0.08

Table 2 shows that in this simplest case the real threshold at which quadratic distortion will be noticeable lies between $k_f = 2\%$ and $k_f = 3\%$, since, when $P_{0a} = 3.5\%$ for the 2000 cps and 1.3% for the 4000 cps band (the values of P_{0a} are calculated for $k_f = 3\%$), we may assume that nonlinear distortion will exist during transmission and will be noticeable to the ear even though present only for a short time. For $k_f = 5\%$, up to 14-19% of the entire transmitted intelligence may be spoiled by distortion which is audible. It is interesting to note still another fact: if the dynamic range of the transmitted intelligence is compressed, then a smaller value of k_f is required to obtain the same probability P_{0a}. Let us assume for example that L_{max} is not 20 but 15 db greater than L_{av}. Then the same value of $(\sigma^2_{2\omega}/\sigma^2_{1\omega})\,\beta^2$ and of all other quantities included in the calculation of P_{0a} will be obtained for a smaller k_f. The same probability of 3.5 % will be obtained for $k_f = 1.7\%$. Here it is assumed that the average level of transmission has not changed. If, however, the average level is diminished, then we may once again lower the requirements of the apparatus as far as nonlinearity is concerned.

The method of calculating the audibility of nonlinear distortion which is suggested in this paper is, of course, based upon a series of assumptions. In particular we can conceive that the audibility of distortion may be different depending on the amount by which $A_{n\omega}$ exceeds $A_{1\omega}$ or $A_{0\omega}$. We can also indicate that the threshold $A_{0\omega}$, strictly speaking, is not constant with respect to time and may depend to some degree or other upon the transmitted program itself. It seems to us, however, that the calculation procedure we have proposed is nevertheless very promising, and that its perfection, when it becomes necessary, will not present any difficulties in principle.

LITERATURE CITED

[1] V. A. Bunimovich, "Fluctuating Processes in Radio-Receiving Units," Soviet Radio, Moscow, 1951: A. V. Rimskii-Korsakov, "Nonlinear Distortion of a Non-Periodic Signal in an Electroacoustical Channel," Acoust. J. 1, 2, 165-170 (1955).

[2] S. N. Rzhevkin, Hearing and Speech in Light of Modern Research in Physics, United Sci.-Tech. Press, Moscow-Leningrad, 1936.

[3] B. A. Fersman, Theses of Papers Read at the Scientific-Technical Conference of the Leningrad M. A. Bonch-Bruevich Electrical Engineering Communications Institute, Leningrad, March, 1955.

Received February 28, 1955

Leningrad Bonch-Bruevich
Electrical Engineering Communications Inst.

DIELECTRIC AND PIEZOELECTRIC PROPERTIES OF SOLID SOLUTIONS OF $(Ba, Sr)TiO_3$, $(Ba, Pb)TiO_3$, $Ba(Ti, Sn)O_3$ and $Ba(Ti, Zr)O_3$

N. A. Roi

The paper experimentally defines the temperature variation of the dielectric permeability of several solid solutions with a barium titanate base; their piezomoduli are measured and the magnitudes of their coercive forces at room temperature are found. It is established that the most interesting solutions from the point of view of their application as electromechanical transducers are solid solutions of barium titanate and lead titanate, barium titanate and barium stannate.

In the lattice of barium titanate, the substitution of calcium, strontium and lead ions for the barium ion, and the substitution of zirconium and tin ions for the titanium ions causes a substantial change in the properties of this substance [1]. It is known, for example, that a partial substitution of strontium ions for barium ions [2-4] or the substitution of zirconium ions for the titanium ions [2] results in a state where the high-temperature phase transition maximum of the dielectric permeability is displaced in the direction of low temperatures. The paper cited in [5] indicates an increase in the coercive force of the ceramic after the substitution of lead ions for a portion of the barium ions.

The replacement of one of the ion types by others is accomplished by forming solid solutions of isomorphous substances during the baking of the ceramic. For example, in order to form a ceramic in which a partial substitution of strontium ions for barium ions is effected, we proceed in the following manner. Barium titanate and strontium titanate ceramic is prepared in the ordinary manner; then after a thorough grinding the resulting substances are formed into powder mixes containing specified amounts of the original components which are expressed in molecular percentages. The resulting mixtures are pressed and baked in the ordinary manner. At a temperature of the order of 1360° C a reaction occurs in solid phase of the mixture; as a result of this reaction a solid solution is formed in whose lattice several barium ions are replaced by strontium ions.

For the purpose of clarifying which substances are of interest from the point of view of their application as electromechanical transducers, we investigated the variation in the properties of barium titanate, which occurred as a result of substituting strontium and lead ions for the barium ions in the lattice of barium titanate, and the substitution of zirconium and tin ions for the titanium ions. At our disposal were samples of solid solutions of $(Ba, Sr)TiO_3$, $(Ba, Pb)TiO_3$, $Ba(Ti, Sn)O_3$ and $Ba(Ti, Zr)O_3$ which were prepared in the Scientific Research Physics-Mathematical Institute of the V. M. Molotov Rostov State University and provided to us through the courtesy of N. S. Novosil'tsev; these solutions were of the following composition;

The original samples were cut up and milled down to dimensions of 2 x 3 x 5 mm^3. The electrodes were applied at the boundaries of the 3 x 5 mm^2 surface.

TEMPERATURE DEPENDENCY OF THE DIELECTRIC PERMEABILITY OF SOLID SOLUTIONS

By means of a KV-1 Q-meter, measurements of the dielectric permeability of the solid solutions listed above were made at various temperatures. Figures 1, 2, 3, 4 show the temperature dependency of the dielectric permeability of several of these solid solutions. On the basis of the results obtained, it can be seen that the substitution of Sr ions for Ba ions and the substitution of Sn and Zr ions for Ti ions causes a displacement of the ε maximum corresponding to the high-temperature phase transition in the direction of low temperatures. The temperature points which correspond to the maxima of ε for the above solid solutions with additive components of varying content are recorded in Figure 5. On the basis of the data appearing in that figure it is evident that the temperature corresponding to the maximum of ε depends linearly upon the concentration of the additive components and that the straight line which is plotted for solid solutions of the type Ba(Ti, Sn)O$_3$ has the maximum slope; i.e., the most rapid displacement of the high-temperature phase transition toward low temperatures is caused by the substitution of Sn ions for Ti ions.

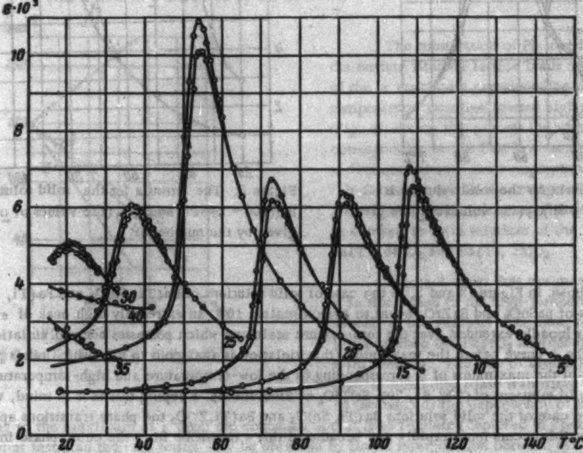

Figure 1. The formula of the solid solution is [(100 − n)% Ba, n%Sr]TiO$_3$ (the values of n are given by the numbers).

A comparison of the measurements made on samples of the solid solutions (Ba, Sr)TiO$_3$ and Ba(Ti, Zr)O$_3$, which were at our disposal, with the results cited in the paper by G. A. Smolenskii [2] shows that the rates of displacement for the high-temperature phase transitions were the same for our samples as they were for the samples of Smolenskii. Let us note that on the basis of the measurements of the dielectric permeability of the solid solutions (Ba, Sr)TiO$_3$ conducted by Smolenskii over a wider interval, it can be seen that the first low temperature phase transition which takes place near zero degrees in barium titanate is displaced more slowly than the high-temperature transition in the direction of low temperatures when Sr ions are partially substituted for Ba ions. Because of this, the region of temperatures in which a tetragonal phase exists diminishes and disappears entirely when the $SrTiO_3$ content equals approximately 70-80%. This evidently means, for such a relationship of components in a solid solution of $(BaSr)TiO_3$, that a transition of material from the cubic phase directly into the orthorhombic phase occurs when the temperature is lowered.

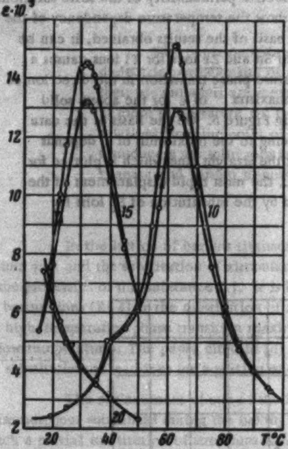

Figure 2. The formula for the solid solution is $Ba[(100-n)\%Ti, n\% Sn]O_3$ (the values of n are given by the numbers).

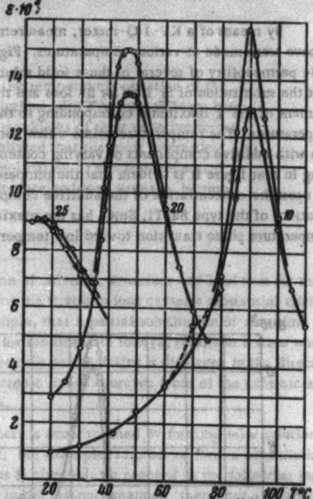

Figure 3. The formula for the solid solution $Ba[(100-n)\%Ti, n\%Zr]O_3$ (the values of n are given by the numbers).

As is shown in Figures 2 and 3, in the case of solid solutions of $Ba(Ti, Sn)O_3$ and $Ba(Ti, Zr)O_3$ containing amounts of $BaSnO_3$ and $BaZrO_3$ equal to approximately 10%, an extremely high peak of ε is observed which is broadly extended over the temperature scale and which possesses a small violation of the smoothness of the ε curve before the maximum. (this violation is analogous to that which takes place during the merging of the maximums of ε corresponding to the low-temperature and high-temperature transitions in the solid solutions of (30% Ba, 70% Sr)TiO_3 of Smolenskii). Keeping this fact in mind, we may postulate that in the case of the solid solutions $Ba(Ti, Sn)O_3$ and $Ba(Ti,Zr)O_3$ the phase transitions approach each other; however this occurs more rapidly and because of this a transition from the cubic phase into the orthorhombic and possibly even to the trihedral phase begins to take place in solid solutions of these types when they contain 10% of an additive component.

The linear extrapolation of the dependency of the temperature corresponding to the maximum of ε at the high-temperature phase transition upon the concentration of $SrTiO_3$ in solid solutions of the type $(Ba, Sr)TiO_3$ out to a 100% $SrTiO_3$ content points out the fact that the phase transition of strontium titanate from a non ferro-electric phase to a ferroelectric phase must take place at a temperature which is approximately equal to 70°K. In one of the latest papers by Smolenskii [6] this is proven experimentally. If such a linear extrapolation is valid for the solid solutions $Ba(Ti, Sn)O_3$ and $Ba(Ti, Zr)O_3$ as well, we may then expect that $BaZrO_3$, as well as $SrTiO_3$ must undergo a transition to a ferroelectric phase at low temperatures of the order of 10°K, while $BaSnO_3$ will not be transformed into a ferroelectric at any temperature.

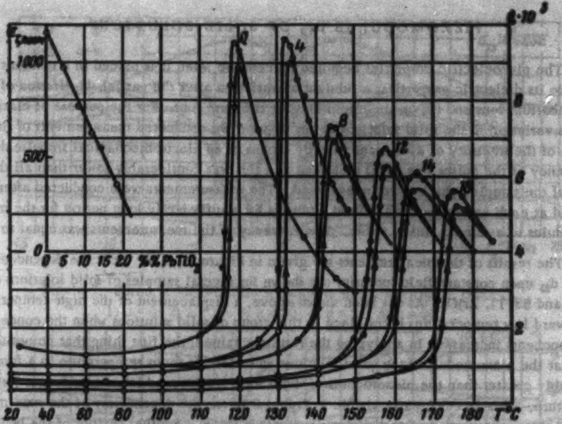

Fig. 4. The formula for the solid solution is $[(100 - n)\%Ba, n\%Pb]TiO_3$ (the values of n are given by the numbers).

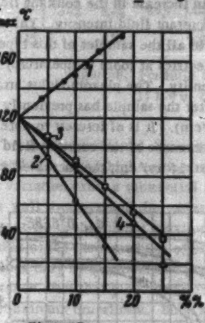

Figure 5.
1) $PbTiO_3$; 2) $BaSnO_3$; 3) $SrTiO_3$; 4) $BaZrO_3$.

The substitution of Pb ions for Ba ions in the barium titanate lattice leads to a displacement of the ε maximum corresponding to the high-temperature transition toward high temperatures (Fig. 4); during this process the small peak of ε corresponding to the first low-temperature transition is displaced toward low temperatures, and as a result the region where the tetragonal phase exists is widened in solid solutions of the type $(Ba,Pb)TiO_3$, in contrast to solid solutions of the type $(Ba, Sr)TiO_3$, $Ba(Ti, Sn)O_3$ and $Ba(Ti, Zr)O_3$.

Figure 4 shows that the maximum value of ε in the region of the high-temperature transition, as well as the value of ε at room temperature, is lowered when the $PbTiO_3$ content is increased in the solid solution. The rate of displacement of the high-temperature phase transition, which is found on the basis of the dependency of the temperature corresponding to the maximum of ε upon the concentration of lead titanate (depicted in Figure 5), proves to be somewhat less than the rate which may be obtained by linear interpolation between temperature points corresponding to pure barium titanate and pure lead titanate; according to Smolenskii and [7], the transition temperatures are approximately equal to 515° C and 490 °C respectively. The decrease in ε at room temperature occurs more rapidly when the concentration of lead titanate in the solid solution is increased than would be expected on the basis of the linear interpolation of the dielectric permeability between the values for pure lead titanate for which the value of ε is given in the paper by Smolenskii. It should be noted that the temperature coefficient of dielectric permeability for solid solutions of the type $(Ba, Pb)TiO_3$, as may be concluded on the basis of the data provided in Figure 4, is extremely small over a wide region of temperatures extending approximately from 10 to 110° C.

PIEZOMODULUS d_{33} OF SOLID SOLUTIONS

The piezoelectric properties acquired by ceramic when it is placed in a constant electric field undergo, as do its dielectric properties, a substantial variation after the partial substitution of strontium or lead ions for barium ions and tin or zirconium ions for titanium ions. For the purpose of clarifying the nature of this variation in the solid solutions at our disposal we conducted measurements of the piezomodulus as a function of the intensity of a constant field by means of an electromechanical impulse diprod [8]. The carrier frequency of the pulses was equal to 150 kc and this was considerably lower than all the natural frequencies of the samples which were investigated. The measurements were conducted after the sample had been held at each value of constant field intensity for a sufficiently long period for the magnitude of the piezomodulus to assume a steady value. The accuracy of the measurements was equal to 10-15 %.

The results of the measurements are given in Figures 6, 7, 8. Here the dependencies of the piezomoduli d_{33} upon constant field intensity are shown for several samples of solid solutions of $(Ba,Sr)TiO_3$, $Ba(Ti,Sn)O_3$ and $Ba(Ti, Zr)O_3$. As has been shown above, a displacement of the high-temperature phase transition toward low temperatures takes place in this group of solid solutions when the concentration of additive components increases. In analyzing the results obtained, the first thing that comes to the attention is the fact that the piezomoduli of the solid solutions which are at room temperature in a ferroelectric phase are considerably greater than the piezomoduli of those solid solutions which are no longer ferroelectric at that temperature. This fact is clearly visible in Figure 9 where the dependency of the maximum piezomodulus upon the concentration of additive components is shown. Another feature of the behavior of the piezomoduli of these solid solutions is the fact that in those solid solutions which are at room temperature in the ferroelectric phase, the piezomodulus at first increases with an increase in the constant field intensity and then evidences a tendency to decrease for a further increase in constant field intensity. This tendency is most clearly evident in solid solutions of the type $Ba(Ti, Sn)O_3$. In all the samples of this type in which the $BaSnO_3$ content does not exceed 15% (i.e., until they are ferroelectrics at room temperature) a maximum of the piezomodulus occurs for some value of the constant field intensity. The piezomodulus attains especially large values when the constant field intensity is lowered after the sample has previously been subjected to a relatively large constant field (of the order of 15 kv/cm). It is of interest to note that upon repeated increases of the field intensity and, in general, during the increase of the constant field intensity within the limits of zero to 15 kv/cm or within the limits of zero to − 15 kv/cm, the increased values of the piezomodulus are repeated fairly accurately.

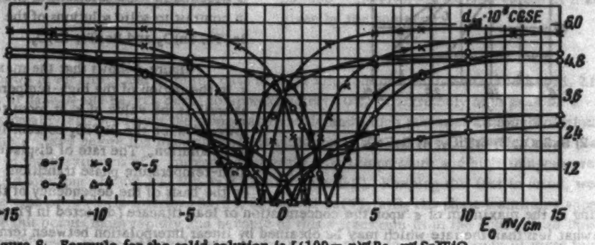

Figure 6. Formula for the solid solution is $[(100-n)\%Ba, n\%Sr]TiO_3$:
1) n = 0; 2) n = 10; 3) n = 20; 4) n = 25; 5) n = 28.

For the purpose of clarifying whether the increased values of the piezomodulus which were obtained when the field was lowered to 1 − 1.5 kv/cm after a preliminary subjection of the sample to a large field were stable with respect to time, repeated measurements of the piezomodulus were made after the sample had been kept for three hours in a field which produced the maximum value of the piezomodulus. As a result it became clear that the piezomodulus does not diminish. From this we may conclude that the observed increases in the values of piezomodulus for these solid solutions are not due to relaxation processes which are similar to the processes which establish the dielectric permeability when a mechanical stress is applied as is described in [9].

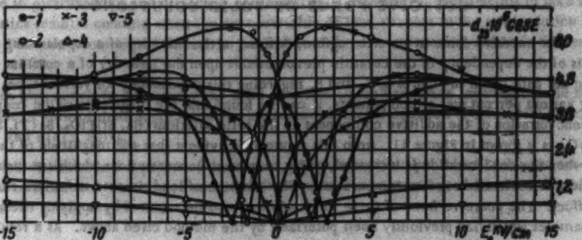

Figure 7. Formula for the solid solution is Ba[(100−n)%Ti, n%Sn]O$_3$.
1) n = 0; 2) n = 10; 3) n = 20; 4) n = 25; 5) n = 30.

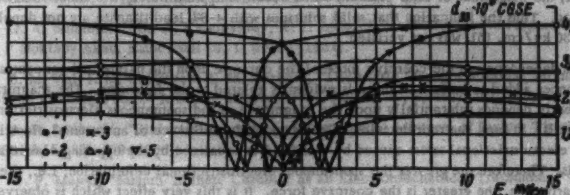

Figure 8. Formula for the solid solution is Ba[(100−n)%Ti, n%Zr]O$_3$.
1) n = 0; 2) n = 10; 3) n = 20; 4) n = 25; 5) n = 30.

The above-mentioned decrease of the piezomodulus for large constant fields may be explained if it is postulated that in the high-temperature portion of the ferroelectric region the processes of domain wall structure variation exert a substantial influence upon the magnitude of the piezomodulus. The variation of the domain wall structure and the variation in the dimensions of the ceramic which is related to it ceases for large constant fields in which a maximum orderliness of the domain wall structure is attained. Because of this, the value of the piezomodulus of ceramic which is in such a condition proves to be somewhat less, and is determined only by the magnitude of the piezomodulus of a single-domain wall monocrystal of the specified substance after that piezomodulus has been averaged over all the domain wall orientations for conditions of maximum orderliness. Such are the results of investigating the dependencies of piezomoduli upon constant field intensity for solid solutions of (Ba, Sr)TiO$_3$, Ba(Ti, Sn)O$_3$ and Ba(Ti, Zr)O$_3$.

The results obtained for the investigation of the piezoelectric properties of solid solutions of (Ba, Pb)TiO$_3$ differ to a considerable degree from the results described above. The first fact that was clarified here was that the ordinary polarization of these solid solutions is not able to achieve a piezomodulus which is to any extent substantial. Therefore we utilize the method of polarization by heating which is cited in [5] and which has been investigated by B. M. Vul and R. Ia. Razbash. This method consists of heating the samples which are in a comparatively small constant field of the order of 5–10 kv/cm to a temperature in the region of high-temperature phase transition, and then slowly cooling them to room temperature with the field still acting. As a result of such a process the samples are polarized to saturation and possess a maximum residual polarization after the constant field is removed. The results of the piezomodulus measurements for solid solutions of (Ba, Pb)TiO$_3$ which have been polarized in such a manner are given in Figure 10 (above) where it is evident that the piezomodulus becomes twice as small when the concentration of lead titanate in the solid solution increases to 15%.

COERCIVE FORCE OF SOLID SOLUTIONS

The coercive force in a static regime, defined as the intensity of a depolarizing field, may be found on the basis of the dependency of the ceramic piezomodulus upon the intensity of a constant field. Basing ourselves upon the data given in Figures 6, 7, and 8, regarding this dependency for various types of solid solutions containing various percentages of components, it can be found that the magnitude of the coercive force depends upon the concentration of the additive component in the solid solutions $(Ba, Sr)TiO_3$, $Ba(Ti, Sn)O_3$ and $Ba(Ti, Zr)O_3$ as is shown in Figure 11; from this figure it is evident that the magnitude of the coercive force decreases when the concentration is increased, going to zero at concentrations which are such that the substance ceases to be a ferroelectric at room temperature. The addition of lead titanate to barium titanate produces an opposite effect. The coercive force of these solid solutions was determined by applying reverse-field depolarization to samples which had previously been polarized by the method cited above. As a result it was found that the coercive force of solid solutions of $(Ba, Pb)TiO_3$ increases when the concentration of lead titanate increases (Figure 10). Solid solutions with a lead-titanate content of the order of 10-15% do not show any signs of a decreasing piezomodulus in fields of the order of 5 kv/cm, while for solid solutions with a lower lead-titanate content, the magnitude of their piezomodulus becomes approximately 2-3 times smaller when such fields are applied. Thus the indication that solid solutions with 4-8% lead titanate are not depolarized in fields of the order of 30 kv/cm, [5], was not verified.

The dependency of the coercive force of the ceramic upon the nature and concentration of the isomorphous substances added to barium titanate is evidently related to the following. The magnitude of the coercive force evidently depends substantially upon the magnitude of the spontaneous electrostrictional deformation of elementary cells. In fact, the reorientation of cells under the influence of an external electric field will occur when the electrostrictional stress caused by this field is equalized by the opposing elastic stresses of the surrounding cells. Therefore the greater the spontaneous electrostrictional deformation, i.e., the greater the spontaneous polarization, the greater is the coercive force. It is this very effect which is observed in solid solutions. In those solid solutions where an additive displaces the phase transition towards the low temperatures, and where at room temperature there is thus a decrease in the spontaneous polarization and the electrostrictional deformation which accompanies it, the coercive force decreases when the concentration of the additive is increased; conversely, when lead titanate is added, an increase in the spontaneous polarization and the electrostrictional deformation which accompanies it results in an increase of the coercive force.

On the basis of the results developed above for the investigation of the properties of solid solutions, we may draw the following conclusions.

The addition of up to 15% barium zirconate to barium titanate results in a growth of the dielectric permeability and in a decrease of piezomodulus and coercive force (all quantities are referred to room temperature). These variations are evidently of no interest when this type of solid solution is to be used as an electromechanical transducer.

The addition of up to 20% of strontium titanate to barium titanate causes an increase in dielectric permeability at room temperature to 2000, an increase in piezomodulus to $5.5 \cdot 10^6$ CGSE and to the reduction of the coercive force to 1.2 kv/cm. In order to maintain a large magnitude for the piezomodulus, constant polarization is required by means of a constant electric field with an intensity of the order of 3-5 kv/cm.

The addition of up to 10-15% of barium stannate to barium titanate permits a maximum piezomodulus of the order of $6.5 - 8 \cdot 10^6$ CGSE to be obtained under the conditions of constant polarization by a constant field with an intensity of the order of 1.5 kv/cm. Under these conditions the dielectric permeability is of the order of 5000. Let us note the extremely strong and practically reversible dependency of the dielectric permeability of these solid solutions upon the intensity of the constant field. When constant polarization is present, the elastic and piezoelectric properties of solid solutions with the indicated composition are stable in the temperature range of from 10 to 30° C; we may consider this to be true on the basis of the temperature dependencies of the resonant frequencies and Young's moduli found in experiments on the radial vibrations of a thin disc.

The addition of lead titanate to barium titanate causes a substantial increase in the coercive force of the substance, and this allows such a solution to be used in ultrasonic high-power radiators. In solid solutions of this type a decrease in piezomodulus and dielectric permeability is observed; it is of interest to note that the ratio of these characteristics remains constant when the concentration of lead titanate in the solid solution is increased from zero to 18%. The piezoelectric and dielectric properties of these substances are stable in the temperature range of from 0 to 110°C.

Thus we may conclude that among the solid solutions which have been investigated the most interesting from the point of view of their application as electromechanical transducers are the solid solutions of the type (Ba, Pb) TiO_3 and $Ba(Ti, Sn)O_3$.

The work discussed in the papers of the author, which have been published in the current and previous issues of the Journal of Acoustics, was carried out in 1952-53 under the supervision of Academician M. N. Andreev, to whom the author expresses his appreciation.

LITERATURE CITED

[1] G. A. Smolenskii, "Polarization and Dielectric Losses of Zirconates, Stannates and Several Titanates of Bivalent Metals," J. Tech. Phys. (USSR) 22, 1,3-11 (1952).

[2] G. A. Smolenskii, M. A. Karamyshev, K. I. Rozgachev, "Ferroelectric Properties of Several Solid Solutions," Doklady Akad. Nauk SSSR 79, 1, 53-56 (1951).

[3] B. M. Vul, I. M. Gol'dman, R. Ia. Razbash, "Dielectric Strength of Metal Titanates of the Second Group of the Periodic Table," J. Exptl.-Theoret. Phys. (USSR) 20, 5, 465-470 (1950).

[4] A. K. Ishkhneli, "Dielectric Properties of Isomorphous Mixtures of Barium Titanate," Bull. Acad. Sci. Georgian SSR 11, 5, 275-279 (1950).

[5] W. P. Mason, "Barium Titanate Ceramic as an Electromechanical Transducer," Bell. Lab. Record 27, 8, 285-288 (1948).

[6] G. A. Smolenskii, "Ferroelectric Properties of Several Crystals," Doklady Akad. Nauk SSSR 85, 5, 985-987 (1952).

[7] G. Shiranc, K. Suzuki, "On the Phase Transition in Barium-Lead Titanate," J. Phys. Soc. Japan, 6, 274-278 (1951).

[8] N. A. Roi, "Temperature Dependency of the Electrostrictional and Elastic Properties of Barium Titanate Ceramic," Acoust. J. 1, 3, 264-271 (1955).

[9] N. A. Roi, "The Coercive Force and Dielectric Permeability of Barium Titanate Ceramic as Functions of Mechanical Stress," Acoust. J. 1, 4, 352-355 (1955).

Received January 31, 1955

Acoustical Institute of the
Academy of Sciences USSR, Moscow

ACOUSTICAL PROPERTIES OF A THINLY LAMINATED MEDIUM*

S. M. Rytov

A medium which consists of alternating laminations of two isotropic substances behaves on the average as a homogeneous but isotropic medium when the wave field varies little over the thickness of an individual lamina (thin laminations). The anisotropy is that of a hexagonally symmetrical crystal. Expressions are obtained for the effective elasticity constants of the crystal as functions of the parameters of both substances and of the lamination thicknesses. The article examines the alternation of laminations of two solid substances and the alternation of solid and liquid laminations.

Artificial thinly-laminated media whose preparation is not complex and whose properties may be extremely varied (anisotropy of the propagation velocities and absorptions both for compression waves and for shear waves) are of a known practical interest, in particular for the purpose of isolating vibrations.

1. A medium composed of alternating laminations of two homogeneous and isotropic substances behaves "on the average", i.e., when the laminations are sufficiently thin, as a homogeneous but anisotropic medium. The condition concerning the thinness of the laminations means that their thicknesses are small in comparison to the compression and shear wave lengths in their materials.

The problem of finding the effective parameters (the moduli of elasticity) of a thinly-laminated medium may be approached in various ways. One of the methods is based upon the postulate that layers alternate periodically. The problem of the propagation of waves then becomes a problem of solving a wave (and then an ordinary) equation with periodic coefficients. Since the parameters are constant within the laminations and change discontinuously only at the boundaries between laminations, a solution may be found in the general case of laminations which are not thin. As a result of a transition in the limit, a solution for a thinly-laminated medium follows from this general solution, and by applying corrective terms it is possible to make the conditions for applying the indicated limiting results more precise.

By such a method the author has earlier examined the problem of the electromagnetic properties of a thinly-laminated medium [1]. They proved to be, naturally, the same as those of a uniaxial crystal; i.e., they are described by single-decomposition tensors of the dielectric and magnetic permeabilities. It should be remarked that in the approximation indicated (sufficiently thin laminations) the losses and, generally speaking, the quadratic quantities may be calculated by ordinary formulas which are based directly upon the averaged field equations with effective values of ϵ and μ. When the thickness of the lamination is increased, the relationship between the mean and mean-square values becomes more complex and it is therefore necessary to average the true quadratic values for the purposes of calculation.

In relation to its elastic properties, a thinly-laminated medium is a hexagonally symmetrical crystal; i.e., it is characterized by five elastic moduli. In the electromagnetic problem it was sufficient to examine waves which were propagated solely in directions perpendicular and parallel to the laminations in order to find the effective values of ϵ and μ; in the latter case it is necessary to consider two types of polarization

---

* Read July 1, 1955 at the Electroacoustical Conference called in Kiev by the Acoustical Commission, the Acoustical Institute Acad. Sci. USSR and the Kiev Polytechnic Institute.

(the electrical vector parallel or perpendicular to the laminations). In the acoustical problem there are two compression waves in addition to three analogous transverse waves (shear waves). Nevertheless, if we limit the problem solely to the two indicated directions of propagation, then it is only possible to determine four of the five moduli of elasticity.

Let us place the z axis in a direction perpendicular to the laminations. The free energy of a unit volume of a hexagonally symmetrical crystal can then be written in the form

$$F=\frac{\lambda_1}{2}u_{zz}^2+\frac{\lambda_2}{2}(u_{xx}+u_{yy})^2+\lambda_3 u_{zz}(u_{xx}+u_{yy})+$$
$$+2\lambda_4(u_{xy}^2-u_{xx}u_{yy})+2\lambda_5(u_{xz}^2+u_{yz}^2),$$

where u_{ik} are the components of the deformation tensors: $u_{ik}=\frac{1}{2}(\partial U_i/\partial x_k+\partial U_k/\partial x_i)$. In the (x, y) plane, the medium is isotropic. The transition to complete isotropy takes place for

$$\lambda_1=\lambda_2=\lambda+2\mu,\quad \lambda_3=\lambda,\quad \lambda_4=\lambda_5=\mu, \tag{1}$$

where λ and μ are Lamé coefficients. If we define the density of the crystal by ρ, then the squares of the propagation velocities for waves in the x and z directions are expressed in the following manner:

$$c_{xx}^2=\lambda_2/\tilde{\rho},\ c_{xz}^2=c_{zx}^2=\lambda_5/\tilde{\rho},\ c_{xy}^2=\lambda_4/\tilde{\rho},\ c_{zz}^2=\lambda_1/\tilde{\rho}. \tag{2}$$

Here the first index of c indicates the direction of wave propagation; the second index indicates the direction of the vector describing the displacement of the particles of the medium, U.

The modulus of elasticity λ_3 is not included in (2). In order to determine λ_3 we must know the velocity of wave propagation at an angle with the z axis which differs from zero and $\pi/2$. We shall first examine wave propagation in the directions of the x and z axes.

2. Let us separate the total displacement of the particles of the medium in the material of a lamination, **U**, into its non-turbulent and solenoidal portions **u** and **v**:

$$\mathbf{U}=\mathbf{u}+\mathbf{v},$$
$$\ddot{\mathbf{u}}-c_l^2\,\mathrm{grad\,div}\,\mathbf{u}=0,\quad \mathrm{rot}\,\mathbf{u}=0,$$
$$\ddot{\mathbf{v}}-c_l^2\,\mathrm{rot\,rot}\,\mathbf{v}=0,\quad \mathrm{div}\,\mathbf{v}=0, \tag{3}$$

where c_l and c_t are the propagation velocities of the compression and shear waves respectively:

$$c_l^2=(\lambda+2\mu)/\rho,\ c_t^2=\mu/\rho. \tag{4}$$

Let us examine the propagation parallel to the laminations, let us say, along the x axis. Evidently the shear wave with a displacement which is parallel to the laminations (U_y) is autonomous, i.e., is not related to the compression wave. On the contrary, the shear transverse to the laminations (U_z), generally speaking, is related to the longitudinal displacement U_x. Let us initially take the case of a longitudinal-transverse wave with a shear along the z axis, i.e., the case when only the components U_x and U_z which depend upon x and z are different from zero. For a harmonic wave with a frequency ω, Equations (3) then acquire the form

$$\frac{\partial^2\mathbf{u}}{\partial x^2}+\frac{\partial^2\mathbf{u}}{\partial z^2}+k_l^2\mathbf{u}=0,\quad \frac{\partial u_z}{\partial x}=\frac{\partial u_x}{\partial z},$$
$$\frac{\partial^2\mathbf{v}}{\partial x^2}+\frac{\partial^2\mathbf{v}}{\partial z^2}+k_l^2\mathbf{v}=0,\quad \frac{\partial v_x}{\partial x}=-\frac{\partial v_z}{\partial z}, \tag{5}$$

where $k_l^2=\omega^2/c_l^2$, $k_t^2=\omega^2/c_t^2$.

It is useful to write the general solution in terms of specially selected partial solutions, namely in terms of an even and an odd solution with respect to the center of the laminations. For a lamination I of the material lying between z = 0 and z = a (Figure 1) we have the following solutions of Equations (5):

$$u_x = P(z)\,e^{-ikx},\; u_z = -\,\frac{P'(z)}{ik}\,e^{-ikx},$$

$$v_x = \frac{Q'(z)}{ik}\,e^{-ikx},\; v_z = Q(z)\,e^{-ikx}, \tag{6}$$

and for these conditions,

$$P(z) = A\cos\alpha\,(z - a/2) + B\sin\alpha\,(z - a/2),\; \alpha^2 = k_l^2 - k^2,$$

$$Q(z) = C\cos\beta\,(z - a/2) + D\sin\beta\,(z - a/2),\; \beta^2 = k_t^2 - k^2. \tag{7}$$

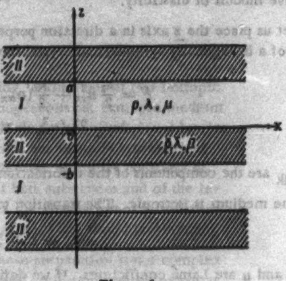

Figure 1.

We shall define the quantities relating to a layer II which lies between z = − b and z = 0 by the same letters but shall draw a line above them. Thus, in layer II

$$\overline{u}_x = \overline{P}(z)\,e^{-ikx},\; \overline{u}_z = -\frac{\overline{P}'(z)}{ik}\,e^{-ikx},\quad \overline{v}_x = \frac{\overline{Q}'(z)}{ik}\,e^{-ikx},\; \overline{v}_z = \overline{Q}(z)\,e^{-ikx}, \tag{8}$$

where

$$\overline{P}(z) = \overline{A}\cos\overline{\alpha}(z + b/2) + \overline{B}\sin\overline{\alpha}(z + b/2),\; \overline{\alpha}^2 = \overline{k}_l^2 - k^2,$$

$$\overline{Q}(z) = \overline{C}\cos\overline{\beta}(z + b/2) + \overline{D}\sin\overline{\beta}(z + b/2),\; \overline{\beta}^2 = \overline{k}_t^2 - k^2. \tag{9}$$

For the components of the deformation tensor in layer I we obtain

$$u_{xx} = -(ikP + Q')\,e^{-ikx},\; u_{xy} = 0,\; u_{xz} = \left(P' + \frac{k^2 - \beta^2}{2ik}Q\right)e^{-ikx},$$

$$u_{yy} = u_{yz} = 0,\; u_{zz} = \left(\frac{\alpha^2}{ik}P + Q'\right)e^{-ikx},$$

whence the components σ_{ik} of the stress tensor $(\sigma_{ik} = \lambda u_{\alpha\alpha}\,\delta_{ik} + 2\mu u_{ik})$ prove to be equal

$$\sigma_{xz} = 2\mu\left(P' + \frac{k^2 - \beta^2}{2ik}Q\right)e^{-ikx},\; \sigma_{yz} = 0,$$

$$\sigma_{zz} = \left(\frac{\lambda k_l^2 + 2\mu\alpha^2}{ik}P + 2\mu Q'\right)e^{-ikx}. \tag{10}$$

In an analogous manner we may express the components $\overline{u}_{ik}$ and $\overline{\sigma}_{ik}$ in layer II.

Two sets of conditions must be fulfilled at the boundaries between layers for $U_x = u_x + v_x$, $U_z = u_z + v_z$, σ_{xz} and σ_{zz}: in the first place, the continuity conditions for z = 0 must be fulfilled, and in the second place, the conditions of periodicity must be fulfilled (i.e., the indicated quantities in layer I for z = a − 0 must equal the corresponding quantities in layer II, z = − b + 0):

$$\begin{aligned} &U_x(0)=\overline{U}_x(0), && U_x(a-0)=\overline{U}_x(-b+0),\\ &U_z(0)=\overline{U}_z(0), && U_z(a-0)=\overline{U}_z(-b+0),\\ &\sigma_{xz}(0)=\overline{\sigma}_{xz}(0), && \sigma_{xz}(a-0)=\overline{\sigma}_{xz}(-b+0),\\ &\sigma_{zz}(0)=\overline{\sigma}_{zz}(0), && \sigma_{zz}(a-0)=\overline{\sigma}_{zz}(-b+0). \end{aligned} \tag{11}$$

The substitution of the solutions of (6-10) into (11) yields eight equations for the constants A, B, ..., $\overline{D}$; these equations separate into two independent groups.

a) A wave which, on the average, is longitudinal ($B = C = \overline{B} = \overline{C} = 0$). As can be seen from (7) and (9), in this case the longitudinal displacements are even (symmetrical) relative to the centers of the laminations, while the transverse displacements are odd (antisymmetrical), and because of this there takes place "on the average" only compression, and shear is absent. For the constants A, D, and $\overline{A}$, $\overline{D}$ the following equations are obtained from (11):

$$Aik\cos\frac{\alpha a}{2}+D\beta\cos\frac{\beta a}{2}=\overline{A}ik\cos\frac{\overline{\alpha}b}{2}+\overline{D}\overline{\beta}\cos\frac{\overline{\beta}b}{2},$$

$$A(\lambda k_l^2+2\mu\alpha^2)\cos\frac{\alpha a}{2}+D2ik\mu\beta\cos\frac{\beta a}{2}=\overline{A}(\overline{\lambda}k_l^2+2\overline{\mu}\overline{\alpha}^2)\cos\frac{\overline{\alpha}b}{2}+\overline{D}2ik\overline{\mu}\overline{\beta}\cos\frac{\overline{\beta}b}{2},$$

$$A\alpha\sin\frac{\alpha a}{2}+Dik\sin\frac{\beta a}{2}=-\overline{A}\overline{\alpha}\sin\frac{\overline{\alpha}b}{2}-\overline{D}ik\sin\frac{\overline{\beta}b}{2},$$

$$A2ik\mu\alpha\sin\frac{\alpha a}{2}+D(\lambda k_l^2+2\mu\alpha^2)\sin\frac{\beta a}{2}=-\overline{A}2ik\overline{\mu}\overline{\alpha}\sin\frac{\overline{\alpha}b}{2}-\overline{D}(\overline{\lambda}k_l^2+2\overline{\mu}\overline{\alpha}^2)\sin\frac{\overline{\beta}b}{2}.$$

Setting the determinant of this system equal to zero, we obtain the equation of dispersion which determines the value of the wave number k, i.e., the value of the velocity of propagation for the compression wave $c_{xx} = \omega/k$:

$$\begin{aligned} &4(\mu-\overline{\mu})^2X\overline{X}+\omega^2\rho\left[\frac{\omega^2\rho}{k^2}-4(\mu-\overline{\mu})\right]\overline{X}\tan\frac{\beta a}{2}+\\ &+\omega^2\overline{\rho}\left[\frac{\omega^2\overline{\rho}}{k^2}+4(\mu-\overline{\mu})\right]X\tan\frac{\overline{\beta}b}{2}-\frac{\omega^4\rho\overline{\rho}}{k^2}\left(Y\tan\frac{\overline{\beta}b}{2}+\overline{Y}\tan\frac{\beta a}{2}\right)=0, \end{aligned} \tag{12}$$

where for the sake of brevity we have introduced the definitions

$$X=k^2\tan\frac{\beta a}{2}+\alpha\beta\,\mathrm{tg}\,\frac{\alpha a}{2},\quad Y=k^2\tan\frac{\beta a}{2}-\overline{\alpha}\beta\tan\frac{\overline{\alpha}b}{2},$$

$$\overline{X}=k^2\tan\frac{\overline{\beta}b}{2}+\overline{\alpha}\overline{\beta}\,\mathrm{tg}\,\frac{\overline{\alpha}b}{2},\quad \overline{Y}=k^2\tan\frac{\overline{\beta}b}{2}-\alpha\overline{\beta}\tan\frac{\alpha a}{2}.$$

Equation (12) determines k for any values of lamination thickness a and b in the periodic structure under analysis. The transition to a thinly-laminated medium is effected by replacing all the tangents by their arguments. This leads to a substantial simplification of the equation of dispersion and yields the following expression for the square of the velocity of the compression wave c_{xx}:

$$c_{xx}^2=\frac{(a+b)^2+4ab\,\dfrac{(\mu-\overline{\mu})(\lambda+\mu-\overline{\lambda}-\overline{\mu})}{(\lambda+2\mu)(\overline{\lambda}+2\overline{\mu})}}{\tilde{\rho}(a+b)\left(\dfrac{a}{\lambda+2\mu}+\dfrac{b}{\overline{\lambda}+2\overline{\mu}}\right)}, \tag{13}$$

where the average density of the medium is introduced:

$$\tilde{\rho}=\frac{a\rho+b\overline{\rho}}{a+b} \tag{14}$$

Evidently the periodicity no longer plays a role in the case of thin laminations which is being analyzed. The thicknesses of the alternating layers may be changed in an arbitrary manner so long as the condition governing the thinness of these laminations remains in application. Therefore a and b are included in (13) and (14) only in the form of relative thicknesses or fractions of the materials I and II, just as they are in all subsequent results which relate to the limiting case of a thinly-laminated medium:

$$n = \frac{a}{a+b}, \quad \bar{n} = \frac{b}{a+b}. \tag{15}$$

In terms of these relative thicknesses, we write c_{xx}^2 and $\tilde{\rho}$ in the following manner:

$$c_{xx}^2 = \frac{1 + 4n\bar{n}\dfrac{(\mu-\bar{\mu})(\lambda+\mu-\bar{\lambda}-\bar{\mu})}{(\lambda+2\mu)(\bar{\lambda}+2\bar{\mu})}}{\tilde{\rho}\left(\dfrac{n}{\lambda+2\mu}+\dfrac{\bar{n}}{\bar{\lambda}+2\bar{\mu}}\right)}, \tag{16}$$

$$\tilde{\rho} = n\rho + \bar{n}\bar{\rho}. \tag{17}$$

When we are expanding the tangents in powers of their arguments in Equation (12), if we also take into consideration the next (cubic) terms, then we may obtain the conditions of validity for Equation (16) (i.e., the conditions which determine how thin the laminations must be for the specified frequency and the specified parameters of the materials) from the requirement that the corresponding corrections to c_{xx}^2 must be small. However, we shall not stop at this.*

b) A wave which, on the average, is transverse ($A = D = \bar{A} = \bar{D} = 0$). According to (7) and (9), in this case the transverse displacements are even with respect to the centers of the layers, and the longitudinal displacements are odd. As a result the wave "on the average" is a pure shear wave. Without writing the corresponding equations for B, C, and $\bar{B}$, $\bar{C}$, or the general equation of dispersion obtained from them, we immediately give only the limiting (for thin laminations) expression for the velocity $c_{xz} = \omega/k$. In doing this, we are already utilizing the average density (17) and the relative thicknesses (15):

$$c_{xz}^2 = \frac{1}{\tilde{\rho}(n/\mu + \bar{n}/\bar{\mu})}. \tag{18}$$

3. For the other basic cases of propagation, a solution is obtained in a completely analogous manner, and this permits us to limit our discussion to several clarifying remarks.

In a pure shear wave which is propagated along the x axis but produces a particle displacement parallel to the laminations, only the component $U_y = v_y$ differs from zero. In the layer I we have the following solution for this wave:

$$v_y = Q(z)\,e^{-ikx},$$

$$Q(z) = C\cos\beta(z - a/2) + D\sin\beta(z - a/2), \quad \beta^2 = k_t^2 - k^2,$$

---

*Analogous conditions are examined in detail in [1] for electromagnetic waves. Basically, as we have already noted, they reduce to the requirement that the laminations must be thin in comparison to the wave length of the compression and shear waves in their materials, even though the differences between the parameters of the two materials are of substantial magnitude. Physically it is clear that the laminations may be the thicker the less the differences between the properties of the materials. However, it is also true that when the materials are very different, the conditions are not especially rigid.

and in the layer II we have the solution:

$$\bar{v}_y = \bar{Q}(z)e^{-ikx},$$
$$\bar{Q}(z) = \bar{C}\cos\bar{\beta}(z+b/2) + \bar{D}\sin\bar{\beta}(z+b/2), \quad \bar{\beta}^2 = \bar{k}_t^2 - k^2.$$

It can easily be seen that of the components σ_{1z} of the deformation tensor only the component σ_{yz} differs from zero. The determinant of the four equations for C, D and $\bar{C}$, $\bar{D}$ which are derived from the continuity conditions for U_y and σ_{yz} will yield the following dispersion equation when it is set equal to zero:

$$\varkappa\left(\tan^2\frac{\beta a}{2} + \tan^2\frac{\bar{\beta}b}{2}\right) + (1+\varkappa^2)\tan\frac{\beta a}{2}\tan\frac{\bar{\beta}b}{2} = 0,$$

where $\kappa = \overline{\mu\beta}/\mu\beta$.

From this result it follows that for thin laminations, i.e., when the tangents are replaced by their arguments, we obtain the following expression for the square of the velocity $c_{xy} = \omega/k$:

$$c_{xy}^2 = \frac{n\mu + \overline{n\mu}}{\bar{\rho}}. \tag{19}$$

When propagation takes place along the z axis, we may examine a longitudinal wave in which only the displacement component $U_z = u_z = P(z)e^{-ikz}$ is different from zero and a transverse wave in which the displacement is parallel to the laminations (for example, when the displacement is equal to $U_x = v_x = Q(z)e^{-ikz}$), independently from each other. In accordance with the Floquet theorem [2], P(z) and Q(z) must be periodic functions with the period of the structure, d = a + b. The conditions of periodicity (for z = a − 0 and z = − b + 0) and continuity (for z = 0) must be fulfilled for the amplitudes of U_z and σ_{zz} in the compression wave and for the amplitudes of U_x and σ_{xz} in the shear wave. In the first case the dispersion equation is of the form:

$$\cos k(a+b) = \cos k_l a \cos\bar{k}_l b - \frac{1+\varkappa^2}{2\varkappa}\sin k_l a \sin\bar{k}_l b,$$

and under these conditions,

$$\varkappa = \frac{(\bar{\lambda}+2\bar{\mu})\,\bar{k}_l}{(\lambda+2\mu)\,k_l},$$

in the second case it has the same form, but k_1 and $\bar{k}_1$ are replaced in the arguments of the cosines and sines by k_t and $\bar{k}_t$ respectively, and it has $\kappa = \overline{\mu k_t}/\mu k_t$.

In the case of thin laminations, when the sines may be replaced by their arguments and only second-order terms with respect to a and b are retained in the cosines, we obtain the following squares of the propagation velocities: for the compression wave—

$$c_{zz}^2 = \frac{1}{\bar{\rho}\,[n/(\lambda+2\mu) + \bar{n}/(\bar{\lambda}+2\bar{\mu})]}, \tag{20}$$

and for the shear wave the velocity c_{zx} proves to be equal to c_{xz} [see (18)], since this must follow when there is hexagonal symmetry.

Having found the velocities (2), we immediately obtain the effective moduli of elasticity for the thinly-laminated medium, λ_1, λ_2, λ_4 and λ_5. In order to do this, it is sufficient to compare Formulas (16), (18), (19), (20) with (2). We write the result in the following form:

$$\frac{1}{\lambda_1} = \frac{n}{\lambda+2\mu} + \frac{\bar{n}}{\bar{\lambda}+2\bar{\mu}}, \quad \lambda_4 = n\mu + \bar{n}\bar{\mu},$$
$$\lambda_2 = \lambda_1\left[1 + 4n\bar{n}\,\frac{(\mu-\bar{\mu})(\lambda+\mu-\bar{\lambda}-\bar{\mu})}{(\lambda+2\mu)(\bar{\lambda}+2\bar{\mu})}\right], \quad \frac{1}{\lambda_5} = \frac{n}{\mu} + \frac{\bar{n}}{\bar{\mu}}. \tag{21}$$

As we have already noted, it is necessary to examine the propagation of the wave at any angle with the z-axis in order to find λ_3, i.e., we must examine a wave in which the displacement of the particles of the medium is defined according to Equations (3) by the formulas

$$U_x = \left[P(z) + \frac{Q'(z) - ik_3 Q(z)}{ik_3}\right] e^{-i(k_1 x + k_3 z)},$$

$$U_z = \left[-\frac{P'(z) - ik_3 P(z)}{ik_1} + Q(z)\right] e^{-i(k_1 x + k_3 z)},$$

where P(z) and Q(z) are periodic with a period of d = a + b. The conditions (11) then yield eight equations (which now do not separate into two groups) and the calculation becomes rather ponderous even if we immediately pass on to the case of thin laminations. Having expanded the eighth-order determinant, it is necessary to counterpose the resulting dispersion equation with the corresponding approximate equation for a hexagonally symmetrical crystal; in the case under analysis this equation has the form

$$(\lambda_2 k_1^2 + \lambda_5 k_3^2 - \tilde{\rho}\omega^2)(\lambda_5 k_1^2 + \lambda_1 k_3^2 - \tilde{\rho}\omega^2) - (\lambda_3 + \lambda_5)^2 k_1^2 k_3^2 = 0.$$

The indicated comparison leads to the following expression for λ_3:

$$\lambda_3 = -\lambda_5 + \sqrt{(\lambda_1 - \lambda_5)^2 + 4n\bar{n}\lambda_1^2\lambda_5(1/\bar{\mu} - 1/\mu) \times \atop \times [(\lambda+\mu)/(\lambda+2\mu) - (\bar{\lambda}+\bar{\mu})/(\bar{\lambda}+2\bar{\mu})][n(\lambda+\mu)/(\lambda+2\mu) + \bar{n}(\bar{\lambda}+\bar{\mu})/(\bar{\lambda}+2\bar{\mu})]}. \qquad (22)$$

In the case of an isotropic medium ($\lambda = \bar{\lambda}$, $\mu = \bar{\mu}$, $\lambda_1 = \lambda + 2\mu$, $\lambda_5 = \mu$) this formula yields $\lambda_3 = \lambda$ as is required. In order for the second term under the radical to disappear, it is sufficient if any one of the conditions $\mu = \bar{\mu}$ or $\frac{\lambda}{\mu} = \frac{\bar{\lambda}}{\bar{\mu}}$ is fulfilled. In both cases Formula (22) yields

$$\lambda_3 = \lambda_1 - 2\lambda_5,$$

i.e., for $\mu = \bar{\mu}$

$$\lambda_3 = \frac{1}{n/(\lambda + 2\mu) + \bar{n}/(\bar{\lambda} + 2\mu)} - 2\mu,$$

and for $\frac{\lambda}{\mu} = \frac{\bar{\lambda}}{\bar{\mu}}$

$$\lambda_3 = \lambda/\mu/(n/\mu + \bar{n}/\bar{\mu}).$$

Knowing all five effective moduli of elasticity, i.e., disposing of an exhaustive characterization of "a crystal", it is possible for us to calculate the velocities of wave propagation in directions which are oriented in an arbitrary manner with respect to the laminations.

In the recent paper by White and Angona [3], Formulas (16) and (18-20) for the propagation velocities of the compression and shear waves in directions which are perpendicular and parallel to the laminations were obtained by another method. Keeping the case of thin laminations in mind from the very outset, these authors examine the static deformations of an element of volume (a cube) which is cut out of a thinly-laminated medium. The deformations examined are those very deformations to which this cube is subjected in a wave of a correspondingly selected type.* The formulas of White and Angona differ from those obtained above only in their external form: they express the velocities of the waves in a thinly-laminated medium in terms of the velocities of the compression and shear waves in the materials of the laminations by expressing them in terms of the densities of these materials and their Poisson coefficients σ and $\bar{\sigma}$. The substitution of the indicated quantities for λ and μ will lead to a complete agreement of the results by means of the relationships

$$\lambda + 2\mu = \rho c_l^2, \quad \mu = \rho c_t^2 = \frac{\rho c_l^2}{2}\,\frac{1 - 2\sigma}{1 - \sigma}$$

---

* This method was used still earlier by Iu. V. Riznichenko [5] whose papers [4-5] were brought to my attention by L. M. Brekhovskikh. Examining a laminated medium, and being interested in the seismic aspect of the problem, Riznichenko found only the velocities of the compression waves and found them only in the cases of longitudinal and transverse propagation. By the same token, the problem concerning the modulus λ_3 (as in [3] also) is not touched upon in his papers. Bruggeman [6] gives expressions for all five moduli. His expressions for λ_1, λ_4 and λ_5 are the same as those obtained from (21), but for λ_2 and λ_3 they differ from (21) and (22) and seem to us to be doubtful because of the method by which they were obtained.

The authors of the paper cited in [3] were attracted to the problem we are analyzing by the fact that during the seismic prospecting for oil it was discovered that the velocity of waves propagated along oil-bearing laminations exceeded the velocity of waves propagated perpendicular to the laminations by 3-20%*. An excess of such order is also obtained from the theoretical formulas for the parameter relationships which may be postulated under the actual conditions.

We believe, however, that this special problem does not exhaust the possibilities of applying the results obtained. Of undoubted interest will be the utilization of artificial anisotropic materials whose manufacture will probably not meet with technological difficulties, and whose properties may be extremely varied. In particular, we may speak of vibration-isolating materials and possibly of monochromators for directing the propagation of specified wave-types while maintaining the corresponding properties of these waves over a wide frequency range.

For applications of this type it is important to know not only the velocities of propagation for various types of waves, but also the absorption coefficients. This last problem (not touched upon in the article cited in [3]) is solved very simply if the condition for the thinness of the laminations is also fulfilled when attenuation is taken into consideration. In that case the Formulas (21) still remain in application when the real coefficients λ and μ are replaced by complex coefficients, due to the introduction of volume and shear viscosities:

$$\lambda + \frac{2}{3}\mu \to \lambda + \frac{2}{3}\mu + i\omega\zeta, \quad \mu \to \mu + i\omega\eta,$$

so that

$$\lambda \to \lambda + i\omega\left(\zeta - \frac{2}{3}\eta\right), \quad \lambda + 2\mu \to \lambda + 2\mu + i\omega\left(\zeta + \frac{4}{3}\eta\right).$$

The complex wave numbers are found according to (2) by the formulas

$$k_{xx}^2 = \frac{\omega^2\tilde{\rho}}{\lambda_2}, \quad k_{xz}^2 = k_{zx}^2 = \frac{\omega^2\tilde{\rho}}{\lambda_5}, \quad k_{xy}^2 = \frac{\omega^2\tilde{\rho}}{\lambda_4}, \quad k_{zz}^2 = \frac{\omega^2\tilde{\rho}}{\lambda_1}. \tag{23}$$

Assuming that $k = k_0 - i\varkappa$, it is not difficult to obtain expressions for the amplitude coefficients of absorption $\varkappa$. In the case when the viscosities are so small that we may limit ourselves to first-order terms involving η and ζ, these expressions are of the following form

$$\varkappa_{xx} = \frac{\omega^2\lambda_1}{2}\sqrt{\frac{\tilde{\rho}}{\lambda_2}}\left\{\frac{n\left(\zeta + \frac{4}{3}\eta\right)}{(\lambda + 2\mu)^2} + \frac{\bar{n}\left(\bar{\zeta} + \frac{4}{3}\bar{\eta}\right)}{(\bar{\lambda} + 2\bar{\mu})^2} + \right.$$
$$\left. + \left(\frac{1}{\lambda_1} - \frac{1}{\lambda_2}\right)\left[\frac{\eta - \bar{\eta}}{\mu - \bar{\mu}} + \frac{\zeta - \bar{\zeta} + \frac{\eta - \bar{\eta}}{3}}{\lambda + \mu - \bar{\lambda} - \bar{\mu}} - \frac{\zeta + \frac{4}{3}\eta}{\lambda + 2\mu} - \frac{\bar{\zeta} + \frac{4}{3}\bar{\eta}}{\bar{\lambda} + 2\bar{\mu}}\right]\right\},$$
$$\varkappa_{xz} = \varkappa_{zx} = \frac{\omega^2}{2}\sqrt{\tilde{\rho}\lambda_5}\left(\frac{n\eta}{\mu^2} + \frac{\bar{n}\bar{\eta}}{\bar{\mu}^2}\right), \quad \varkappa_{xy} = \frac{\omega^2}{2\lambda_4}\sqrt{\frac{\tilde{\rho}}{\lambda_4}}(n\eta + \bar{n}\bar{\eta}), \tag{24}$$
$$\varkappa_{zz} = \frac{\omega^2}{2}\sqrt{\tilde{\rho}\lambda_1}\left[\frac{n\left(\zeta + \frac{4}{3}\eta\right)}{(\lambda + 2\mu)^2} + \frac{\bar{n}\left(\bar{\zeta} + \frac{4}{3}\bar{\eta}\right)}{(\bar{\lambda} + 2\bar{\mu})^2}\right],$$

here λ_i ($i = 1, 2, 4, 5$) define the real moduli which are expressed in terms of Lamé coefficients according to Formulas (21).

Worthy of interest is the case when laminations of a material in which the losses may be neglected (for example, metal) alternate with layers of a viscous liquid. If we take into consideration only the shear viscosity in the liquid (lamination II), we have

$$\bar{\lambda} = \bar{\rho}\bar{c}_l^2 - \frac{2}{3}i\omega\bar{\eta}, \quad \bar{\mu} = i\omega\bar{\eta}.$$

---

* See also [5] and [7].

For the sake of brevity, let us use the definitions

$$\overline{\rho}\,\overline{c_l^2} = \overline{K}, \quad \omega\overline{\eta} = \overline{\eta}_1.$$

Then according to (21),

$$\frac{1}{\lambda_1} = \frac{n}{\lambda+2\mu} + \frac{\overline{n}}{\overline{K}+\frac{4}{3}i\overline{\eta}_1}, \quad \lambda_4 = n\mu + i\overline{n}\overline{\eta}_1,$$

$$\lambda_2 = \lambda_1\left[1 + 4n\overline{n}\frac{(\mu - i\overline{\eta}_1)\left(\lambda+\mu-\overline{K}-\frac{i}{3}\overline{\eta}_1\right)}{(\lambda+2\mu)\left(\overline{K}+\frac{4}{3}i\overline{\eta}_1\right)}\right]; \quad \frac{1}{\lambda_6} = \frac{n}{\mu} - \frac{i\overline{n}}{\overline{\eta}_1} \qquad (25)$$

and Formulas (23) permit us to obtain the corresponding expressions for the propagation velocities and the amplitude coefficients of absorption. If $\overline{\eta}_1$ is small (in comparison to $\overline{K}$ and μ), then the viscosity of the liquid is only included as a correction in the expressions for λ_1, λ_2 and λ_4, i.e., the coefficients of absorption κ_{xx}, κ_{zz} for the compression waves and κ_{xy} for the shear wave decrease together with $\overline{\eta}_1$. But in λ_6 the viscosity of the liquid produces an effect which is the stronger the smaller the viscosity is, i.e., $\kappa_{xz} = \kappa_{zx}$ grows with a decrease in $\overline{\eta}_1$ (of course, in order for the formulas being analyzed to be valid, the condition that the liquid laminations must be thin in comparison to the wave length of a viscous wave in a liquid layer, must remain in application). For the velocities and absorptions of the shear waves in the general case of any $\overline{\eta}_1$, we have:

$$c_{xz}^2 = \frac{2\mu}{n\tilde{\rho}\left(\sqrt{1+(\overline{n}\mu/n\overline{\eta}_1)^2}+1\right)}, \quad \kappa_{xz}^2 = \frac{n\omega^2\tilde{\rho}}{2\mu}\left(\sqrt{1+(\overline{n}\mu/n\overline{\eta}_1)^2}-1\right),$$

$$c_{xy}^2 = \frac{1\,(n^2\mu^2+\overline{n}^2\overline{\eta}_1^2)}{n\tilde{\rho}\mu\left(\sqrt{1+(\overline{n}\overline{\eta}_1/n\mu)}+1\right)}, \quad \kappa_{xy}^2 = \frac{n\omega^2\tilde{\rho}\mu}{2(n^2\mu^2+\overline{n}^2\overline{\eta}_1^2)}\left(\sqrt{1+(\overline{n}\overline{\eta}_1/n\mu)^2}-1\right).$$

From this it follows that when $\overline{\eta}_1 = \omega\overline{\eta}$ is sufficiently small,

$$c_{xz}^2 = \frac{2\omega\overline{\eta}}{\overline{n}\tilde{\rho}}, \quad \kappa_{xz}^2 = \frac{\omega\tilde{\rho}\overline{n}}{2\overline{\eta}},$$

$$c_{xy}^2 = \frac{n\mu}{\tilde{\rho}}, \quad \kappa_{xy}^2 = \frac{\omega^4\tilde{\rho}\overline{n}^2\overline{\eta}^2}{4n^2\mu^2},$$

i.e., with a decrease in $\overline{\eta}$, the velocity c_{xz} falls and the absorption κ_{xz} grows while c_{xy} ceases to depend upon $\overline{\eta}$ and κ_{xy} decreases. The frequency dependency of these quantities is also substantially different.

5. In examining the alternation of laminations of a solid body and a liquid in the previous section, we assumed that the condition introduced at the very outset, that the laminations must be thin in comparison with the wave lengths of the compression and shear waves in the lamination material, was fulfilled both for the solid body and for the liquid. But if the viscosity of the liquid is small, then another way of posing the problem may be of interest when the thickness of the liquid laminations is, as before, small in comparison to the wave length of compression but considerably exceeds the shear wave length (the viscous wave length). Under these conditions it is useful to examine the liquid as an ideal liquid in the first approximation, i.e., to take into consideration only the longitudinal waves in it and to require only that at the boundaries with the solid laminations there be continuity of pressure and normal displacement, as well as an absence of tangential stresses in the solid body. From the disruption of tangential velocity obtained under these conditions, it is then possible to find the wave attenuation caused by the viscosity of the liquid.

A medium consisting of laminations of a solid body and an ideal liquid, of course, also behaves "on the average" as a crystal possessing hexagonal symmetry but with effective values of elasticity moduli which are such that they are not possible in actual crystals. In particular, it is clear in advance that the solid laminations are uncoupled with respect to shear in their plane and therefore a shear wave propagated perpendicular to the laminations cannot be obtained.

Thus we now have only longitudinal waves (U = u) in the liquid (layer II), while the pressure is $p = -\bar{K}$ div U, where $\bar{K} = \bar{\rho}\,\bar{c}^2$ ($\bar{c}$ is the velocity of the longitudinal waves and we omit the index l). For the solid body (layer I) Equations (3), (4) are in effect. At the boundaries the following conditions of continuity and periodicity must be fulfilled:

$$\begin{gathered} U_z(0) = \bar{U}_z(0), \quad U_z(a-0) = \bar{U}_z(-b+0), \\ \sigma_{xz}(0) = \sigma_{yz}(0) = 0, \quad \sigma_{xz}(a-0) = \sigma_{yz}(a-0) = 0, \\ \sigma_{zz}(0) = -p(0), \quad \sigma_{zz}(a-0) = -p(-b+0). \end{gathered} \tag{26}$$

We immediately notice that the sole case for which there are no special features in comparison to the alternation of solid laminations is the case of the propagation of a compression wave in a direction perpendicular to the laminations. For c_{zz} we obtain a formula which is analogous to (20):

$$c_{zz}^2 = \frac{1}{\bar{\rho}\,(n/(\lambda+2\mu) + \bar{n}/\bar{K})}, \tag{27}$$

i.e., the problem reduces to a substitution of the compressibility of the liquid $\bar{K}$ for the expression $\bar{\lambda} + 2\bar{\mu}$. In the remaining cases the results will naturally prove to be different from (16), (18) and (19).

Let us again start with propagation along the laminations (along the x axis)and let us examine a longitudinal-transverse wave in which the displacement lies in the plane (x, z). In the solid laminations we have the previous expressions (6), (7) and (10) for the displacements and the stresses, and in the liquid

$$\bar{U}_x = \bar{P}(z)\,e^{-ikx}, \quad \bar{U}_z = -\frac{\bar{P}'(z)}{ik}\,e^{-ikx}, \quad p = -\frac{\bar{\rho}\,\omega^2}{ik}\,\bar{P}(z)\,e^{-ikx},$$

and under these conditions

$$\bar{P}(z) = \bar{A}\cos\bar{\alpha}(z + b/2) + \bar{B}\sin\bar{\alpha}(z+b/2), \quad \bar{\alpha}^2 = \bar{k}^2 - k^2, \quad \bar{k} = \omega/\bar{c}.$$

Conditions (26) provide six equations for the constants A, B, C, D and $\bar{A}$, $\bar{B}$ which here also separate into two groups.

a) A wave which, on the average, is longitudinal (B = C = $\bar{B}$ = 0). The boundary conditions are of the form:

$$\begin{gathered} A\alpha\sin\frac{\alpha a}{2} + Dik\sin\frac{\beta a}{2} + \bar{A}\,\bar{\alpha}\sin\frac{\bar{\alpha} b}{2} = 0, \\ A2ik\alpha\sin\frac{\alpha a}{2} + D\gamma\sin\frac{\beta a}{2} = 0, \\ A\mu\gamma\cos\frac{\alpha a}{2} + D2ik\mu\beta\cos\frac{\beta a}{2} - \overline{A\rho}\,\omega^2\cos\frac{\bar{\alpha} b}{2} = 0, \\ (\gamma = k_t^2 - 2k^2), \end{gathered}$$

whence follows the dispersion equation:

$$\bar{\mu}\bar{\alpha}\tan\frac{\bar{\alpha} b}{2}\left(4k^2\alpha\beta\tan\frac{\alpha a}{2} + \gamma^2\tan\frac{\beta a}{2}\right) + \bar{\rho}\,\omega^2\alpha\,(\gamma + 2k^2)\tan\frac{\alpha a}{2}\tan\frac{\beta a}{2} = 0.$$

Passing over to the case of thin laminations (the tangents are replaced by their arguments) and substituting

$$\mu = \omega^2\rho/k_t^2, \quad \alpha^2 = k_l^2 - k^2, \quad \bar{\alpha}^2 = \bar{k}^2 - k^2, \quad \gamma = k^2 - 2k^2,$$ we obtain:

$$\bar{n}\rho\,(\bar{k}^2 - k^2)\,[4k^2(k_l^2 - k_t^2) + k_t^4] + n\bar{\rho}\,k_t^4\,(k_l^2 - k^2) = 0.$$

If we introduce the definitions

$$x = (k/k_t)^2, \quad \xi = n\bar{\rho}/\bar{n}\rho, \quad \eta = (k_l/k_t)^2, \quad \zeta = (\bar{k}/k_t)^2, \tag{28}$$

then the equation will acquire the form:

$$4(1-\eta)x^2-[4\zeta(1-\eta)+\xi+1]x+\xi\eta+\zeta=0,$$

whence

$$x_{1,2}=\frac{4\zeta(1-\eta)+\xi+1\pm\sqrt{[4\zeta(1-\eta)+\xi-1]^2+4\xi[1-4\eta(1-\eta)]}}{8(1-\eta)}. \qquad (29)$$

It is not difficult to verify that in the region $\eta < 1$, which is actually the only region of real interest, both the roots x_1 and x_2 are real and positive, i.e., two velocities exist for the compression wave c_{xx}. For several particular cases let us provide the expressions for x_1 and x_2, for the propagation velocities corresponding to them, c_{xx}, and for the relationships between the amplitudes $A:D:\bar{A}$ of compression and shear in the solid laminations and compression in the liquid.

For $\eta=\frac{1}{2}\left(c_l=\sqrt{2}\,c_t\right)$ we have

$$x_1=\zeta+\frac{\xi}{2},\ c_{xx1}=\frac{\bar{c}c_l}{\sqrt{\bar{c}^2+c_l^2}},\ A:D:\bar{A}=1:\sqrt{\frac{\xi+2\zeta}{\xi+2\zeta-2}}:\frac{\rho}{\bar{\rho}},$$

$$x_2=\frac{1}{2},\ c_{xx2}=c_l,\ A:D:\bar{A}=1:0:0.$$

Thus the second root is related to a pure compression wave in the solid laminations, which is not accompanied by shear in view of the special relationship between the velocities c_l and c_t.

For $\xi \longrightarrow 0$, i.e., for a thinning of the solid laminations or for an increase in their density,

$$x_1=\zeta,\ c_{xx1}=\bar{c},\ A:D:\bar{A}=0:0:1,$$

$$x_2=\frac{1}{4(1-\eta)},\ c_{xx2}=\frac{2c_t\sqrt{c_l^2-c_t^2}}{c_l},\ A:D:\bar{A}=\frac{\eta}{1-2\eta}:\frac{-1}{\sqrt{4\eta-3}}:\frac{2a(1-\eta)}{b[4\zeta(1-\eta)-1]}.$$

Here x_1 corresponds to a pure compression wave in the liquid for solid laminations which are immobile.

When ξ increases, i.e., when the density of the liquid increases or when its laminations become thinner (however only until they become comparable to the viscous wave length), we obtain

$$x_1=\frac{\xi}{4(1-\eta)},\ c_{xx1}=\frac{2c_t}{c_l}\sqrt{\frac{c_l^2-c_t^2}{\xi}},\ A:D:\bar{A}=1:1:\frac{2\rho(1-\eta)}{\bar{\rho}},$$
$$x_2=\eta,\ c_{xx2}=c_l,\ A:D:\bar{A}=1:0:0.$$

The velocity c_{xx1} decreases with a growth in ξ. The root x_2 yields the compression wave in the solid laminations— without shear, because the liquid is practically absent.

b) A wave which, on the average, is transverse ($A=D=\bar{A}=0$). In this case the transverse displacement in the solid lamination is even with respect to its center, and the longitudinal displacement is odd, i.e., a bending of the solid laminations must take place. The dispersion equation in the general case is of the form

$$\bar{\mu}\bar{\alpha}\left(4k^2\alpha\beta\tan\frac{\beta a}{2}+\gamma^2\tan\frac{\alpha a}{2}\right)+\bar{\rho}\omega^2\alpha(\gamma+2k^2)\tan\frac{\bar{\alpha}b}{2}=0.$$

In the case of thin laminations, if we only retain the first-order terms involving a and b, we obtain a condition which cannot be fulfilled: $\tilde{\rho}=n\rho+\overline{n\rho}=0$. In other words, the determinant of the equations for B, C and $\bar{B}$ is different from zero and therefore the wave we are analyzing is impossible in a thinly-laminated medium.

If in the transition to small a and b we take the next (cubic) terms in the expansions of the tangents into account in the dispersion equation, we obtain

$$k_t^2\{a^2[x(3-4x)+\eta(2x-1)^2]+b^2\xi_1(\zeta-x)\}+12(1+\xi_1)=0,$$

where the definitions (28) are utilized as well as $\xi_1 = \overline{n\rho}/n\rho$. For small $k_t a$ and $k_t b$, one of the roots of this equation is positive and very large. In particular, when $a = b$, it is equal to

$$x\approx\frac{1}{k_t a}\sqrt{\frac{3(1+\xi_1)}{1-\eta}}.$$

Thus a shear wave exists which possesses a very small velocity c_{xz} which depends explicitly upon the thickness of the laminations. In the limit, when the laminations are very thin, we must assume that

$$c_{xz} = 0 \tag{30}$$

6. We must still examine the shear waves with the velocities c_{xy} and c_{zx}. When a pure shear wave with a displacement along the y axis is propagated along the x axis, there is no interaction between the solid laminations and the liquid. Therefore only a shear wave is possible in the solid laminations which slide along the stationary liquid when this wave is propagated:

$$U_y=v_y=[C\cos\beta(z-a/2)+D\sin\beta(z-a/2)]\,e^{-ikx},\ \overline{U}_y=0.$$

The boundary conditions reduce to the fact that on both sides of the solid sheet the tangential stress σ_{yz} is equal to zero; this yields two equations for the constants C and D:

$$C\sin\frac{\beta a}{2}+D\cos\frac{\beta a}{2}=0,$$

$$-C\sin\frac{\beta a}{2}+D\cos\frac{\beta a}{2}=0.$$

The conditions for the resolution of these equations is $\sin\beta a = 0$, i.e., $\beta a = n\pi$ or

$$k=\sqrt{k_t^2-(n\pi/a)^2}.$$

Since conditions specify that $k_t a \ll 1$, all the guided waves are below critical and only the wave with $n = 0$ ($\beta = 0$) will be a traveling wave. In this wave the displacement is constant over the thickness of the solid lamination ($U_y = Ce^{-ikx}$) and $k = k_t$, i.e.,

$$c_{xy} = c_t \tag{31}$$

The computation of the attenuation of this wave (from the magnitude of the losses introduced by the viscosity of the liquid η when the solid laminations slide relative to the liquid laminations) yields the following value for the amplitude coefficient of absorption:

$$\varkappa_{xy}=\frac{1}{2a}\sqrt{\frac{\tilde{\rho}\omega\eta}{\rho\mu}}.$$

When a pure shear wave is propagated in the direction of the z axis we again do not have interaction between the solid laminations and liquid; there is no shear elasticity for the vibrations of the solid laminations in their natural plane and therefore, $c_{zx} = 0$, as must be true in a hexagonally symmetrical crystal in view of the applicability of (30).

As a result, by comparing Formulas (27), (29) and (30) with (2), we obtain the following values for four (of the five) effective moduli of elasticity for a medium consisting of laminations of a solid body and an ideal liquid:

$$\frac{1}{\lambda_1}=\frac{n}{\lambda+2\mu}+\frac{\bar{n}}{\bar{K}},\ \lambda_4=\mu\frac{\tilde{\rho}}{\rho},\ \lambda_5=0,$$

$$\lambda_3=\lambda_4\frac{4\zeta(1-\eta)+\xi+1\mp\sqrt{[4\zeta(1-\eta)+\xi-1]^2+4\xi[1-4\eta(1-\eta)]}}{2(\zeta+\xi\eta)},$$

where $\overline{K} = \overline{\rho c^2}$ is the compressibility of the liquid and where the definitions (28) are utilized anew. Thus the modulus λ_2 is bivalent. The transition to an isotropic medium is, of course, impossible; this can be seen from the fact that λ_4 and λ_5 cannot be equal.

LITERATURE CITED

[1] S. M. Rytov, "Electromagnetic Properties of a Thinly Laminated Medium," J. Exptl.-Theoret. Phys. (USSR) 29, 5 (11) 605-616 (1955).

[2] G. Floquet, Ann. Ecole Norm. 12, 47-88 (1883).

[3] J. E. White and F. A. Angona, "Elastic Wave Velocities in Laminated Media," J. Acoust. Soc. Am. 27, 311-317 (1955).

[4] Iu. V. Riznichenko, "The Propagation of Seismic Waves in Discrete and Heterogeneous Media," Bull. Acad. Sci. USSR, Geographical and Geophysical Series 13, 2, 115-128 (1948).

[5] Iu. V. Riznichenko, "Seismic Quasi-anisotropy," Bull. Acad. Sci. USSR, Geographical and Geophysical Series 13, 6, 518-544 (1949).

[6] D. A. G. Bruggeman, "Berechnung Verschiedener Physikalischer Konstanten von Heterogenen Substanzen, III," Ann. Physik 29, 2, 160-178 (1937).

[7] I. S. Berzon, "Indices of Average Seismic Velocities in the Case of Laminated Media," Bull. Acad. Sci. USSR, Geographical and Geophysical Series 13, 2, 129-142 (1949).

Received September 15, 1955

P. N. Lebedev Physics Institute
of the Academy of Sciences, USSR
Moscow

A HIGH-POWER ULTRASONIC INSTALLATION FOR IRRADIATING MICROORGANISMS

I. V. Skards

The article describes a high-power ultrasonic installation for the irradiation of biological preparations in ampules, and discusses the special measures which are taken in the electrical and acoustical sections of the installations in order to guarantee a constant ultrasonic intensity in the irradiated sample.

At the present time ultrasonic irradiation is being utilized more and more widely in the most varied fields of science and engineering. The utilization of ultrasonics in biology, and especially in microbiology, has great possibilities. The research which has been conducted in recent years has accumulated a significant amount of material which verifies the possibility of utilizing ultrasonics in several fields of industry for the purposes of sterilization, for the extraction of biologically active substances which are found in cells, and which may be utilized in the production of vitamins, vaccine preparations, fermented substances, etc. It has also been noted that under particular conditions of irradiation it is possible to achieve a directional variation of several properties of microorganisms; these variations are of significance in engineering microbiology. In relation to this there arises the necessity of creating an ultrasonic apparatus which would guarantee the ability to study the mechanism of ultrasonic effects, and which would take into consideration all of the many varied aspects of these effects.

We cannot fail to note that the construction of the ultrasonic apparatus which is in use at the present time suffers from substantial shortcomings which hinder the obtaining of uniform and repetitive results, and which limit the possibilities of utilizing this apparatus in microbiology and in other fields of science and engineering. Having as our purpose the elimination of several of these shortcomings, we considered it necessary to design an ultrasonic apparatus which would satisfy the following basic requirements.

1) The installation must be equipped with a cooling system which can be adapted to maintain a specified temperature in the irradiated object;

2) The installation must be so designed that the ultrasonic intensity which acts upon the irradiated object is stable;

3) It is necessary for the installation to be especially adapted to monitor the cavitation which arises in the irradiated substratum.

A quartz plate was utilized in the capacity of a radiator in the apparatus which we have designed. There are indications in the literature according to which it is possible to obtain an ultrasonic intensity which is very high by means of quartz plates. Thus, for instance, Selman and Wilkin [8], having immersed a quartz plate in purified transformer oil, obtained an ultrasonic intensity of up to 55 watts/cm^2. Such an ultrasonic intensity is fully sufficient for the vast majority of work with microbiological objects [1, 4].

In designing an ultrasonic installation which wuld fulfill the above-indicated basic requirements, it was necessary to grapple with a series of subsidiary problems which it was necessary to resolve in order to reach the goal which we had set.

OBTAINING A HIGH ULTRASONIC INTENSITY

A high-frequency oscillator, whose circuit is shown in Figure 1, is utilized for feeding the quartz radiator.

The oscillator consists of three stages and this allows us to obtain a stable frequency. By means of an auxiliary unit, the oscillator is automatically cut off when electrical breakdown occurs in the oil. Such a breakdown is accompanied by the development of considerable quantities of heat, and this may lead to damage to the crystal; in addition, the oil becomes acidic at high temperatures. The automatic unit cuts off the high-frequency oscillator when breakdown occurs, by means of blocking the grid of the tube in the exciter stage; it effects this so rapidly that the crystal is fully protected from damage, and the oil is prevented from becoming dirty.

The automatic blocking action consists of the following: a battery of dry cells with a voltage of 150 v is connected in series with the quartz radiator circuit; when the oil insulation in the quartz circuit is broken down, a direct current appears which by flowing through the resistor $R^1 = 50$ megohms creates a voltage drop; this voltage is applied to the grid of an auxiliary electronic tube. In order that the high-frequency voltage which supplies the ultrasonic radiator should not affect the grid of this tube, a series resonant circuit is connected in parallel with the grid of the tube; this circuit is tuned to the fundamental ultrasonic frequency. The tuned circuit consists of a variometer L and a condenser C; a condenser cannot be used in place of the tuned circuit since it would be necessary to use a condenser with a comparatively large capacity and this would increase the time constant and lower the sensitivity of the automatic blocking action. When a negative voltage appears on the grid of the auxiliary tube its plate current decreases, the plate voltage increases and a neon lamp (which is shown in the figure) lights. The voltage drop in the cathode circuit of the neon lamp blocks the exciter stage, and simultaneously a relay signals that the insulation has been damaged.

It should be noted that the blocking action also takes place when there is a sharp change in the current supplying the ultrasonic radiator. Such a sharp current variation may arise when the irradiated substratum is torn away from the quartz sheet or from the bottom of the irradiated vessel. Under these conditions voltages are created across the series resonant circuit which are sufficient to cut off the auxiliary tube. Therefore the blocking unit is so designed that it may operate in two regimes. The second regime differs from the ordinary regime in that several tens of seconds after the oscillator has been blocked, the oscillator is automatically turned on again by means of a relay. If the irradiation regime has not yet been stabilized, which occurs, for example, when the insulation in the oil has broken down, then the oscillator is blocked once again. The blocking repetition rate is so short that even when multiple blocking takes place the oil does not become dirty and the crystal is not damaged. For the purpose of limiting the number of times that blocking and reconnection take place, a couting circuit may be utilized; after a specified number of pulses the couting unit cuts off the oscillator permanently.

Harden, Andersen [6] et al., assuming that the maximum obtainable ultrasonic intensity was limited by the dielectric strength of the transformer oil, postulate that this maximum intensity may be easily raised to some limit by lengthening the discharge path, i.e., by locating the edges of the electrodes at some distance from the edges of the quartz crystal. However, it should be noted at the same time that the authors who obtained the geatest ultrasonic intensity placed the edges of the electrodes comparatively close to the edges of the crystal.

Evidently the dielectric strength of the transformer oil is lowered during the ultrasonic action. Figure 2 shows the breakdown voltage of diffusion-pump oil as a function of the static pressure with and without ultrasonic radiation. It is clear from the curves that when ultrasonic radiation is present, the breakdown voltage is considerably lowered.

In a degassed oil the breakdown voltage is considerably raised; this can be seen from Figure 3 which shows the breakdown voltage as a function of the degassing time of the oil. Investigation has shown that the lowering of the dielectric strength of the oil due to ultrasonic radiation is caused by the appearance of cavitation, and that the discharge does not occur between the plates of the crystals but between electrodes (Figure 4) notwithstanding the fact that the geometric path of this discharge proves to be longer.

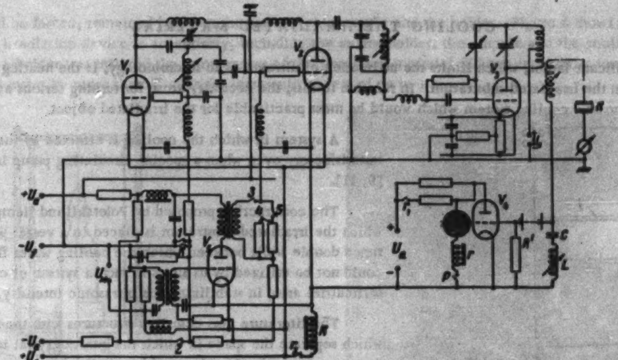

Figure 1. Circuit diagram illustrating the principle of the high-frequency oscillator: V$_1$) oscillator; V$_2$) buffer stage; V$_3$) final stage; V$_4$) automatic unit; V$_5$) modulator; K) radiator; 1,2,3,4,5) contacts; modulated oscillation—contacts 3, r$_2$, R are closed; unmodulated oscillations—contacts 5, 2, r$_2$, R are closed.

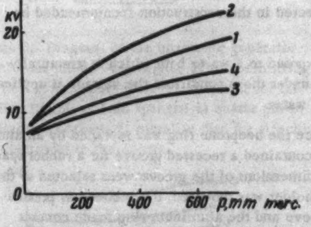

Figure 2. Breakdown voltage of the oil as a function of static pressure.
1) Without ultrasonic action, in a pressure-lowering phase (when the pump is withdrawing); 2) without ultrasonic action, in a phase of increasing pressure; 3) with ultrasonic action in a phase of diminishing static pressure; 4) with ultrasonic action in an increasing pressure phase. 1 and 2) for a frequency of 387 kc which corresponds to resonance for the quartz plate; 3 and 4) at 420 kc.

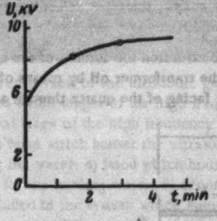

Figure 3. Breakdown voltage for the oil as a function of degassing time.

In light of what has been said, it is understandable why Selman and Wilkin were able to achieve a relatively high ultrasonic intensity when the quartz plates were so placed that the oil located under the surface of the plate was separated from the oil surrounding the edge of the crystal by means of a cylindrical quartz holder.

In the ultrasonic installation which we designed, it proved possible to attain ultrasonic intensities of up to 70 watts/cm^2 in the irradiated vessel; this corresponds to a maximum intensity of 100 watts/cm^2 directly above the quartz plate. The method of measuring the intensity is described in [10]. The average ultrasonic intensity over the surface of the quartz plate proves to be considerably lower. The diameter of the irradiated vessel equals 3.5 cm, the diameter of the quartz crystal is 6 cm; the ultrasonic intensity above the central portion of the quartz is considerably higher than at the periphery.

COOLING THE IRRADIATED MATERIAL

A significant factor, which limits the utilization of ultrasonics in microbiology, is the heating which takes place in the irradiated substratum. In relation to this, the necessity arose for turning serious attention to the creation of a cooling system which would be most practicable for the irradiated object.

A system in which the cooling is effected by the oil is unsatisfactory even when a special circulating pump is utilized [9, 11].

The construction proposed by Polotskii and Hempsh, in which the irradiated substratum is placed in a vessel with untuned double walls between which the cooling water flows, could not be utilized by us since in such a system of cooling difficulties arise in stabilizing the ultrasonic intensity.

The literature also describes structures with tuned walls which separate the space in which the quartz crystal is located from a water bath. We also could not utilize a construction in which a layer of transformer oil is located between the tuned plate and the surface of the radiating quartz. In this case, the oil is subjected to the effects of intensive ultrasonic radiation, and because of this it is difficult to prevent the appearance of cavitation in the oil; this cavitation is detrimental from the point of view of retaining the dielectric strength of the oil in the ultrasonic field. We also rejected a construction in which the tuned plate was directly attached to the quartz, since better cooling of the crystal is effected in the construction recommended by Samsel, Fetra and Henry.

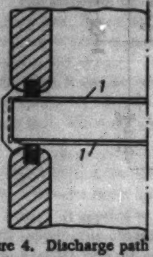

Figure 4. Discharge path in the oil. Solid line) true discharge path; broken line) shortest path; 1) silvered surfaces of the quartz.

In this construction the surface of the quartz is directly exposed to a water bath which is structurally isolated from the transformer oil by means of a neoprene ring; under these conditions the voltage is applied to the external facing of the quartz through a solution of salt in water.

In our device the neoprene ring was replaced by an aluminum ring which contained a recessed groove for a rubber spacer (Figure 5). The dimensions of the groove were selected so that when the crystal holder was mounted, the rubber was pressed down into the groove and the aluminum ring made contact with the silvered surface of the crystal; such contact was necessary for the application of the supply voltage. The homogeneous silver coating of the crystal was obtained by means of reducing a silver salt with a solution of dextrose and sucrose [9].

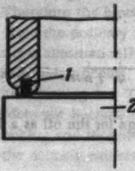

Figure 5. Construction of the crystal holder with the rubber spacer: 1) Rubber spacer; 2) quartz crystal.

Under test it was discovered that notwithstanding the tight fit of the rubber spacer, the transformer oil leaked into the water when acted upon by the ultrasonic radiation. This was observed even when there was a small excess of pressure on the water side, and this makes us believe that a specific suction effect occurs. The best material for the spacer proved to be lead; the lead spacer was soldered into the groove and then milled down. When the lead spacer was used, the oil was not sucked through into the water. Over a period of time, lead spacers are abraded by the ultrasonic action, and therefore a steel disc which provides a flexible attachment for the crystal is utilized in our construction.

In the construction recommended by the "Zeiss" Company the irradiated material is placed in a vessel with a tuned bottom. However, as was admitted at the conference of German manufacturers of ultrasonic apparatus [4], the cooling of the irradiated material proves to be incomplete in such a vessel. Therefore we thought it more practical to place the irradiated material into a thin-walled, flat-bottomed glass ampule which was fastened into a special holder in such a manner that a thin slit, through which a rapid stream of water could be forced, remained between the walls of the ampule and the holder. Figure 6 shows the construction of the irradiation device in its entirety, including the quartz holder, the ampule and the cooling system. When such a holder was utilized the temperature of the irradiated material did not exceed the temperature of the cooling water by more than 5° even for ultrasonic powers of up to 1 kw.

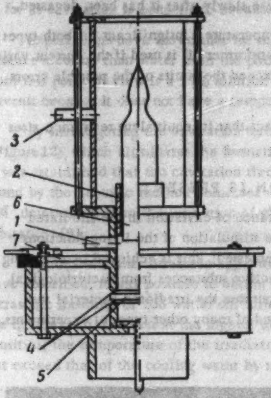

Figure 6. Diagram of the ultrasonic generator. 1) Inlet for the cooling liquid; 2) slit permitting the flow of the cooling liquid; 3) outlet for the cooling liquid; 4) lead spacers; 5) quartz plate; 6) irradiated vessel; 7) metallic disc for attaching the electrodes to the quartz.

Figure 7. Overall view of the ultrasonic generator. 1) Exciter and buffer stages of the high frequency generator; 2) final stage of the high frequency current generator; 3) hood which houses the ultrasonic radiator for degassing the water; 4) hood which houses the circulating pump for the cooling water; 5) counting device which is included in the system which automatically cuts off the current when the oil breaks down.

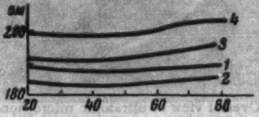

Figure 8. Resistance of the radiator as a function of temperature.
1) For diffusion pump oil; 2) for transformer oil (both for a voltage of 5 kv; 3) for transformer oil when the voltage is 7 kv; 4) for transformer oil when the voltage is 10 kv.

OBTAINING A STABLE ULTRASONIC INTENSITY

When a vessel with an untuned bottom is used as a container for the irradiated material, it is necessary to take into account the variation of the ultrasonic intensity in the irradiated substratum as a function of the distance from the bottom of the vessel to the quartz crystal or as a function of the velocity of sound propagation in the cooling medium.

It should be remarked that in experiments where it is necessary to suppress cavitation in the contact medium, the device is housed under a hood (Figure 7); therefore an accurate determination of the distance between the quartz and the bottom of the vessel containing the irradiated material is difficult for engineering reasons. This situation forced us to design the device in such a manner that the ultrasonic intensity in the vessel containing the irradiated material did not vary with the distance between the bottom of the vessel and the quartz crystal. For this purpose, the resistance of the radiator was matched to the sum of the internal resistance of the high-frequency generator and the resistance which defines the losses in the quartz holder and in the oil (see [10]). In order to attain stability for the electromotive force of the high-frequency generator, we supplied the latter from stabilized voltage sources.

In order that the ultrasonic intensity be stable, it is necessary that the losses in the crystal supports be constant during the period of operation. Figure 8 shows the resistance of the radiator as a function of temperature, and the frequency of the supply current (320 kc) differs from the resonant frequency of the quartz plate, which is equal to 387 kc. The curves are obtained on the basis of testing two types of oils – ordinary transformer oil and high-molecular oil which can be used with a diffusion pump. The advantage of the latter, according to Buchholz [2], is that it saturates with gas considerably more slowly after it has been degassed.

As is evident from the curves, the variation of resistance with temperature is insignificant for both types of oil. However, the resistance varies approximately by 15% when transformer oil is used if the current varies; when diffusion oil is used the variations which were observed did not exceed the limits of the possible errors of measurement.

One of the disadvantages of using diffusion oil, however, is the fact that its equivalent resistance rises noticeably after electrical breakdown.

DETERMINING WHETHER CAVITATION IS PRESENT

In ultrasonic work it is necessary to be able to control the appearance of caviation in the irradiated object. In several cases, for instance, if an attempt is made to achieve stimulation of the living functions of microorganisms, irradiation should be carried out with cavitation suppressed; this is achieved by degassing the irradiated suspension. If we are to be able to extract biologically active substances from bacteriological bodies, cavitation must occur in the cells of the bacteria, and for this purpose the irradiated bacterial suspension is also subjected to degassing. To insure the success of these and of many other types of experiments, the operator must be able to continuously observe the cavitation.

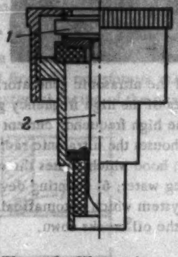

Figure 9. Ultrasonic receiver circuit. 1) quartz crystal; 2) voltage drive.

Figure 10. Overall view of ultrasonic microphone.

This can be done by means of an ultrasonic receiver which is an absolute necessity for any ultrasonic installation. The ultrasonic receiver (Figures 9 and 10) consists of a quartz plate located in a holder and connected to an ordinary radio-receiver by means of a shielded cable. Since the ultrasonic receiver is built to detect cavitation, the natural frequency of the piezo-quartz must be higher than the ultrasonic frequency which is used [7]. Thus, for instance, for an ultrasonic frequency of 380 kc and a receiver with a natural frequency of 500 kc, the radio-receiver is tuned to a frequency of 500 kc. When cavitation appears, noise appears in the radio-receiver.

When the appearance of cavitation in the irradiated substratum is being detected by the acoustic method, it is necessary to suppress cavitation in the contact liquid between the quartz crystal and the irradiated vessel. With this in mind, experiments were conducted for the purpose of finding the cavitation threshold as a function of degassing time for water and oil, as well as for several other liquids. The degassing was effected at a pressure equal to the boiling pressure of the liquid under investigation. In order to speed up the degassing process, the substratum was subjected to an ultrasonic radiation intensity of 4 watts/cm^2. The results obtained are shown by the curves in Figure 11.

After the water had been degassed for 8 minutes at an intensity of 26 watts/cm², no cavitation was observed. In order that cavitation should not take place in the oil at an intensity of 26 watts/cm², it was necessary to degas the oil for 30 minutes. We did not use greater ultrasonic intensities in our tests, since we could not completely avoid the formation of a fountain in the test liquid when the ultrasonic intensity was increased further. This same factor explains why gasoline and benzene and comparatively less stable as far as cavitation is concerned; because of their lower surface tension, a fountain is more easily formed.

Experiments have shown that for the ultrasonic intensities used in biology, oil is less applicable as a contact medium than water from the point of view of the suppression of cavitation. The best contact medium from this point of view is a 17% solution of ethyl alcohol in water. This sound-conducting liquid is also of interest because it does not have a temperature coefficient of sound velocity [3].

By investigating the cavitation threshold in double-distilled water placed in a special bent ampule (Figure 12) which eliminates the formation of a fountain, it was established that the cavitation threshold which is found by the acoustic method coincides with the threshold determined from the formation of chemically active substances [9].

By means of the ultrasonic apparatus which we have described, it was possible to obtain a maximum ultrasonic intensity of 100 watts/cm² directly above the quartz crystal. Even at the highest ultrasonic intensities, the temperature of the irradiated liquid did not exceed that of the cooling water by more than 5°.

Diffusion-pump oil proves to be more advantageous than transformer oil for the purpose of obtaining a stable ultrasonic intensity.

The utilization of the ultrasonic receiver provided us with the possibility of controlling the cavitation in the irradiated substratum.

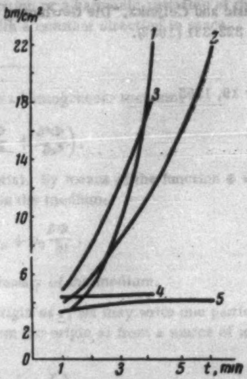

Figure 11. Ultrasonic intensity at which cavitation occurs as a function of degassing time. Duration of observation is 10 seconds. The temperature during degassing is 22°C. The determination of the threshold of cavitation was carried out at atmospheric pressure.
1) For 17% solution of ethyl alcohol in water; 2) for pure water; 3) for automobile gasoline; 4) for cryoscopic benzene; 5) for transformer oil.

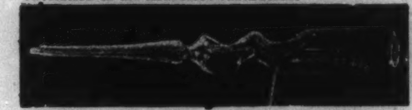

Figure 12. Illustration of ampoule which eliminates formation of a fountain in the irradiated substratum.

LITERATURE CITED

[1] E. Ackerman, "Pressure Thresholds for Biologically Active Cavitation," J. Appl. Phys. 24, 11, 1371-1373 (1953).

[2] H. H. Buchholz, "Einfluss des Gasgehaltes auf das Dielektrische Verhalten von Isolieroelen," ETZ Ausgabe A. J. 22, 763-768 (1954).

[3] A. Eckardt, Linding, K. Nietzsche, "Zur Homogenisierung von Ultraschallfeldern in Wasser," Ann. Physik 12, 4-6, 237-239 (1953).

[4] R. Goebel, "Die Anwendung des Ultraschalls in der Biologie," Nachrichtentechnik 3, 12, 549-551 (1953).

[5] F. Gutmann, "Crystalholder Permitting Direct Supersonic Irradiation of Conducting Liquids," J. Sci. Instr. 24, 276-277 (1947).

[6] Harden, Andersen, Epstein, "High Intensity Ultrasonics," J. Acoust. Soc. Am. 19, 1, 248-253 (1947).

[7] Th. Lange,"Methoden zur Untersuchung der Schwingungskavitation in Flüssigkeiten mit Ultraschall," Akust. Beihefte 2, 75-82 (1952).

[8] Selman and Wilkin, "The Production of High Intensity Ultrasonics at Megacycle Frequencies," J. Sci. Instr. 26, 7, 229-231 (1949).

[9] I. Skards, "Investigation of the Mechanism of the Effect of Ultrasonics Upon Bacteria," Dissertation, Agricultural Academy of the Latvian SSR, Riga, 1955.

[10] I. Skards, "Obtaining Ultrasonic Radiation of a Constant Intensity for Irradiation in a Vessel With an Untuned Bottom," Acoust. J. 1, 3, 274-285 (1955).

[11] V. Lopasic and Celjuska, "Die Gewinnung einiger Antigene mittels Ultraschall," Schweiz. Z. allg. Path. u. Bakt. 15, 322-331 (1952).

Received February 19, 1955

Institute of Microbiology
Academy of Sciences, Latvian SSR,
Riga

SOUND RADIATION BY A ROTATING DIPOLE

L. N. Sretenskii

The axis of a dipole whose moment varies periodically with time has some type of motion in space. The paper studies the acoustic field of such a dipole when the indicated motion is either a uniform rotation or a harmonic variation of the angle which the axis of the dipole makes with a constant direction in space.

---

1. Let us examine the equation of sound propagation in a homogeneous medium:

$$\frac{\partial^2\Phi}{\partial t^2} = c^2\left(\frac{\partial^2\Phi}{\partial x^2}+\frac{\partial^2\Phi}{\partial y^2}+\frac{\partial^2\Phi}{\partial z^2}\right), \qquad (1)$$

where c is the velocity of sound, and Φ is the velocity potential. By means of the function Φ we may define the compression of the gaseous medium, s, and the pressure in the medium:

$$s = \frac{1}{c^2}\frac{\partial\Phi}{\partial t}, \quad p = p_0 + \rho_0\frac{\partial\Phi}{\partial t}.$$

Here p_0 is the normal pressure, and ρ_0 is the normal density of the medium.

Defining the distance of any point in space from the origin as r, we may write one particular solution of Equation (1), which depicts spherical waves emanating from the origin as from a source of sound:

$$\Phi = -\frac{1}{4\pi}\,\frac{F_1\left(t-\frac{r}{c}\right)}{r} \qquad (2)$$

$F_1(\alpha)$ is an arbitrary function of its own argument. Differentiating the solution (2) with respect to x we find another solution for the wave equation:

$$\Phi = -\frac{1}{4\pi}\,\frac{\partial}{\partial x}\,\frac{F_1\left(t-\frac{r}{c}\right)}{r}$$

which defines the propagation of sound from a dipole moment $M = F_1(t)$; the axis of the dipole is directed along the axis OX.

Further, the function

$$\Phi = -\frac{1}{4\pi}\,\frac{\partial}{\partial y}\,\frac{F_2\left(t-\frac{r}{c}\right)}{r}$$

defines the velocity potential of the motion caused by a dipole which has a moment $M = F_2(t)$, and has an axis directed along the coordinate OY.

From all this it follows that the function

$$\Phi = -\frac{1}{4\pi}\left\{\frac{\partial}{\partial x}\frac{F_1\left(t-\frac{r}{c}\right)}{r} + \frac{\partial}{\partial y}\frac{F_2\left(t-\frac{r}{c}\right)}{r}\right\} \tag{3}$$

is the velocity potential of the acoustic field formed by a dipole whose moment is

$$M = \sqrt{F_1^2(t) + F_2^2(t)} \tag{4}$$

and whose axis, which is located in the plane XOY, forms an angle χ with the OX axis; this angle is defined by the formula

$$\cos\chi = \frac{F_1(t)}{\sqrt{F_1^2(t) + F_2^2(t)}}\,. \tag{5}$$

2. Let us examine several particular cases of the propagation of sound waves, which have been described by the formulas in this section.

Let us first assume that

$$F_1(t) = m\cos\sigma t\cos\omega t, \quad F_2(t) = m\cos\sigma t\sin\omega t, \tag{6}$$

where m, σ, ω are specified quantities. From formula (4) it follows that the dipole moment has the following value:

$$M = m\cos\sigma t$$

and that the angle χ which the axis of the dipole makes with the OX axis will vary uniformly with time, rotating with an angular velocity ω. Thus, the formula

$$\Phi = -\frac{m}{4\pi}\left\{\frac{\partial}{\partial x}\frac{\cos\sigma\left(t-\frac{r}{c}\right)\cos\omega\left(t-\frac{r}{c}\right)}{r} + \frac{\partial}{\partial y}\frac{\cos\sigma\left(t-\frac{r}{c}\right)\sin\omega\left(t-\frac{r}{c}\right)}{r}\right\}$$

defines the velocity potential of the gas vibrations due to the propagation of sound waves formed by a dipole which has a harmonically varying moment and an axis rotating uniformly in the plane XOY.

We may also rewrite the preceding formula in the following form:

$$\Phi = -\frac{m}{8\pi}\left\{\frac{\partial}{\partial x}\frac{\cos\mu\left(t-\frac{r}{c}\right)}{r} + \frac{\partial}{\partial x}\frac{\cos\nu\left(t-\frac{r}{c}\right)}{r} + \frac{\partial}{\partial y}\frac{\sin\mu\left(t-\frac{r}{c}\right)}{r} + \frac{\partial}{\partial y}\frac{\sin\nu\left(t-\frac{r}{c}\right)}{r}\right\}, \tag{7}$$

where

$$\mu = \omega + \sigma, \quad \nu = \omega - \sigma.$$

Therefore, the acoustic field which is created due to the uniformly rotating dipole may be described by the sum of the acoustic fields created by two pairs of dipoles: the axis of one pair coincides with the axis OX, and the axis of the other pair coincides with the axis OY; the vibration frequencies in each pair of dipoles are defined by the sum and difference frequencies of the rotation of the dipole axis and the frequency of the dipole itself.

Let us define the energy flux Q which passes through a sphere (S) with radius R in a direction away from the dipole. We then have

$$Q = -\iint\limits_{(S)} (p - p_0)\frac{\partial\Phi}{\partial r}\,ds. \tag{8}$$

In order to calculate the magnitude of Q we introduce the polar coordinates of the point (x,y,z), into formulas (7) and (8), assuming that

$$x = r\sin\theta\cos\psi,\quad y = r\sin\theta\sin\psi,\quad z = r\cos\theta.$$

We obtain

$$\Phi = -\frac{m}{8\pi c}\frac{\sin\theta}{r}[\mu\sin(\mu\tau - \psi) + \nu\sin(\nu\tau - \psi)] + \cdots$$

In this expression, for the sake of brevity, we have set $\tau = t - \frac{r}{c}$ and have not explicitly written out the terms which go to zero, such as $\frac{1}{r^2}$.

To the same degree of accuracy we also obtain the following two formulas:

$$\frac{\partial\Phi}{\partial r} = \frac{m}{8\pi c^2}\frac{\sin\theta}{r}[\mu^2\cos(\mu\tau - \psi) + \nu^2\cos(\nu\tau - \psi)] + \cdots,$$

$$\frac{\partial\Phi}{\partial t} = -\frac{m}{8\pi c}\frac{\sin\theta}{r}[\mu^2\cos(\mu\tau - \psi) + \nu^2\cos(\nu\tau - \psi)] + \cdots$$

On the basis of these formulas let us now evaluate the magnitude of Q: we have

$$Q = \frac{m^2\rho}{64\pi^2c^3}\int\limits_0^{2\pi} d\psi\int\limits_0^{\pi}[\mu^2\cos(\mu\tau - \psi) + \nu^2\cos(\nu\tau - \psi)]^2\sin^3\theta\,d\theta,$$

or, carrying out the integration,

$$Q = \frac{m^2\rho}{12\pi c^3}[4\omega^2\sigma^2\sin^2\sigma\tau + (\omega^2 + \sigma^2)^2\cos^2\sigma\tau].$$

As a result, the average value $\overline{Q}$ of the quantity Q over a period of vibration of the dipole will be equal to:

$$\overline{Q} = \frac{m^2\rho}{24\pi c^3}(\omega^4 + 6\omega^2\sigma^2 + \sigma^4).$$

This is the expression for that energy which the rotating dipole radiates into an infinite medium during one period of its vibration.

We then find the value of the internal energy E at each point in space far from the dipole:

$$E = \frac{1}{2}\rho c^2 s^2.$$

Carrying out the indicated operations, we obtain

$$E = \frac{\rho m^2\sin^2\theta}{128\pi^2c^4r^2}[\mu^2\cos(\mu\tau - \psi) + \nu^2\cos(\nu\tau - \psi)]^2.$$

We then find the average value $\overline{E}$ of the internal energy according to this formula; we evaluate it thus:

$$\overline{E} = \lim_{T\to\infty}\left\{\frac{1}{T}\int\limits_0^T E\,dt\right\}.$$

Carrying out the indicated operations we obtain:

$$\overline{E} = \frac{\rho m^2}{128\pi^2c^4}(\omega^4 + 6\omega^2\sigma^2 + \sigma^4)\frac{\sin^2\theta}{r^2}.$$

3. Let us now suppose that the axis of the dipole changes its angle χ of inclination with the axis OX according to the law

$$\chi = \gamma \cos ht, \tag{9}$$

where γ and $\underline{h}$ are specified numbers.

Let us further assume that the dipole moment varies in time according to the harmonic law

$$M = m \cos \sigma t.$$

The functions F_1 and F_2 from § 1 will in this case be defined by the following expressions:

$$F_1(\tau) = m \cos \sigma\tau \cos(\gamma \cos h\tau),$$
$$F_2(\tau) = m \cos \sigma\tau \sin(\gamma \cos h\tau).$$

The velocity potential Φ is written thus:

$$\Phi = -\frac{m}{8\pi}\left\{\frac{\partial}{\partial x}\frac{\cos(\sigma\tau + \gamma\cos h\tau)}{r} + \frac{\partial}{\partial x}\frac{\cos(\sigma\tau - \gamma\cos h\tau)}{r} + \right.$$
$$\left. + \frac{\partial}{\partial y}\frac{\sin(\sigma\tau + \gamma\cos h\tau)}{r} - \frac{\partial}{\partial y}\frac{\sin(\sigma\tau - \gamma\cos h\tau)}{r}\right\}.$$

Let us rewrite this expression in a new form using a formula which is known from the theory of Bessel functions:

$$e^{i\gamma\cos ht} = \sum_{p=-\infty}^{\infty} i^p J_p(\gamma)\, e^{phti};$$

we obtain

$$\Phi = -\frac{m}{4\pi}\left\{\frac{\partial}{\partial x}\sum_{p=-\infty}^{\infty}\frac{J_p(\gamma)}{r}\cos\frac{1}{2}\pi p\cos(\sigma + ph)\tau + \frac{\partial}{\partial y}\sum_{p=-\infty}^{\infty}\frac{J_p(\gamma)}{r}\sin\frac{1}{2}\pi p\cos(\sigma + ph)\tau\right\}.$$

As a result we find the following formulas for large $\underline{r}$:

$$\frac{\partial\Phi}{\partial t} = -\frac{m}{4\pi c r}\sin\theta\,[\Gamma_1(\tau)\cos\psi + \Gamma_2(\tau)\sin\psi],$$
$$\frac{\partial\Phi}{\partial r} = \frac{m}{4\pi c^2 r}\sin\theta\,[\Gamma_1(\tau)\cos\psi + \Gamma_2(\tau)\sin\psi],$$

where

$$\Gamma_1(\tau) + i\Gamma_2(\tau) = \sum_{p=-\infty}^{\infty}(\sigma + ph)^2 e^{\frac{1}{2}\pi p i} J_p(\gamma)\cos(\sigma + ph)\tau.$$

By means of these formulas, we find the amount of energy radiated through a sphere of large radius:

$$Q = -\rho\iint\frac{\partial\Phi}{\partial t}\frac{\partial\Phi}{\partial r}\,dS = \frac{\rho m^2}{12\pi c^3}[\Gamma_1^2(\tau) + \Gamma_2^2(\tau)].$$

From this it is possible to find the average value $\overline{Q}$ of the quantity Q, assuming that $\overline{Q}$ is defined by the following limit:

$$\overline{Q} = \lim_{T\to\infty}\left\{\frac{1}{T}\int_0^T Q\,dt\right\}.$$

Carrying out the indicated operations, we find that

$$\overline{Q} = \frac{\rho m^2}{24\pi c^3}\sum_{p=-\infty}^{\infty}(\sigma + ph)^4 J_p^2(\gamma); \tag{11}$$

it is assumed here that no relationship of the form

$$\sigma = \frac{1}{2} Nh$$

exists between σ and h when N is a whole number; when there is such a relationship, the preceding formula becomes somewhat more complex.

Formula (11) may be substantially simplified if we pay attention to the known formulas

$$\sum_{p=-\infty}^{\infty} p^2 J_p^2(\gamma) = \frac{1}{2}\gamma^2, \quad \sum_{p=-\infty}^{\infty} p^4 J_p^2(\gamma) = \frac{3}{8}\gamma^4 + \frac{1}{2}\gamma^2.$$

We obtain

$$\overline{Q} = \frac{\rho m^2}{24\pi c^3}\left[\sigma^4 + 3\sigma^2 h^2 \gamma^2 + h^4 \gamma^2\left(\frac{1}{2} + \frac{3}{8}\gamma^2\right)\right].$$

Then we find the expression for the internal energy of the gas; we have

$$E = \frac{1}{2}\frac{\rho}{c^2}\left(\frac{\partial \Phi}{\partial t}\right)^2.$$

For large values of r this expression acquires the following simplified form:

$$E = \frac{\rho m^2}{32\pi^2 c^4 r^2}\left[\Gamma_1(\tau)\cos\psi + \Gamma_2(\tau)\sin\psi\right]^2 \sin^2\theta.$$

We shall now find the average value $\overline{E}$ of the internal energy at a specified locus far from the origin by using this formula:

$$\overline{E} = \lim_{T=\infty}\left\{\frac{1}{T}\int_0^T E\,dt\right\} = \frac{\rho m^2}{32\pi^2 c^4 r^2}\sin^2\theta \cdot \lim_{T=\infty}\left\{\frac{1}{T}\int_0^T \left[\Gamma_1(\tau)\cos\psi + \Gamma_2(\tau)\sin\psi\right]^2 dt\right\}.$$

Carrying out the indicated operations, we obtain

$$\overline{E} = \frac{\rho m^2}{64\pi^2 c^4 r^2}\sin^2\theta\left\{\sin^2\psi \sum_{p=-\infty}^{\infty}{}' (\sigma + ph)^4 J_p^2(\gamma) + \cos^2\psi \sum_{p=-\infty}^{\infty}{}' (\sigma + ph)^4 J_p^2(\gamma)\right\}, \tag{12}$$

where the first infinite sum is only propagated for odd values of the summing index p, and the second one is propagated for even values.

Formula (10) shows that the acoustic field created by a dipole whose axis vibrates according to the law given in Formula (9) may be composed of the acoustic fields of an infinite number of stationary dipoles whose axes coincide with the OX axis or the OY axis. Each individual term of the infinite series (11), (12) and others indicates what effect each of the stationary dipoles will produce upon the sum of each corresponding series. Particularly interesting factors are noted here when the values of the quantity γ are large, i.e., in the case when the axis of the dipole makes a sufficiently large number of complete turns around the point O. If, for example, we assume that γ is equal to 24, and that the ratio σ/h is small, then

$$\left(\frac{\sigma}{h} + p\right)^4 J_p^2(24)$$

will have a maximum value equal to 12,858 for p = 22; for the remaining values of p we have considerably smaller values for this monomial. It would also be appropriate to remark that for a σ/h which is small and a γ which is of substantial magnitude, the terms in which $p \approx \gamma$ will be of primary significance.

Thus in the case we are examining, one dipole plays the fundamental role in the formation of the acoustic field of a vibrating dipole (or several dipoles which are closest to it by number).

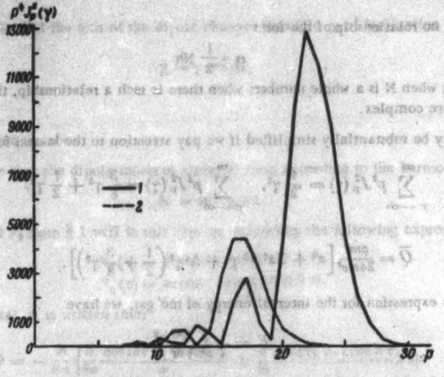

1) $\gamma = 24$; 2) $\eta = 18$.

The figure shows values of $p^4 J_p^2(\gamma)$ as a function of the index p for two values of γ.

Received July 19, 1955

Marine Hydrophysical Institute of the Academy of Sciences, USSR, Moscow

CHRONICLE

V. S. GRIGOR'EV

(On His Fiftieth Birthday)

In December 1955 the talented and broadly experienced specialist in the field of acoustics and electroacoustics, Victor Sergeevich Gregor'ev, the director of the laboratory of the Acoustical Institute of the Acad. Sci. USSR and assistant editor of the "Acoustical Journal", celebrated his fiftieth birthday.

At the present time Victor Sergeevich is one of the most important acoustical scientists, the author of many experimental works, and of approximately thirty published books and reports. Possessing a broad scientific erudition, and talent as an experimental scientist, he has successfully headed a series of projects conducted by the Acoustical Institute.

His practical bent, the newness of his research, the originality of his methods— all these are characteristic features of his work.

V. S. Grigor'ev began his scientific activity in the All-Union Electrical-Engineering Institute (VEI) after finishing engineering college in 1930. From 1932 on, he worked in the Scientific-Research Cinema Photo Institute, and from 1938 on, he directed the acoustical laboratory attached to the construction of the Palace of Soviets. From 1944 on, Victor Sergeevich has been working in the Academy of Sciences, at first in the acoustical laboratory of the P. N. Lebedev Physics Institute, and then in the Acoustical Institute.

In the early period of his work— from 1930 to 1932— Victor Sergeevich was engaged in the application of amplifier techniques to sound recording and sound reproducing in sound films. From 1932 on, he has worked in the field of film projection and electroacoustics, engaging in particular in sound reproduction for film-projecting installations. During this period Victor Sergeevich has been working as an engineer-inventor and as a researcher. The first of his research projects on problems of cinema projection for large auditoriums made important contributions to the successful completion of the project involving the construction of an outdoor sound cinema theatre seating 20,000 in the M. Gorky Central Park of Culture and Rest in Moscow. At that time it was the largest cinema theatre in the world. During the same period he devoted great attention to the development of the theory and methods of engineering calculation and design for sound reproducing systems. On the basis of ideas which have been developed in several of his works, the first high-power, high efficiency loudspeaker in the Soviet Union was created. The models worked out by him were, as a result, used as the basis for a series of units which are widely utilized in the field of sound cinematography. During this same period, while working on research on the properties of passive fourpoles, Victor Sergeevich worked out some original mechanical filters for quenching the oscillations of cinema film, which produce distortion in the reproduction of sound.

V. S. Grigor'ev, while working in the acoustical laboratory attached to the Palace of Soviets, designed acoustical installations and systems for sound amplification in the Palace. However, he worked most actively and showed his experience and creativity to the highest degree in the development of laboratory acoustic measuring devices and in the creation of an acousticometric proving ground for this type of construction. This proving ground was the first and only one in the Soviet Union and various research was conducted with its aid; this research facilitated the development of Soviet architectural acoustics and electroacoustics. Simultaneously, Victor Sergeevich was working out a method for architectural acoustical measurements, for problems involving the use of feedback in electroacoustical transducers, and was continuing his work in ultra-high-power loudspeakers.

During the period after the war and right up to the present time, V. S. Grigor'ev is successfully heading work on a series of important problems in the field of new engineering and acoustical research. Related to these are research concerning: refractions during the propagation of sound in water, the statistical properties of several acoustic processes, the statistical properties of a wind wave upon the surface of a body of water, the vibration of several bodies; experimental research is being done on dispersion from an uneven surface, propagation of sound in shallow water, investigation of acoustic resonators et. al. In addition, he directs the design and construction of large complexes of measuring apparatus for various types of acoustical experiments.

This incomplete list of the projects which Victor Sergeevich is himself working on, as well as the projects under his direction, illustrates the breadth of his scientific interests.

V. S. Grigor'ev is helping to develop a staff of young researchers. In carrying out his scientific supervision he skillfully directs the efforts of the researcher toward a true solution of the problem without depriving him of his independence and initiative. Victor Sergeevich is also engaged in pedagogical work. In addition to the courses in acoustics and hydroacoustics which he gives in various universities, he directs the diplomate projects of a large number of students.

During his fifty years Victor Sergeevich has been full of creative ideas. We wish him health and a fruitful attainment of his scientific goals.

IN THE ACOUSTICAL COMMISSION OF THE ACAD. SCI. USSR

Conference Devoted to Methods of Investigating Speech

On October 25-27, 1955, the fourth conference of the section of the Acoustical Commission of the USSR devoted to the investigation of speech took place in Moscow; it was devoted to the methods of investigating speech.

Physicists, physiologists, psychologists, linguists and communications engineers from scientific-research institutes and universities in Moscow, Leningrad, Kiev, Odessa, Tibilisi, Baku and other cities participated in the conference. The following papers were read at the conference:

I. M. Litvak. Physical Methods for Investigating the Characteristics of Speech Sounds (Leningrad).

L. A. Varshavskii. Methods for Investigating the "Formant" Composition of Speech Sounds (Leningrad).

N. B. Pokrovskii. Investigation of the Integral Characteristics of Speech (Leningrad).

V. G. Ginzburg. X-Ray Study of Speech Articulation (Moscow).

L. V. Dmitriev. The X-Ray Method for Studying the Voice Apparatus of Singers (Moscow).

T. A. Brovchenko. Methods of Photographing Speech Articulation (Odessa).

V. A. Artemov. Methods for the Psychological Study of Speech (Moscow).

N. I. Zhinkin. Complex Method for Investigating the Mechanism of Speech Process (Moscow).

B. V. Bogdanov. Method for Investigating the Auditory Process by Word Tables in a Clinic (Leningrad).

V. A. Artemov. Methods for the Experimental-Phonetic Study of the Acoustic Composition of Language (Moscow).

P. S. Kuznetsov. The Problem of Dismembering Auditory Speech (Moscow).

At the conference a resolution was adopted which pointed out the necessity for taking measures to organize the work being done on the complex study of speech.

DEVELOPMENT OF ACOUSTICS IN POLAND AND ROMANIA

Poland. In pre-war Poland the few acoustical scientists did not have appropriate conditions under which to work in their specialties. The very sparingly equipped laboratories of the Polish Radio and of the Institute of Telecommunications limited themselves to work on current problems. Therefore, after the new government had been established it became necessary to start work by relying on young cadre who did not have much experience, and by creating a new center of scientific work. Meanwhile construction techniques, industry, cinematographic and radio-broadcasting technology posed serious scientific and pedagogic tasks before Polish acoustical scientists. During the first Five-Year Plan an orderly organization of projects in acoustics is being conducted so that they may be most efficiently carried out in institutions of higher learning; beginning with 1951, research work has been coordinated by the Polish Academy of Sciences and has been developing according to plan. Simultaneously the problems of electroacoustics are being integrated into the courses of industrial institutes.

An important event was the first Polish conference devoted to ultrasonic engineering, which was organized in November 1953 by the Institute of Fundamental Problems of Engineering, of the Polish Academy of Sciences (IFPE). In 1954, in the Medical Academy of Zawiercie, a conference took place which was devoted to physiological acoustics; in 1955 a conference took place at the agricultural university (in Olsztyn) in which the problem of molecular acoustics was discussed. Continuous seminars in acoustics and electroacoustics are being conducted in several scientific centers.

During recent years, the following system has been decided upon for subdividing the research conducted in various fields by the individual institutes.

The general problems of the theory of acoustics are being worked out by the staff of the acoustic department of Poznan University (mostly the investigation of waves of finite amplitude) and in the department of the IFPE which is devoted to the investigation of vibrations (diffraction of sound waves, waves in solid media, energy of a sound wave).

The staff of the electroacoustic department of the Warsaw Polytechnic Institute (WPI) is working on architectural acoustics. This staff worked out the design for the largest theatres and concert halls in the country, in addition to conducting their research work in the field of propagation of sound waves.

Several scientific centers are working in the field of auditory physiology. Work dealing with the sharpness of hearing ability is being conducted by the staff of the acoustic department of Poznan University, and problems of subjective acoustic response are being solved by the electroacoustical staff of the WPI.

The acoustics of speech. The acoustic properties of Polish speech are being investigated in the Phonographic Institute of Poznan University and by the IFPE department which is devoted to the investigation of vibrations. This same department is doing research in the field of telephone acoustics; incidentally, the same department is designing the standards for the artificial voice and the artificial ear. At the present time, work in the field of telephone measurements is being carried out by the communications staff of the Wroclaw Polytechnical Institute.

Electroacoustical transducers is the theme of the theoretical and experimental projects of the electroacoustical staff of the WPI and the department of the IFPE which is devoted to the investigation of vibrations. The result of these projects is that monographs on electroacoustic transducers, the design of a high-efficiency loudspeaker, as well as on the development of the engineering of barium titinate transducers have become available.

The passive application of ultrasonics is being expanded from year to year. Ultrasonic defectoscopes of Polish construction (the electroacoustical staff of the WPI and the department of the IFPE devoted to the investigation of vibrations) have received a fine reception in many countries; also of great interest at international conventions was an original ultrasonic method for geological research. It should be noted that work in this field, which is based upon firm theoretical foundations, is finding application in new fields (the investigation of concretes, engineering porcelain). The radio-engineering staff of the Gdansk Polytechnical Institute is working on sonic depth finders for various systems and the scientific problems related to their construction. The Institute of Metallurgy in Szczecin is also working in the field of ultrasonic defectoscopy. They are also conducting work related to research in the field of the practical application of ultrasonics. Several scientific institutions (in Poznan and Zawiercie, at the Institute of General Chemistry) are working on the problems of coagulation of suspensions in liquids and gases as well as on the construction of high-power ultrasonic sirens.

An ultrasonic installation for the coagulation of non-ferrous metal particles built by the main Institute for the Protection of Labor has already been applied in the field of metallurgy. The Metal-Cutting Institute in Krakow together with the electroacoustical staff of the WPI are now engaged in the perfection of an apparatus for the ultrasonic crystallization of metals. As we can see from what has been said above, research in the field of acoustics and electroacoustics is being broadly developed, although lack of cadre does not yet permit the development of these fields in all of the directions which are necessary for our economy. For example, insufficient research is being conducted on the perfection of the optical and magnetic recording of sound. The Warsaw Polytechnic Institute has already had an electroacoustical specialization course available for a year, and in other similar educational institutions lectures on electroacoustics comprise an important part of the program of the communications faculty.

Polish Academy of Sciences — I. Maletskii

Romania. In the Romanian Peoples Republic acoustics has developed and has attained its deserved position since the end of the second world war. In relation to the construction of a series of buildings of a public and cultural character (the House of Radiobroadcasting, the Cinematographic Combine, theatres and cinema-theatres), as well as in relation to the manufacture of electroacoustical apparatus in the country, the necessity arose for investigating and solving numerous problems in architectural acoustics and electroacoustics. In addition, research in the field of ultrasonics and its various applications has advanced significantly.

As a result of the necessity for coordinating the work in this field of physics, the Acoustical Commission of the Academy of the Romanian People's Republic was established in 1955. The Commission set itself the task of engaging mainly in the study of the problems of electroacoustics, ultrasonics, architectural acoustics, as well as in the study of problems related to the campaign against industrial noise. From now on, the activity of the commission will be considerably broadened, and will also embrace problems of hydroacoustics, physiological and musical acoustics.

Among the outstanding achievements in architectural acoustics, the success of which was due to the cooperative work of outstanding specialists, are the studios of the Radiobroadcasting House in Bucharest and the film-shooting floors of the Cinematographic Combine in Bufta. Original methods of solving the problems which were posed were applied in the construction of these buildings and only national raw materials were used. The necessity for investigating various sound-absorbent structures and materials led to the creation of the Laboratory of Acoustic Measurements. In this laboratory, which was equipped with newest apparatus, it became possible to conduct various acoustical measurements for the purpose of determining the acoustical conditions which exist in various buildings, determining the degree of acoustic isolation of structural elements against air and shock noise, as well as for conducting vibration measurements. Here we should mention the research on sound-absorbent materials and the construction of acoustic isolation with various types of covering, which was conducted in Romania. This research will continue in 1956.

For determining the intelligibility of speech, several research projects on the statistical phonetics of the Romanian language were conducted, and they resulted in the composition of lists of specific logatoms for the Romanian language. In addition, the Institute of Linguistics of the Academy of the RPR worked out problems related to the phonetic analysis of speech.

In the field of ultrasonics, research on the effect of ultrasonic radiation upon the growth and development of plants was successfully conducted. A series of devices was also designed for ultrasonic defectoscopy, both for laboratory research, for the defectoscopy of metal, and to satisfy the requests of our metallurgical industry.

Acoustical science is developing intensively and we believe that under the direction of the Acoustical Commission of the Academy of the RPR our achievements in this field will become more numerous and more outstanding.

Academy of the Romanian Peoples Republic

M. Grumazhescu

LETTERS TO THE EDITOR

THE INVESTIGATION OF THE FIELD PRODUCED BY ULTRASONIC DISPERSION LENSES IN A LIQUID

L. M. Liamshev

Ultrasonic dispersion lenses may be utilized for creating a broad directivity characteristic for radiating systems at high ultrasonic frequencies. Recently a series of papers has been published which is devoted to the theory of such lenses [1, 2] and to the experimental study of their directivity patterns in air [3].

The remarks in this letter provide several results from the measurement of the field nonuniformity of ultrasonic dispersion lenses in a liquid.

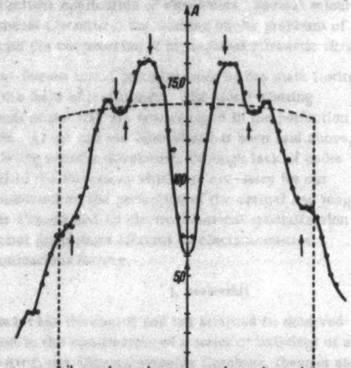

Figure 1.

The measurements were made by means of an installation which consisted of a water filled tube with dimensions of 200 x 60 x 60 cm^3 whose walls were sound-absorbent; an ultrasonic pulse generator which supplied pulses with a square-wave envelope; a quartz dipole made from an X-cut plate with a half-wave thickness and a diameter of about 40 mm; a receiving amplifier with a quartz diprod about 3 mm in size; a pulse oscillograph serving as an indicator of the signal amplitudes. The pulse duration was 30 microseconds, the repetition frequency was 50 cps and the frequency of the carrier was 1 megacycle. The distribution of acoustic pressure was measured at some distance from the lens in a plane perpendicular to the axis of the lense (measurements were made at the same level), and a point on the axis of the lens was taken as the origin. Accelerating spherical lenses made of plexiglass, polystyrol and aluminum were selected for investigation. During the measuring process the lens was fastened (screwed into) the lens mounting at a distance of several millimeters from the quartz plate. A column of water was located between the lens and the quartz plate of the radiator; the dimensions of the column of water were experimentally selected so that the maximum passage of acoustic waves through the lens would be possible.

Below we provide the averaged results of many repeated measurements of the same type for a field from two lenses. Figure 1 shows the pressure distribution for a lens of plexiglass at a distance of 700 mm from the lens. The radius of the output aperture of the lens is a = 16.5 mm, the radius of curvature of the lens is r = 50 mm, the focal length is f/= 100 mm.

The pressure distribution for a polystyrol lens at a distance of 260 mm is given in Figure 2. The parameters of the lens are: a = 16.5 mm, r = 25 mm and f = 64 mm. The pressure in units related to some standard level are laid off along the vertical axis; the distance from the axis of the lens in a plane perpendicular to the axis is laid off in millimeters along the horizontal axis. The broken line shows the shape of the pressure distribution which is derived from beam concepts.

An anaberrational dispersion lens transforms a plane wave front into a spherical wave front. From this it follows that if there is no absorption in the body of such a lens when the lens is an ideal transparent lens with a small angle of divergence, and when the distribution of energy at the output surface of the lens is practically uniform [1], then the lens field may be considered similar to the diffractional field of a point source located at the imaginary focal point of the lens behind an infinite opaque screen with an aperture equal to the output aperture of the lens.

In Figures 1 and 2, the arrows indicate the directions of the minima and maxima on the distribution curve, which were calculated on the basis of the indicated concepts [4]. It was established that if there are an even number of Fresnel zones on a sector of the surface of the spherical wave front (the surface bounded by the output aperture of the lens), then a pressure minimum is observed on the axis of the lens; if there is an odd number of Fresnel zones, then a pressure maximum occurs on the axis of the lens. The number of Fresnel zones k, as we know, is related to the parameters of the lens and to the wave length in the liquid, λ, by the relationship

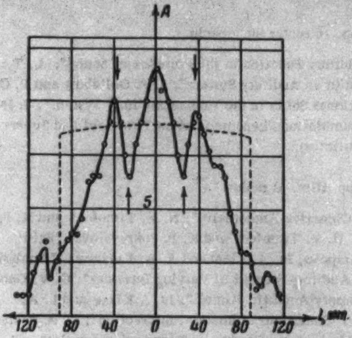

Figure 2.

$$k \approx \frac{a^2}{f\lambda} \quad (1)$$

For lens 1 (Figure 1) k ≈ 2; for lens 2 (Figure 2) k ≈ 3. Measurements of the nonuniformity of the field produced by aluminum lenses showed that their field is substantially nonuniform due to the phenomenon of reverberation in the lens body. The reverberation is caused by the poor transparency of the lens and by the accumulation of acoustic energy in it during the course of a pulse; this leads to a considerable distortion of the shape of an ultrasonic pulse. In order to eliminate the distortion, it is necessary to illuminate aluminum lenses.

LITERATURE CITED

[1] L. D. Rozenberg, Plane-elliptical Sonic Lenses, Trans. Commission on Acoustics, Bull. Acad. Sci. USSR 5, 114-119 (1950); Plane-hyperbolic Sonic Lenses, Trans. Commission on Acoustics, Bull. Acad. Sci. USSR 6, 114-124 (1951).

[2] L. N. Bondareva and M. I. Karnovskii, Directional Properties of Dispersion Lenses, Bull. Acad. Sci. USSR 8, 114-124 (1955); and Acoust. J. 1, 2, 128-133 (1955).

[3] B. G. Belkin, Sonic Lens with Variable Refractive Index, Bull. Acad. Sci. USSR 8, 125-138 (1955); Motion Picture Theater Speaker with Sonic Dispersion Lens, Acoust. J. 1, 3, 200-217 (1955).

[4] E. Grei and G. Met'iuz, Bessel Functions and their Applications in Physics, Foreign Lit. Press, Moscow, p. 235 (1953).

Received November 21, 1955

Acoustical Institute
Academy of Sciences of the USSR
Moscow

FROM THE PRESS OF
THE ACADEMY OF SCIENCES OF THE USSR

Problems of Physiological Acoustics, Vol. I, 1949, 174 pp. 10 rubles 80 kopecks.

Contents: G. V. Gershuni, "Reconstruction of an Auditory Function in the Presence of Sound"; L. T. Zagorul'ko and Iu. A. Klaas, "Serial Sensations (samples) in an Auditory System"; S. P. Gol'dburt and P. O. Makarov, "Dynamic Chronaxie and the Interval of Functional Shifts in the Human Auditory System"; S. Ia. Lifshits, "Fluctuation of Sensitivity, Interruption and Accumulation Phenomena when Threshold and Superthreshold Stimuli Act Upon Sensory Organs" (and other articles).

Problems of Physiological Acoustics, Vol. II, 1950, 176 pp. illus. 8 rubles.

Contents: G. V. Gershuni, "Physiological Bases of Objective Audiometry"; N. V. Timofeev and K. P. Pokryvalova, "Age Changes in the Audibility Threshold"; N. V. Timofeev and K. P. Pokryvalova, "Pain Thresholds for Sensation in a Free Sound Field"; A. A. Arapova, Iu. A. Klaas and A. A. Kniazeva, "Analysis of the Variation of Auditory Sensitivity under the Effect of Auditory Stimuli of Varying Intensity"; G. V. Gershuni, "Quantitative Study of the Limits of the Effects of Nonsensory Acoustic Stimuli"; Iu. A. Klaas and L. A. Chistovich, "Effects of Nonsensory Acoustic Stimuli under Conditions of Binaural Interaction"; K. P. Pokryvalova, "The Problem of the Frequency Range which Is Perceptible by Bone Conduction" (and other articles).

Problems of Physiological Acoustics. Vol. III, 1955, 126 pp. illus. 6 rubles 85 kopecks.

Contents: L. A. Varshavskii and I. M. Litvak, "Investigation of Formant Composition and Several Other Physical Characteristics of the Sounds of Russian Speech"; L. A. Chistovich, "Discrimination of Complex Signals", Part I, "The Changed Perception of Complex Sound When There Is a Varying Relationship Between the Intensities of Its Spectral Components", Part II, "Perception of the Pitch of Complex Sound"; G. V. Gershuni, "Study of the Action of the Human Auditory Analyzer on the Basis of Using Various Reactions"; R. V. Avakian, "Measurement of Threshold Sound Intensities and Differential Frequency Thresholds by Means of Momentary Conditioned Reflexes in a Human"; A. I. Maruseva, "The Problem of Measuring Discrimination Limits for Auditory Signals in a Human".

These books are on sale in "Akademkniga" stores.

Books will be sent to out-of-town subscribers upon receipt of prepaid orders.

Address orders to:

Moscow, Kuibyshev Street, 8, Office of "Akademkniga".

The expanded program of the American Institute of Physics comprises translation of four leading Soviet physics journals, as listed below. These translations, by competent, qualified scientists, will provide all research laboratories and libraries with accurate and up-to-date information of the results of research in the U.S.S.R.

Soviet Physics — Technical Physics

A translation of the "Journal of Technical Physics" of the Academy of Sciences of the U.S.S.R. The 1956 volume, which was originally announced as containing eighteen issues, is instead being issued monthly, in expanded issues. All issues of the original Russian journal for 1956 will be translated. Approximately 4,000 Russian pages. Annually, $90.00 domestic, $95.00 foreign.

Soviet Physics — Acoustics

A translation of the "Journal of Acoustics" of the Academy of Sciences of the U.S.S.R. Four issues per year, approximately 500 Russian pages. Annually, $20.00 domestic, $22.00 foreign. The 1955 issues of "Journal of Acoustics" U.S.S.R. will also be published. Will consist of two volumes, approximately 500 pages, and the subscription price will be $20.00 for the set.

Soviet Physics "Doklady"

A translation of the "Physics Section" of the Proceedings of the Academy of Sciences of the U.S.S.R. Six issues per year, approximately 900 Russian pages. Annually $25.00 domestic, $27.50 foreign.

Soviet Physics — JETP

A translation of the "Journal of Experimental and Theoretical Physics" of the Academy of Sciences of the U.S.S.R. Twelve issues per year, approximately 2,600 Russian pages. Annually $60.00 domestic, $64.00 foreign. Back issues of Volume 1 and 2 are available at a special price of $30.00 for both to subscribers to Volume 3.

Subscriptions should be addressed to the American Institute of Physics, 57 East 55th Street, New York 22, N.Y.